WPW 2022 Coupled Power School

Magnetic developments

Grant Covic and Duleepa Thrimawithana

Overview

- A Brief History at UoA
- Fundamentals & Design Goals
- Industrial Track Systems
- AGV and Robots
- Stationary EV Charging Systems
- Stationary Pad Developments
- SAE Compliance
- Multicoil Systems
- Future Road Systems

IPT History @ University of Auckland

THE UNIVERSITY OF AUCKLAND
NEW ZEALAND

Power Electronics and Wireless Power Transfer
Applications in Industrial, Static and Dynamic EV Charging, Biomedical Systems, Appliance Electronics, Lighting

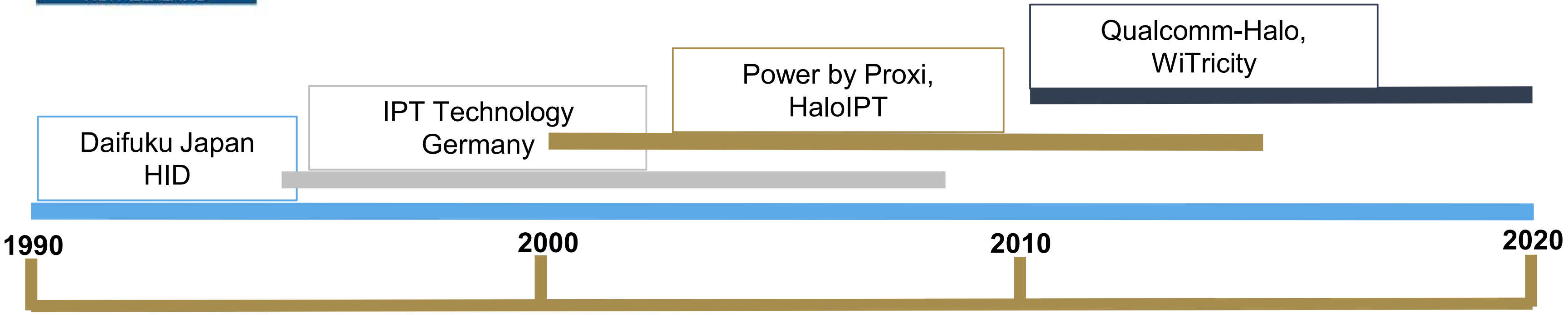

35+ PhDs, 10+ postdocs, 100+ Licensed Patent Families

30 Years Resonant WPT

Terminologies: Magnetic resonance, Highly resonant, IPT.
All use high Q coils & resonance for high efficiency at low coupling in the near field!

Grant Covic and Duleepa Thrimawithana, Department of Electrical, Computer, and Software Engineering (2022)

Fundamentals & Design goals

Fundamentals

Tuning & Operating Methodologies

Fundamentals

- Reliable & convenient
- Tolerant of water, chemicals, and dirt.

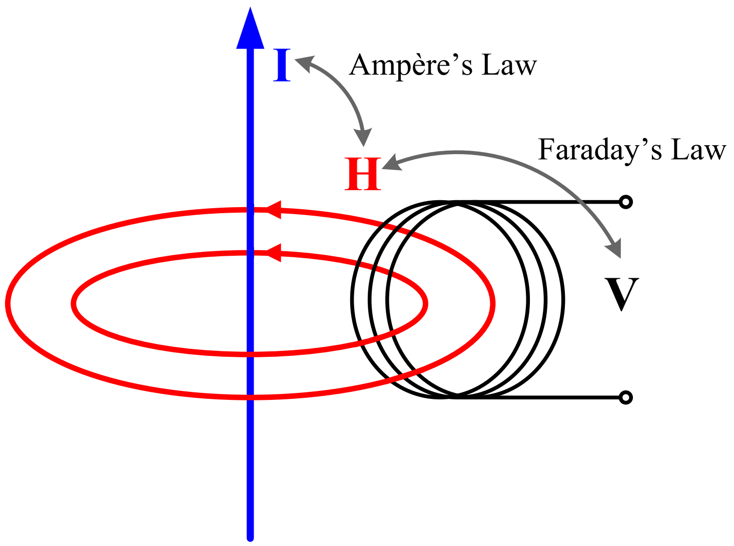

$$P_{su} = V_{oc} I_{sc} = \frac{M^2}{L_1 L_2} \omega L_1 I_1^2 = k^2 V_1 I_1$$

Tuning and Operating Methodologies

Power output when both sides are tuned to resonance:

$$P_{out} = \sqrt{P_{su} V_2 I_2} = k\sqrt{VA_1 VA_2}$$

V_1 and V_2 are limited for safety

I_1 and I_2 increase power (but also losses)

Losses in any pad as function of Pad quality

Higher quality indicates a more ideal inductor

$$Q_L = \frac{\omega L}{r_L}$$

$$P_{loss} = \frac{VA_{Pad}}{Q_{L_{Pad}}}$$

Control Options

Primary side control only:	Only VA_1 varied
Secondary side control only:	Only VA_2 varied
Primary & secondary side control:	Both VA_1 and VA_2 varied to achieve the lowest loss

Industrial Track Systems

Fixed Frequency Resonant Supplies

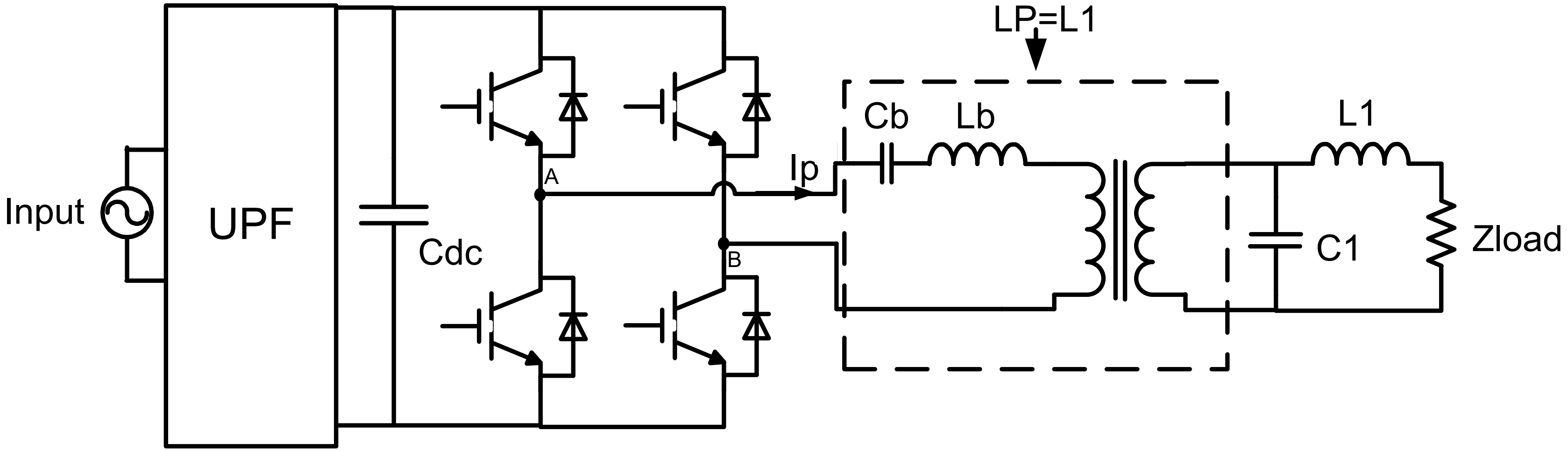

Typical LCL Resonant Track Systems Construction in 1990's

- Added transformer creates isolation and common mode rejection (L_p,C_1, & L_1 at resonance)
- Long track L_1 constructed using series C's and L's to manage the voltages.
- V_p at the H-Bridge output, naturally produces a controlled current source in L_1
- Z_{load} represents the impedance reflected onto the primary "track" from one or more coupled secondaries under operation.

IPT Resonant Track Systems

- Eary current controlled resonant supply were at 20kHz
  - Often around 20 independent secondaries
  - System efficiency > 80% high under load
  - *k* to each pickup ~ 0.01-0.03
- Often no primary core ($Q_{L\text{-track}}$ ~ 200)
- Secondary magnetics has core and is tuned ($Q_{L\text{-secondary}}$ ~ 550)
- Secondaries move along track and regulate VA_2

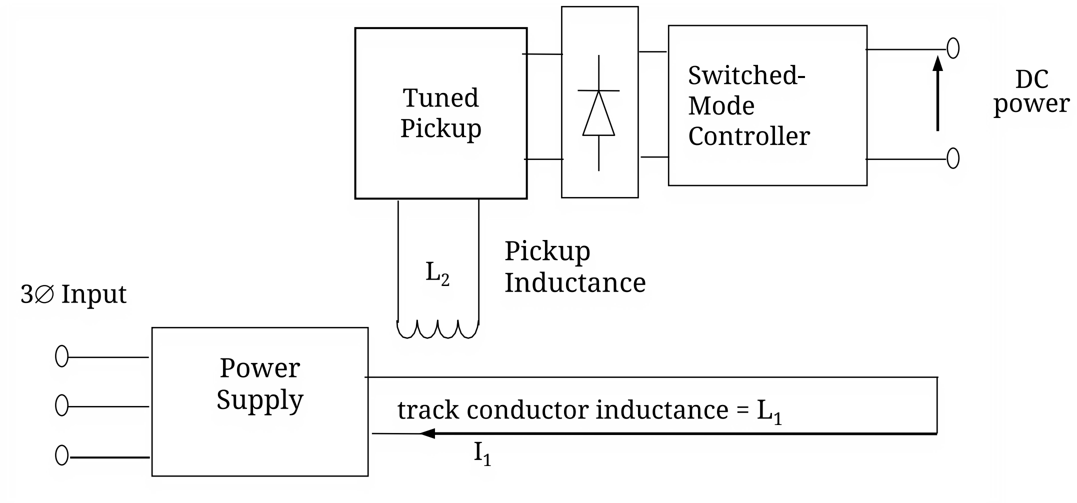

Individual k very low < 0.05

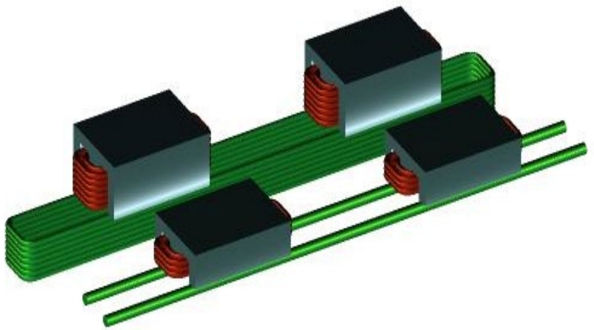

Primary recessed in floor: flat pick-ups

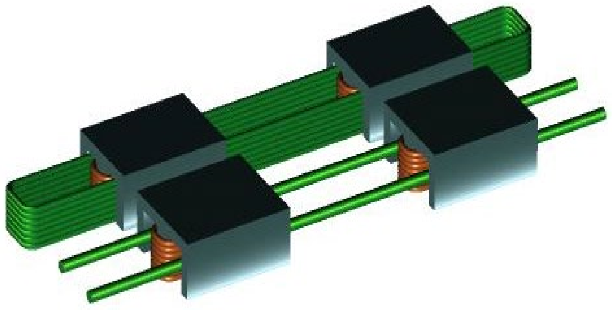

Rail mounted systems: E-core

Prototype Operation

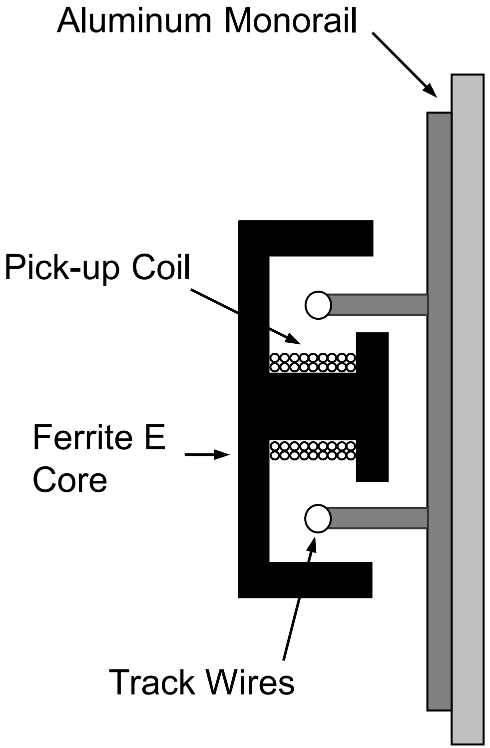

- Allows movement
- Tolerant of misalignment
- Unaffected by the environment

Improving the Magnetic Design

Problem: There is flux cancellation in E-Pick-up

- Evaluate flux paths from the primary coils
- Some of these cannot be measured because they cancelled by the return wire

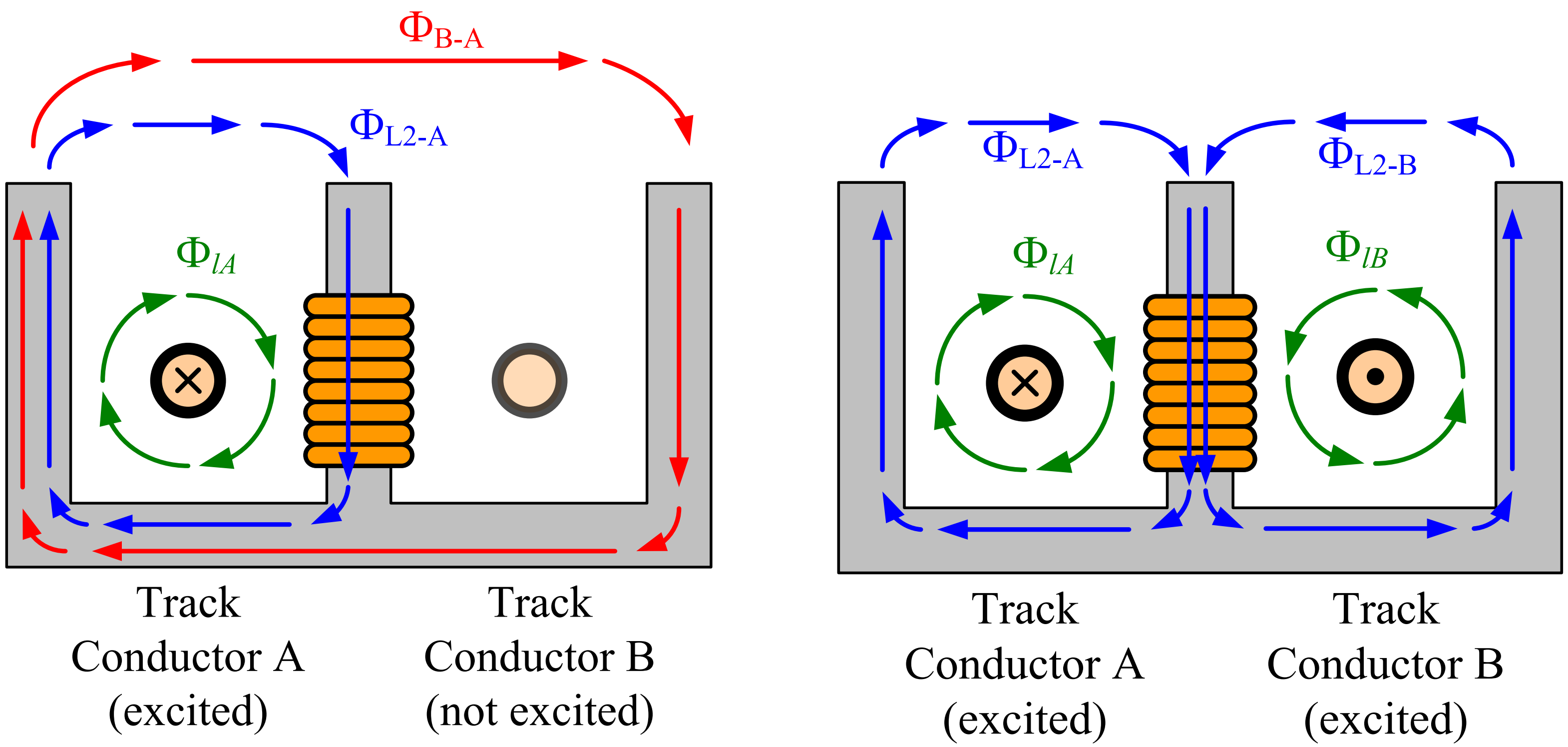

Pickup design: E to S Core

Minimise flux paths that do not couple through the secondary coil

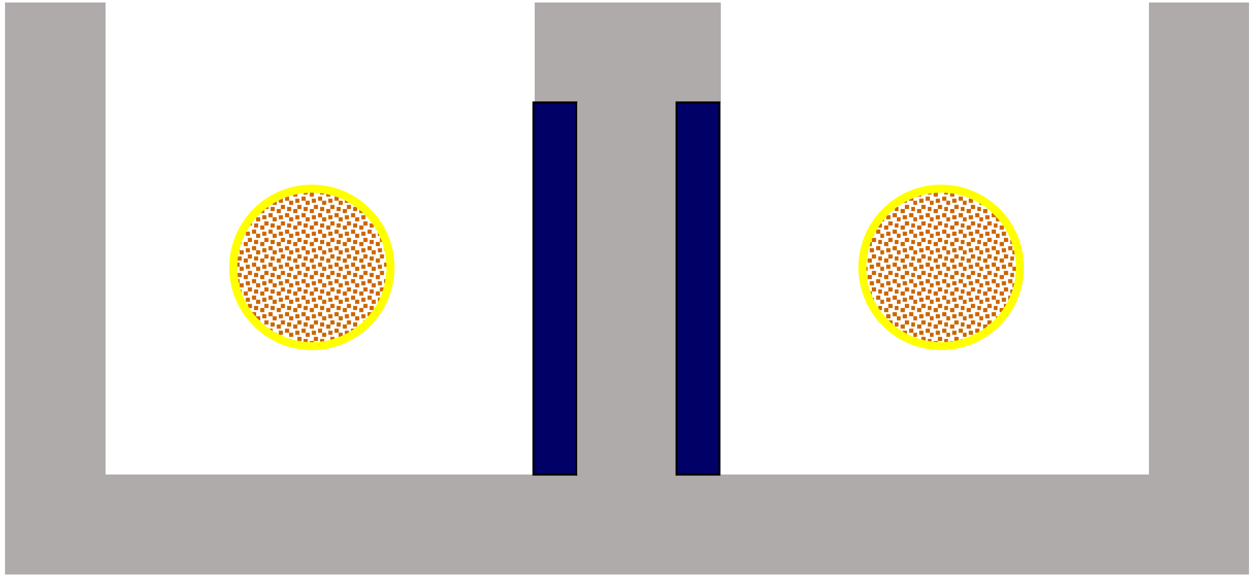

S and E pickups composition:

- Core ~ same ferrite
- Coil is identical

	S-Pickup	E-Pickup
$V_{oc\,(rms)}$	35.7 V	20.1 V
$I_{sc\,(rms)}$	4.4 A	4.0 A
P_{su}	158.5 VA	80.8 VA

Pickup design: S Core

More power but more difficult to use

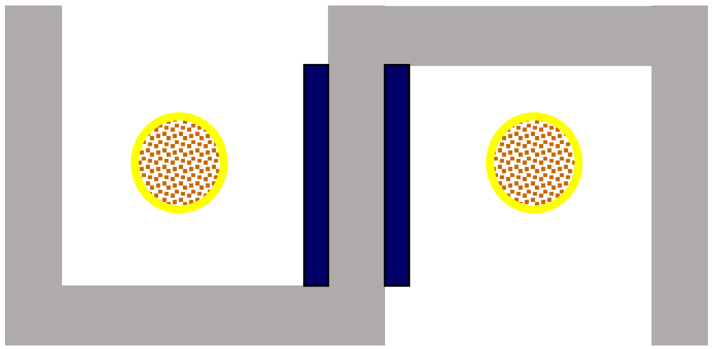

S-pickup on ICPT track

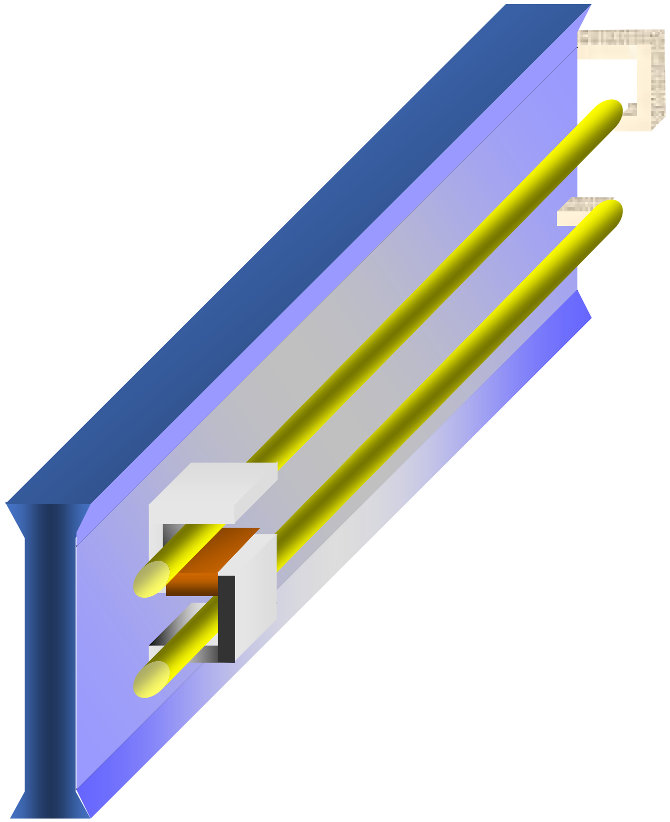

Example Track Systems

Roadway Lighting

3i Innovation

Tunnel (Wellington NZ)

Tunnel (Sydney Australia)

Double left turn (Illinois USA)

Amusement Rides

- Disney Imagineering project
- Single phase track
- Multiple Pickups
- Wide tolerance

1994 Disney Imagineering

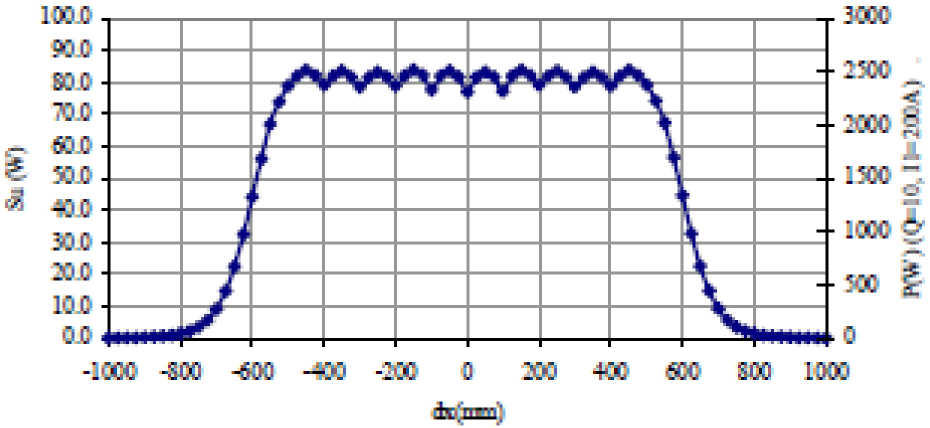

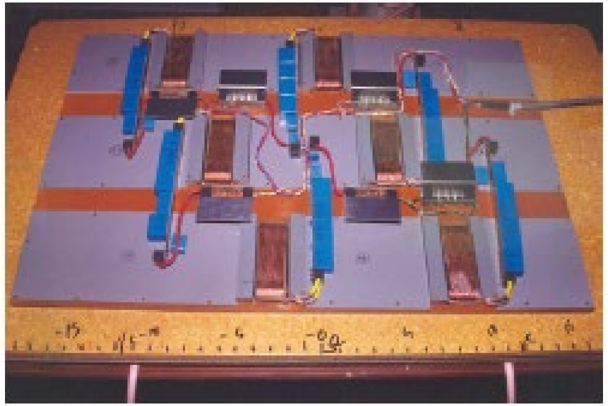

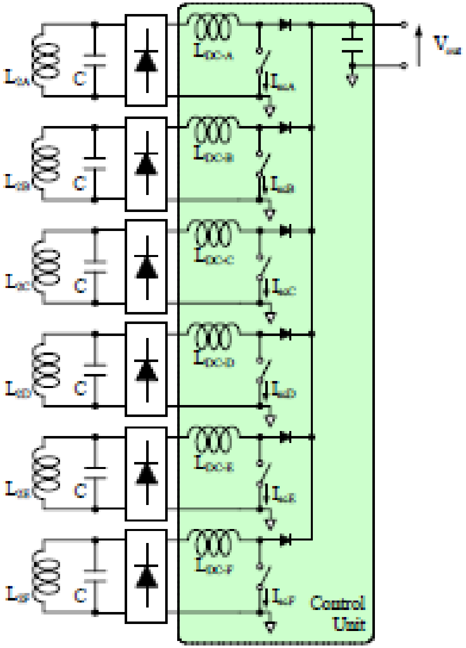

Factory Automation

Daifuku: Materials Handling (Early 1990's)

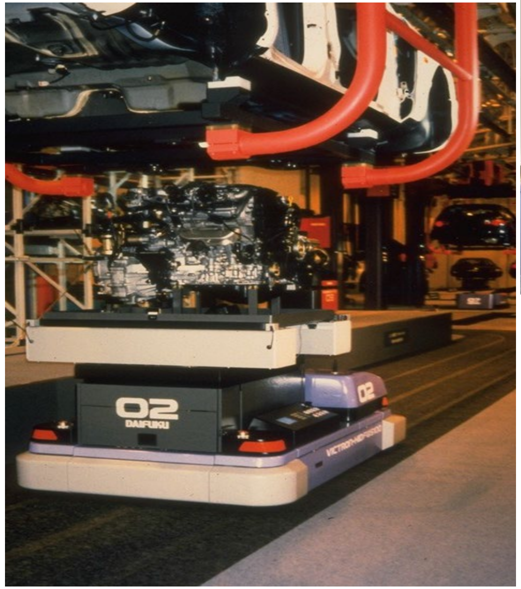

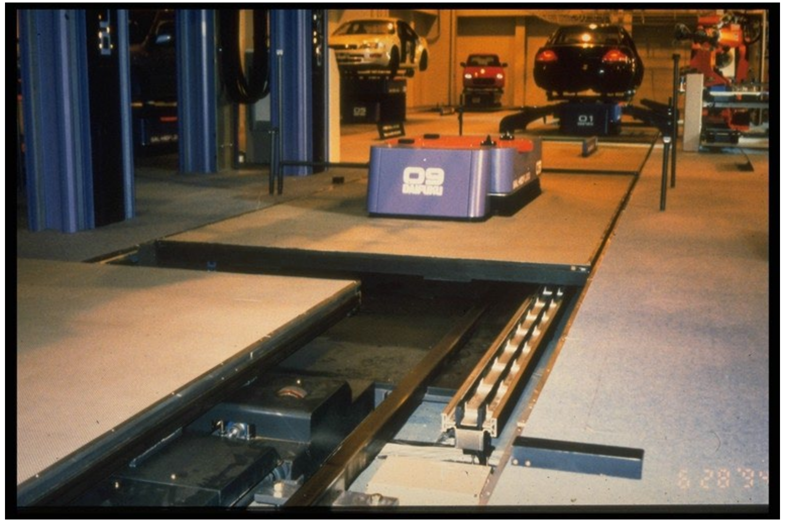

Electronic: Factory Automation

Daifuku: Clean Room Systems (Mid 1990s)





Automotive: Materials Handling

Conductix-Wampfler (IPT Technology) (Late 1990’s)

Automotive:

Wampfler: Rail Applications

10kW Pickup

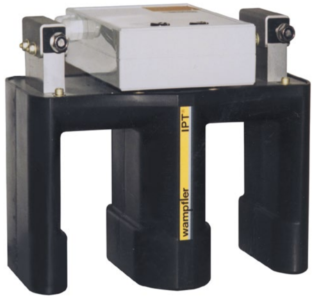

Japan Public Works Research Institute
Test Track for new road pavements

- 1 Vehicle
- 90 kW power
- 165m track length
- Vehicle weight 22 tonne
- Speed 30 km/h

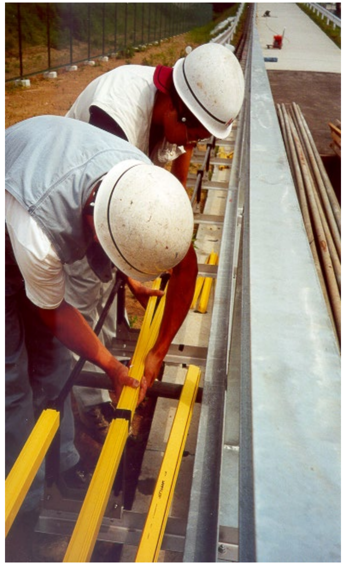

Sorting:

Wampfler: Rail Applications

Paris (Carrefour), London, Italy (Turin)

- 4 x 1.5 kW Power (75 or 48Vdc)
- Track Length ~ 210 - 280 m

AGVs and Robots

Require greater freedom of movement

AGV's and Robots

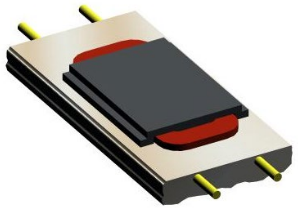

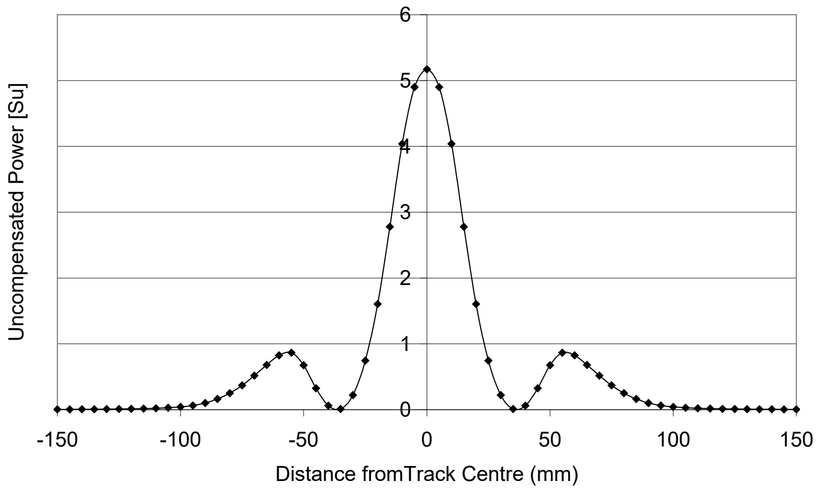

Precision alignment required for power transfer

Multi-phase Industrial Tracks

- Multi phase tracks - ferrite less primaries
    - Parallel layout decoupling mutuals only possible for 2 phase
    - Any M couples opposing voltages in nearby tracks
    - Drives unwanted currents back into the common bridge (circulating currents)
- Solutions include moving track loops to minimise M’s, cancelling mutuals or balancing them

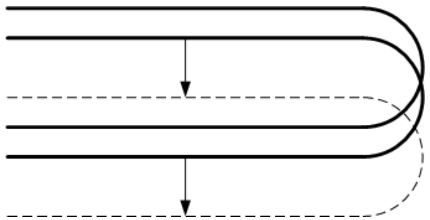

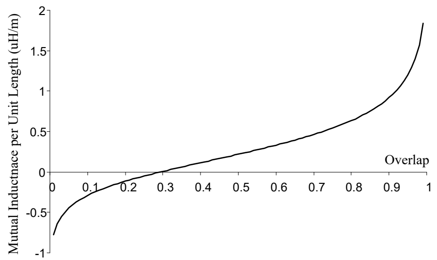

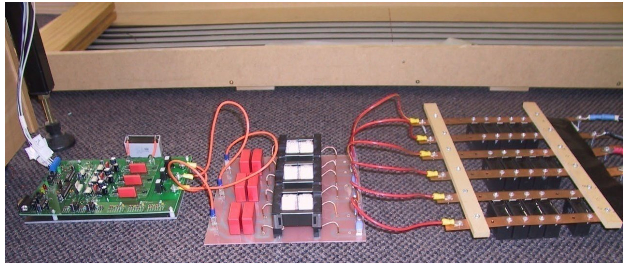

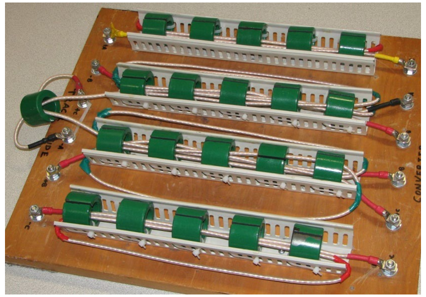

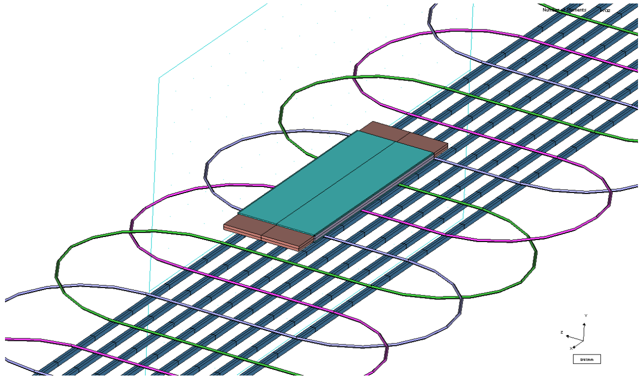

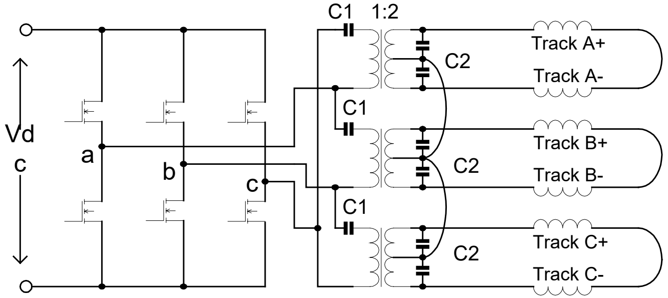

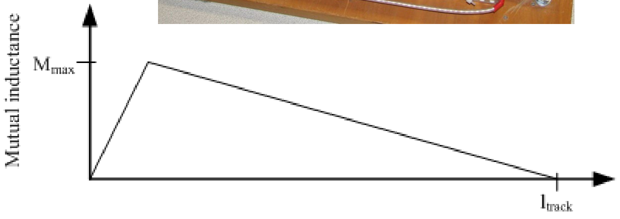

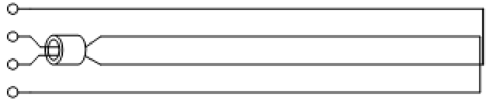

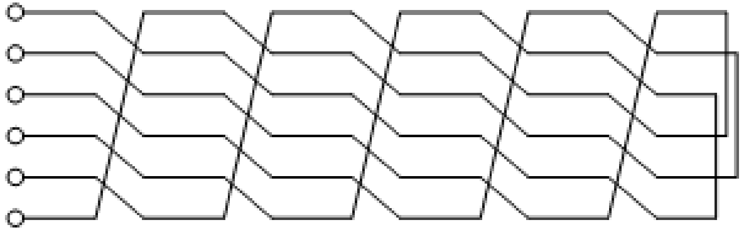

Reference [8],[18]-[20],[71]-[72]

Multiphase tracks

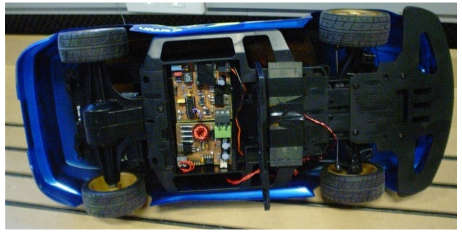

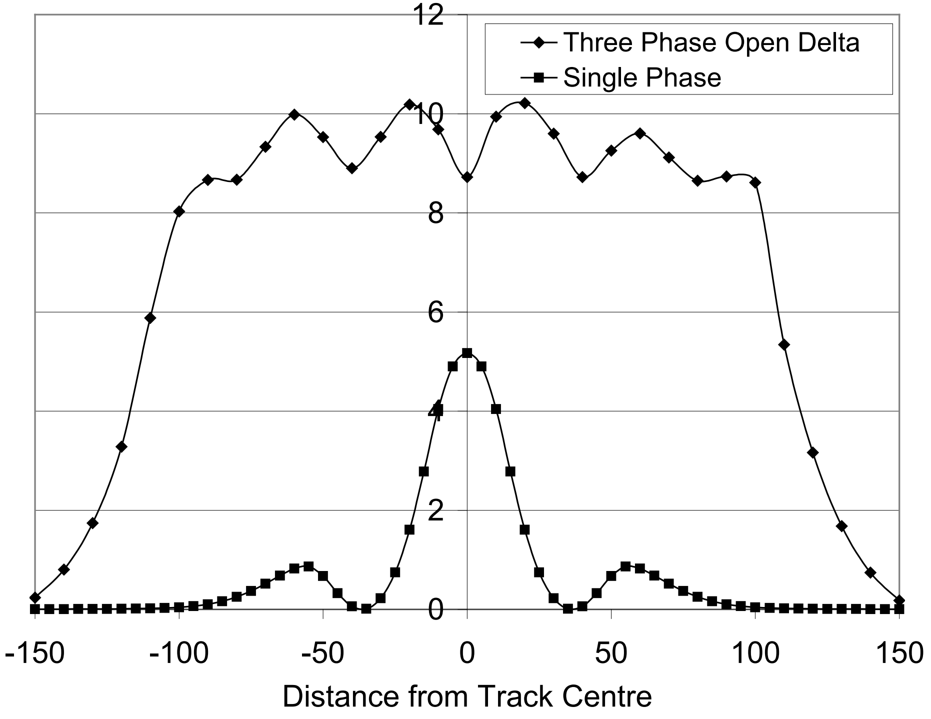

Reference [8],[18]-[20],[71]-[72]

Single & Multi-coil Pickups

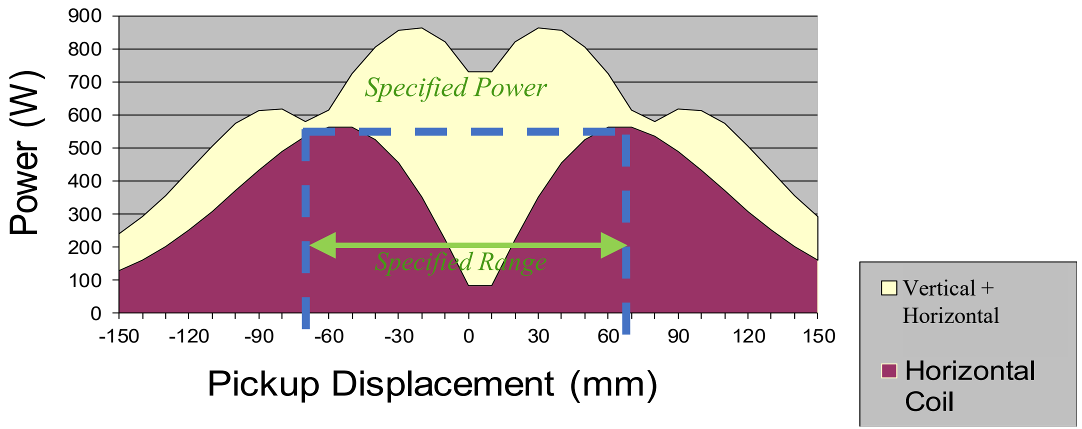

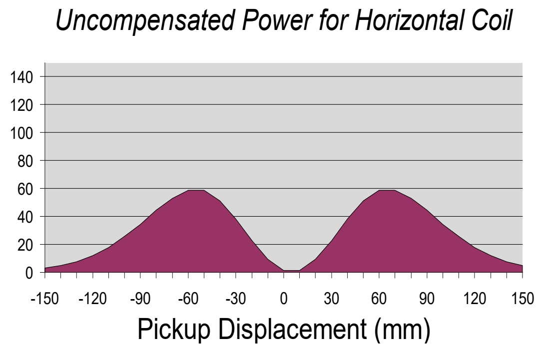

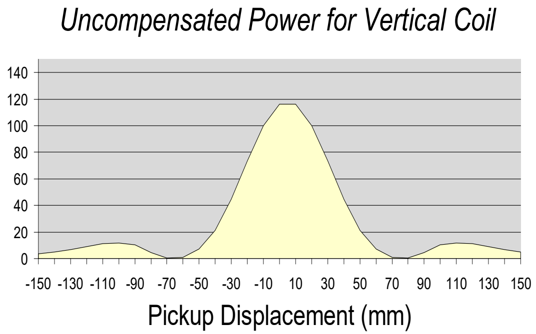

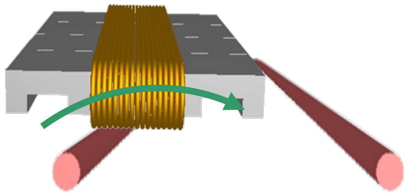

HORIZONTAL FLUX CAPTURE

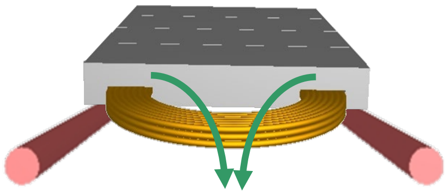

VERTICAL FLUX CAPTURE

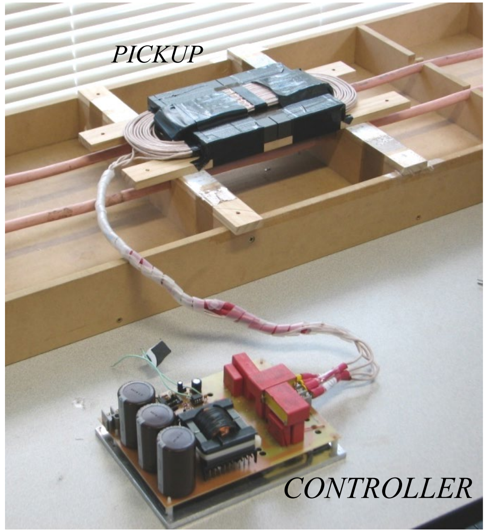

Reference [8],[18]-[20],[71]-[72]

Multiphase Tracks & Pads

- Combined multi-coil
  - Flatter power profile
  - 25-50% more power

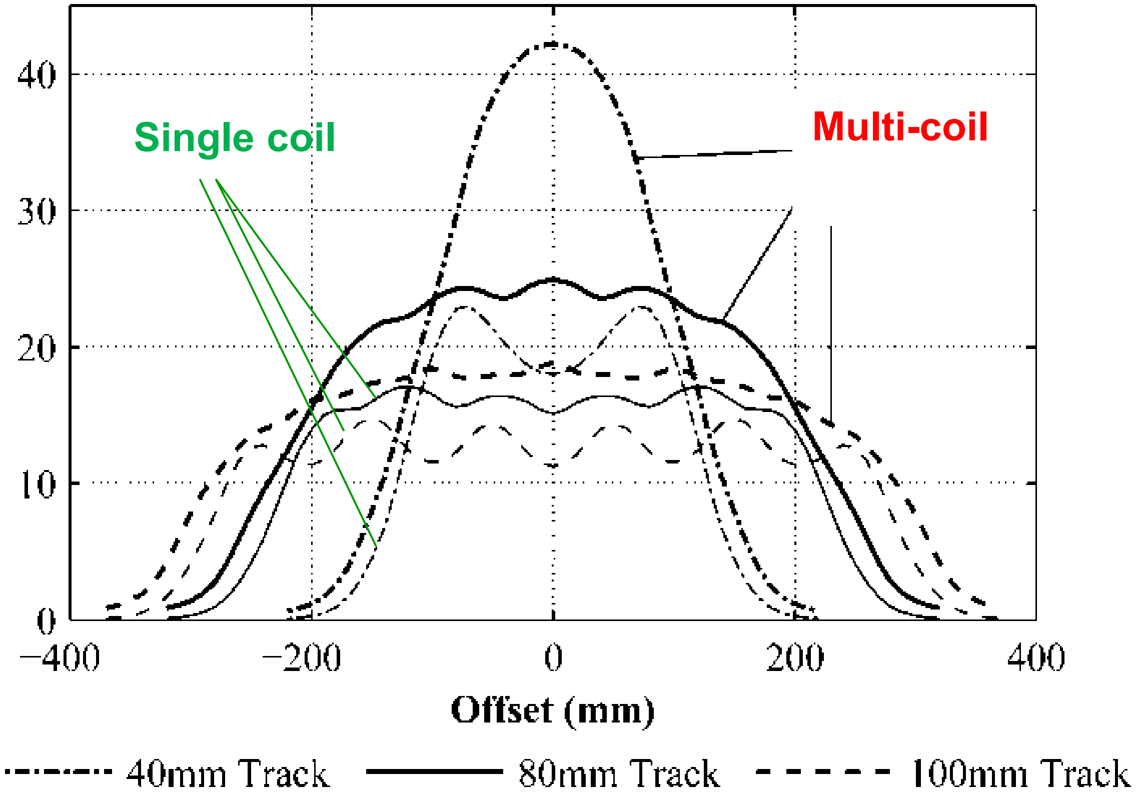

Reference [8],[18]-[20],[71]-[72]

Stationary EV Charging

Early systems

Mobility Vision

Autonomous, Connected, Electric and Wireless

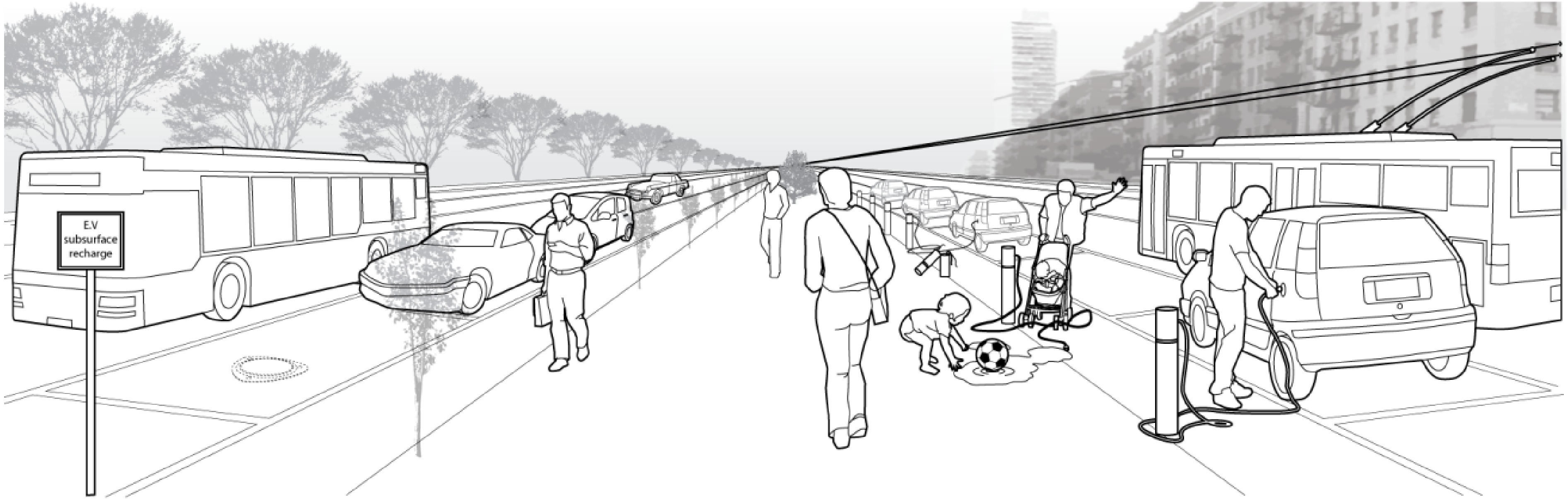

IPT street

Safe and Durable

Easy to use

Aesthetically pleasing

Conductive charge street

EV1 Battery Charger

Charging Paddle system

Autonomous Robotics

50W Chargers

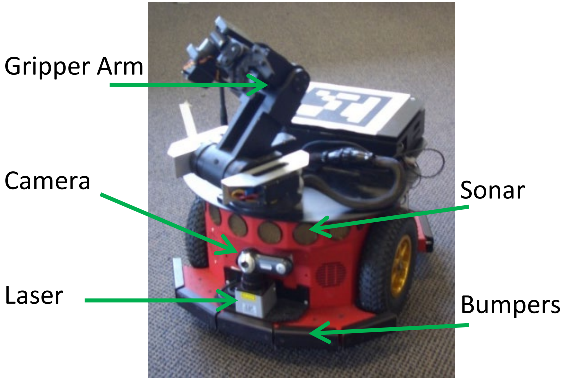

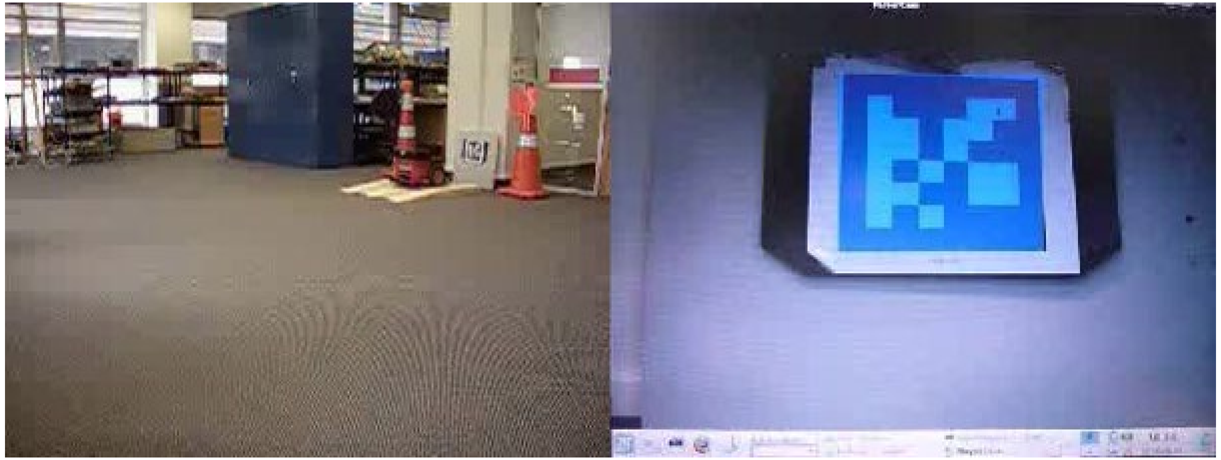

Wireless Charging as required

ID marker identifies
charger position

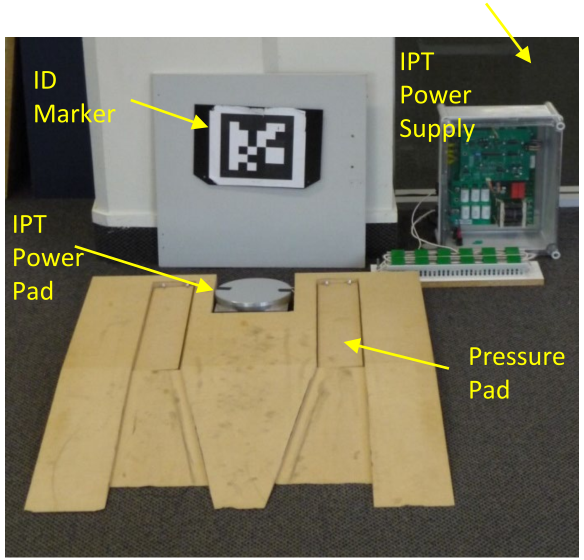

200W Shopping Basket Chargers

Power pad sited under trolley

Charging Station

Charging Mat in Walmart USA

IPT powered shopping baskets

People Moving (Mid-late 1990s)

IPT Technology (Conductix-Wampfler)


ipeNz

Arthur Mead Memorial Environmental Merit Award

Presented to

Wampfler Ag

for the application of environmental awareness to the solution of an engineering problem

People Mover at Maori Arts and Crafts Institute, Rotorua

Chairman

Secretary

June 1999

Date

Whakarewarewa Rotorua Charging Bay

- 5 buses with trailer
- 3 x 10 batteries of 12 V
- Charging: 7min /15-20 min
- Charging power: 20 kW

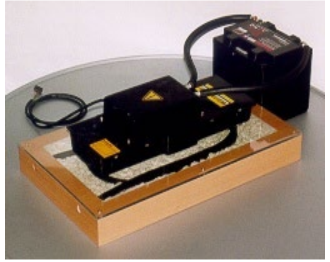

10x 3kW Pickups @ 14kHz

People moving (early 2000s)

IPT Technology (Conductix-Wampfler)

- 3 buses each with 56 x 6V Batteries
- Charging 60kW for 10 minutes/hour

Genoa, Porto Antico

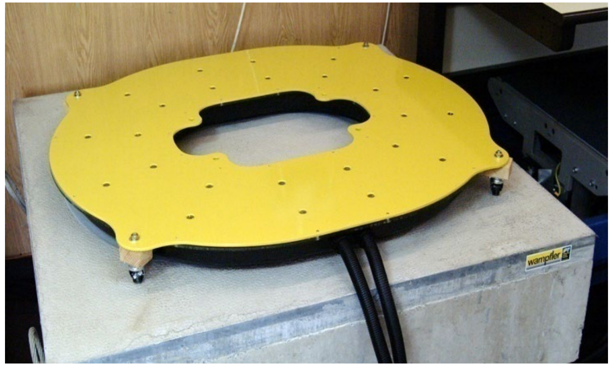

30kW Pickup 20kHz

Automotive: 2000's

Weil-am-Rhein

IPT Technology: Charging- discontinuous power transfer

- Primary side control and Hydraulic levitation
  - Communications system required
  - Only application for 1 to 1 application

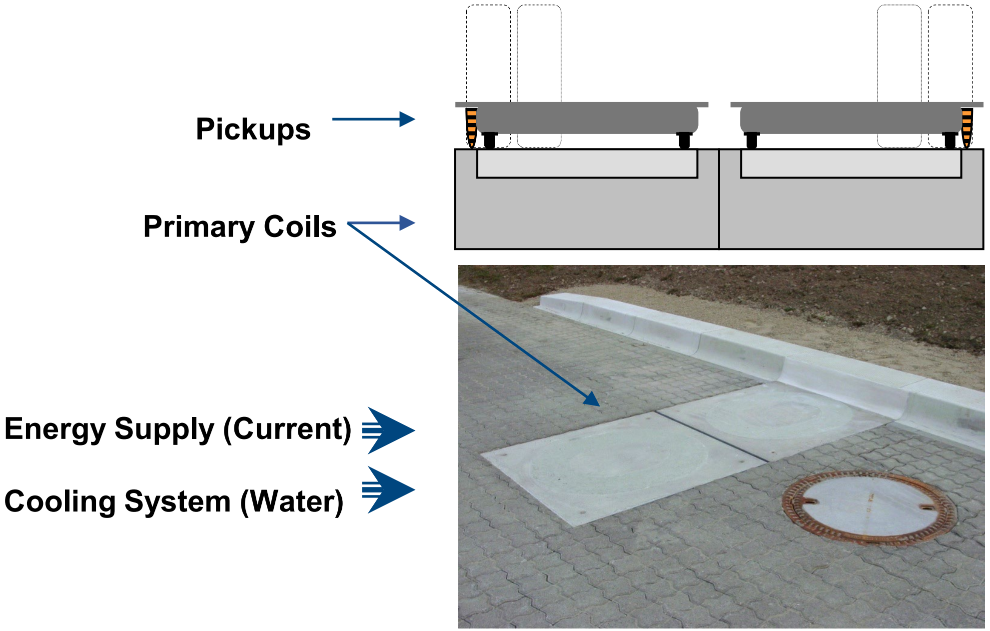

IPT Technology: 60kw Charging station
- 20% Duty Cycle
- 300/600V Output
- Nom. Distance to Ground: 30mm
- Tolerances: H/L +/-50mm; V +/-10mm
- IP 67 -20°C / +50°C
- 70 kg, 1025 x 875 x 61mm

Automotive: 2000's

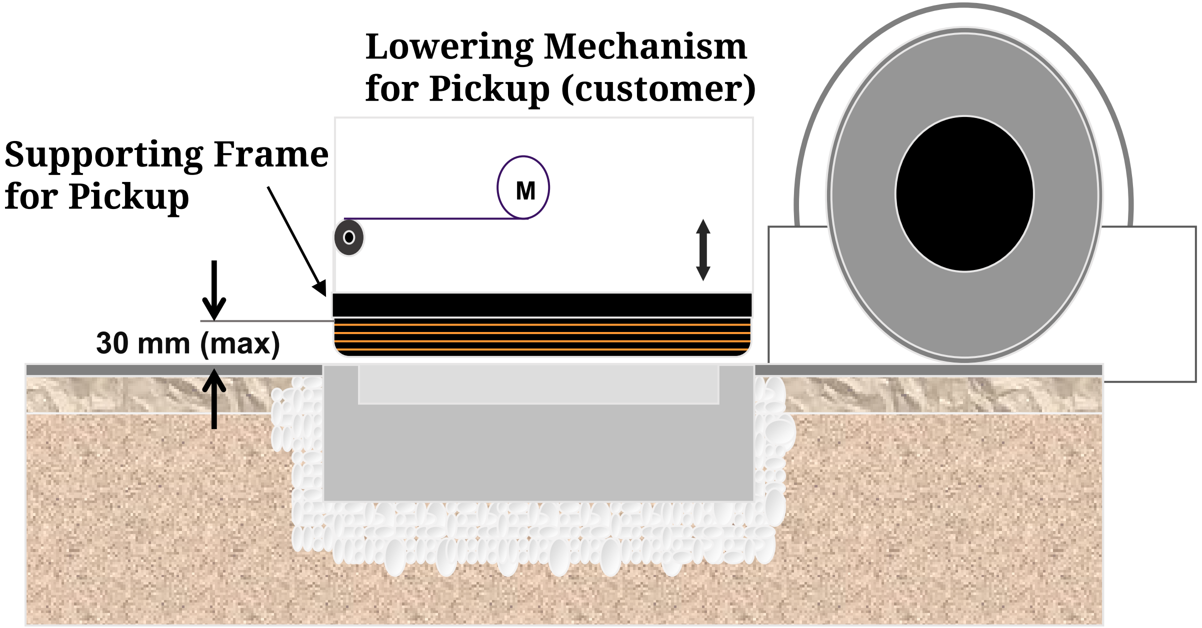

IPT Technology: Charging

Genoa, Porto Antico

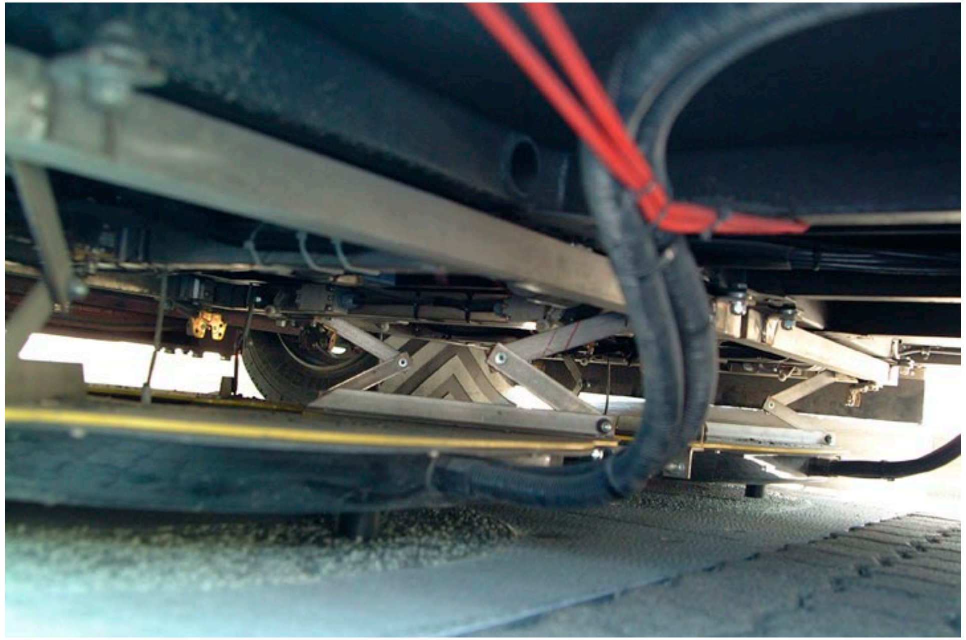

Automotive: Late 2000's – Greater Gaps Required

The EV Charging System

- Power Supply
- Ground Assembly (GA)
- Magnetic field
- Vehicle Assembly (VA)
- Data Transmission
- Controller
- Battery
- User Interface
- Multiple Ground Pads

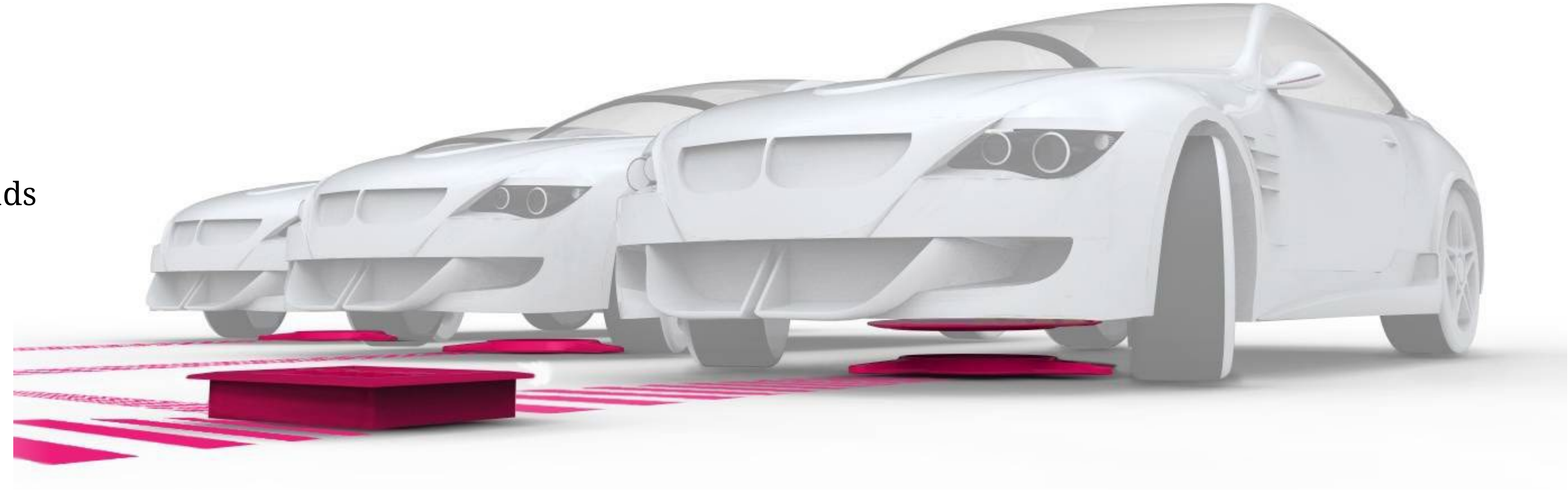

Pad development

Non polarised Couplers

Polarised Couplers

Multi-coil Topologies

Non-Polarised Couplers

Circular Non-polarized

Circular Q_L (~ 300 at 20kHz)

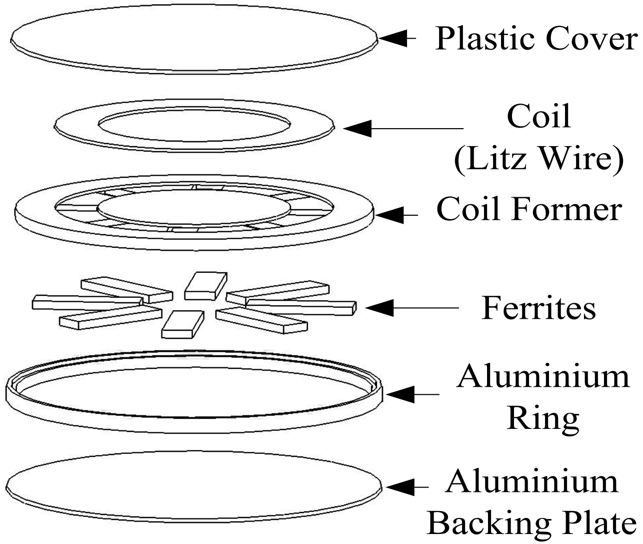

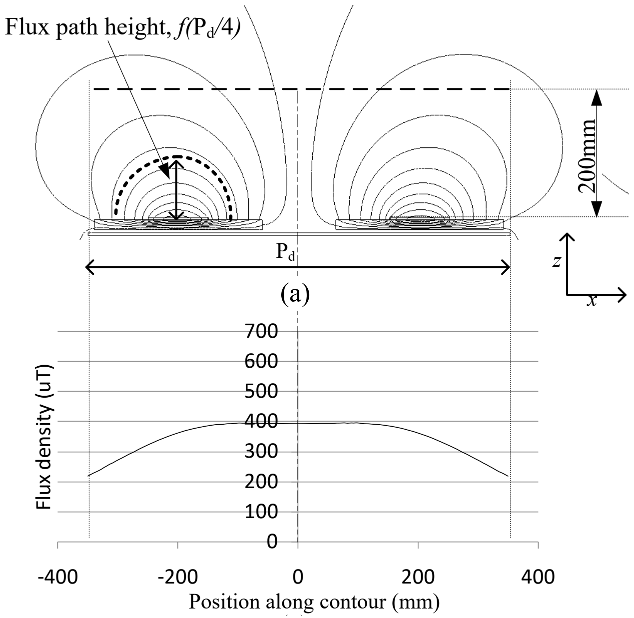

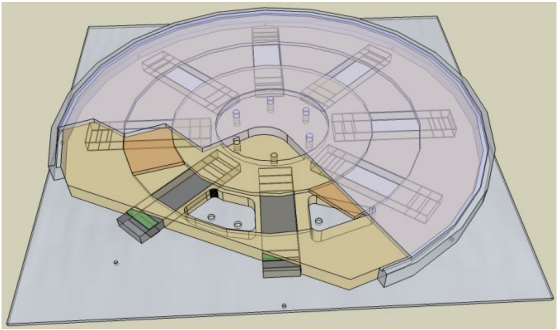

Reference [8],[21],[22]

Coupler Leakage & Shielding

Installation - EV chassis and field leakage considerations

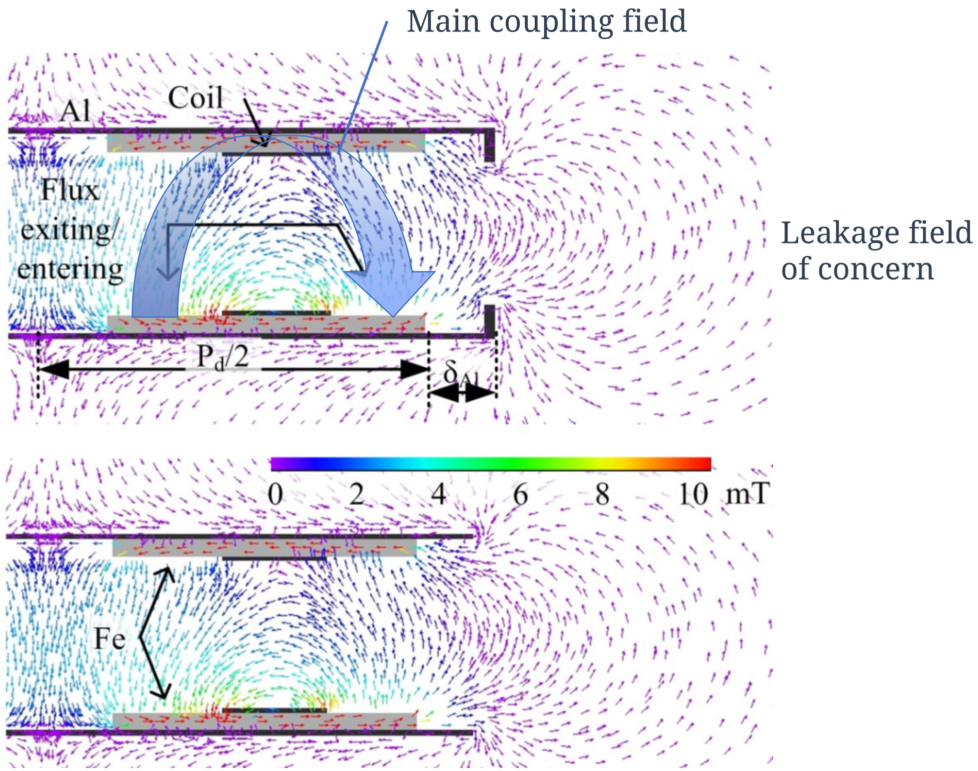

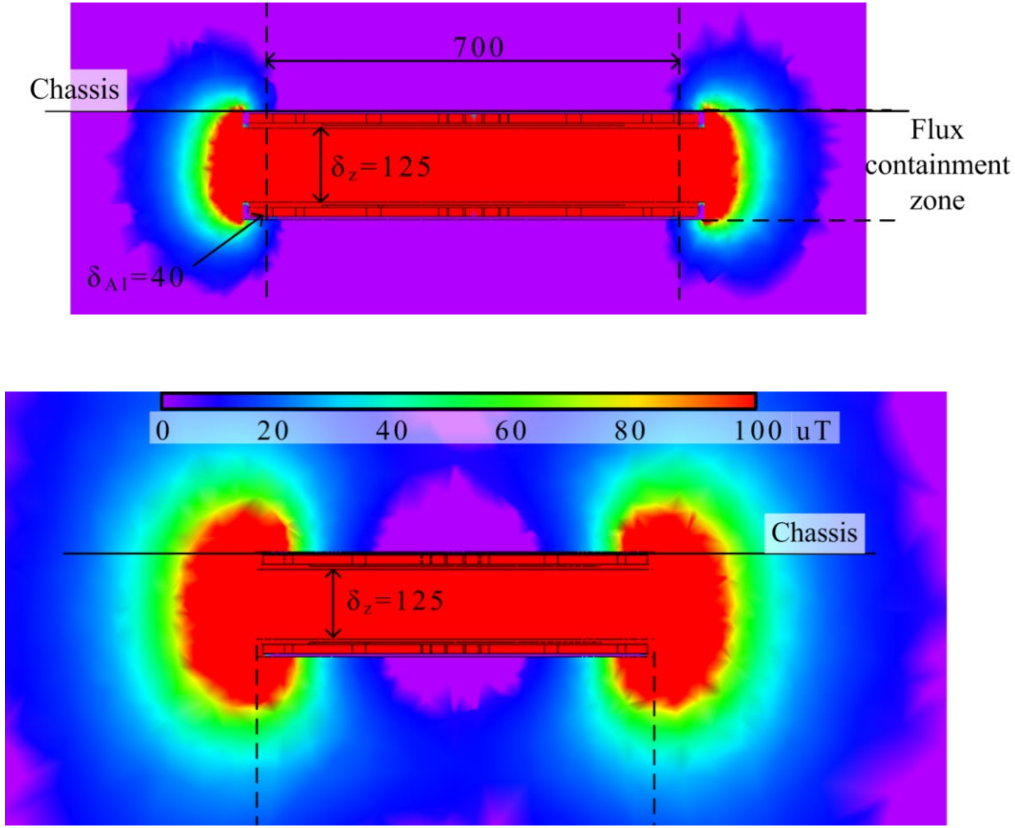

Reference [8],[21],[22]

Stationary Application

Power null (in all directions ~ 80% pad radius)

- good leakage control
- poor misalignment tolerance & challenging for dynamic

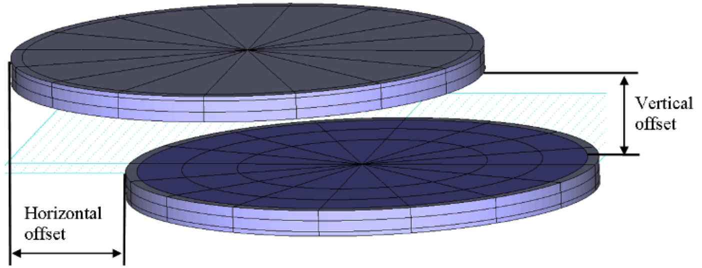

$$P_{su} = k^2 VA_1$$

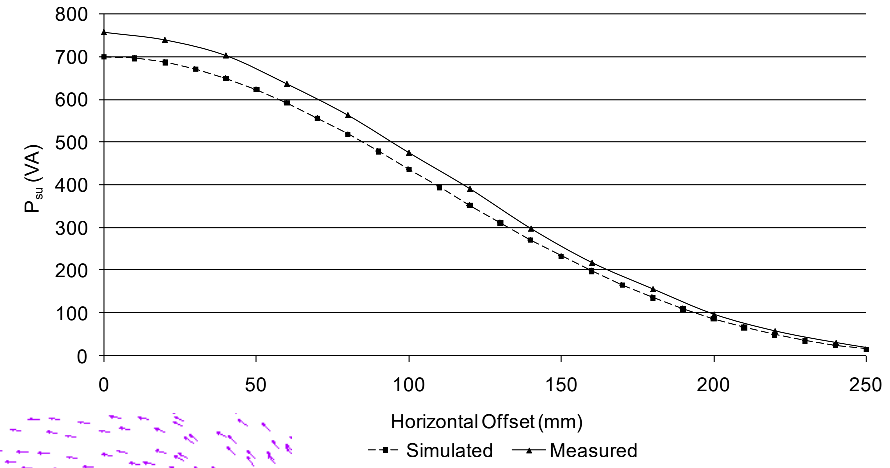

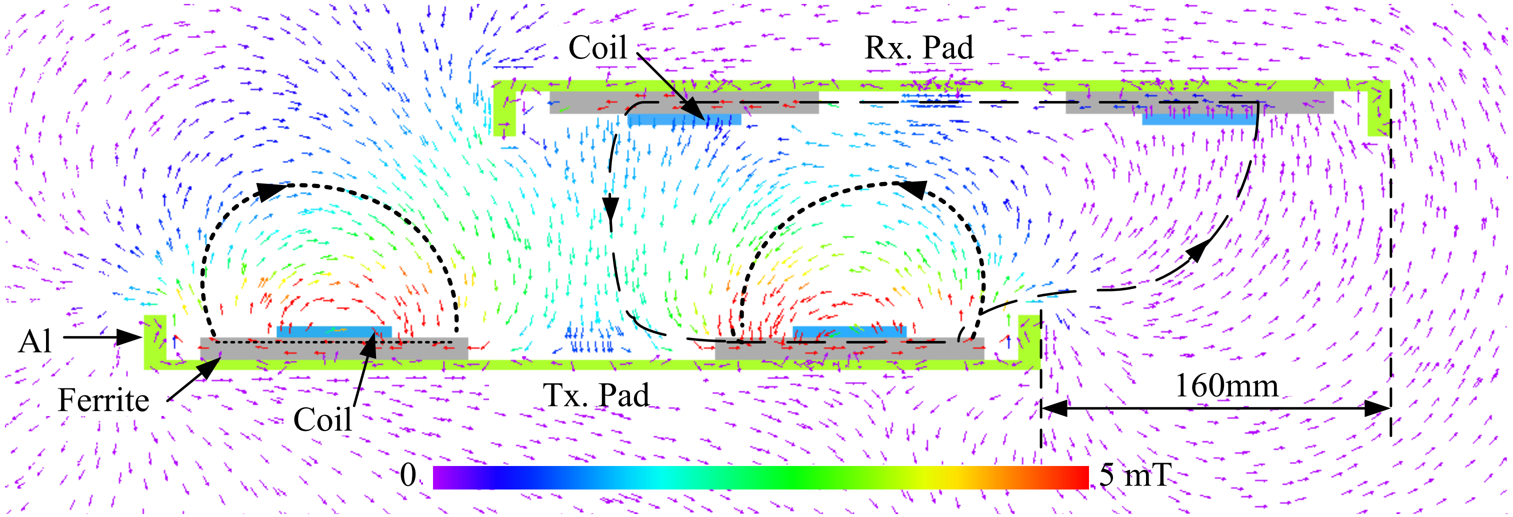

Reference [8]

Fe-less LC Reflector

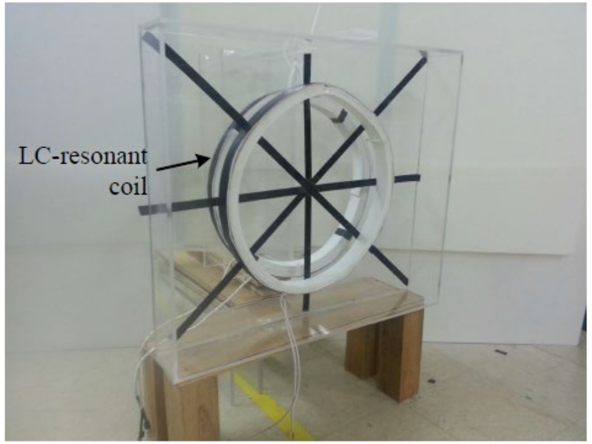

Fig. 9. A prototype fabrication of MFS using the LC-resonant coil.

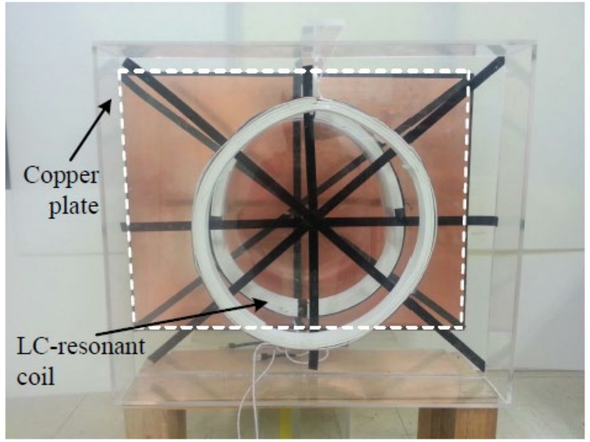

Fig. 10. A prototype fabrication of MFS using the combination of the conductive plate and LC-resonant coil.

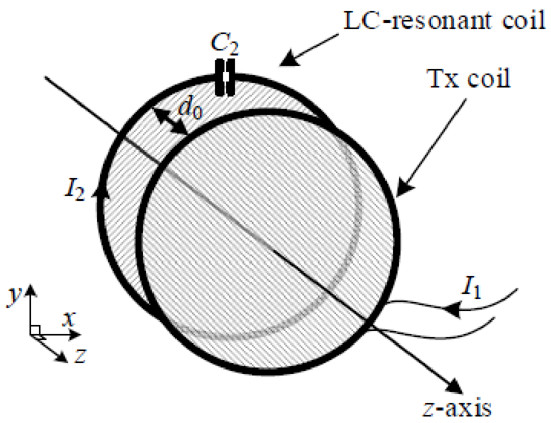

(a) MFS utilizing the LC-resonant coil.

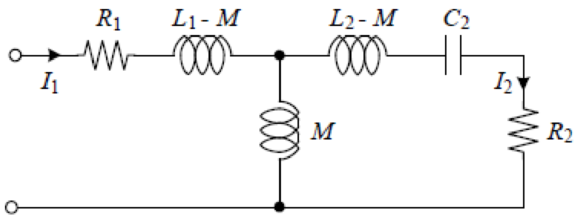

(b) Simplified equivalent electric circuit.

Fig. 4. MFS utilizing the LC-resonant coil and its equivalent electric circuit.

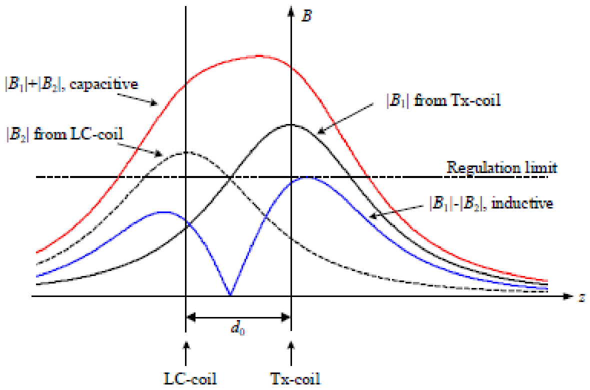

Fig. 5. Magnetic field density profile with MFS utilizing LC-resonant coil.

Reference [33] C.T. Rim

Ferrite-less Circular Primaries

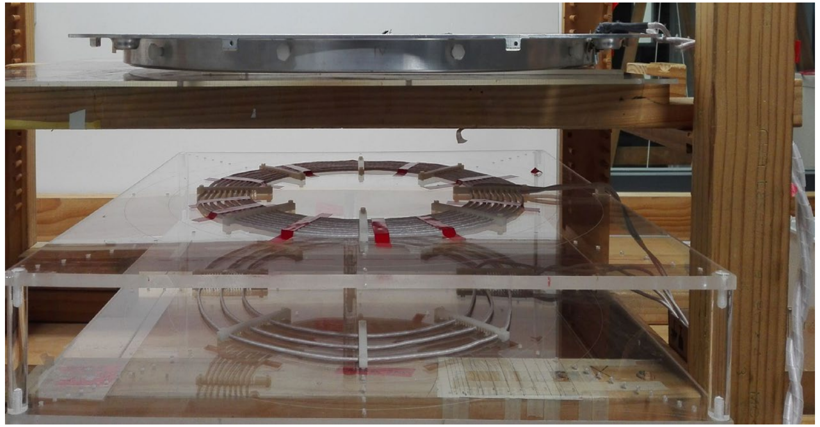

CP Secondary offset: X=150mm, Z=150mm

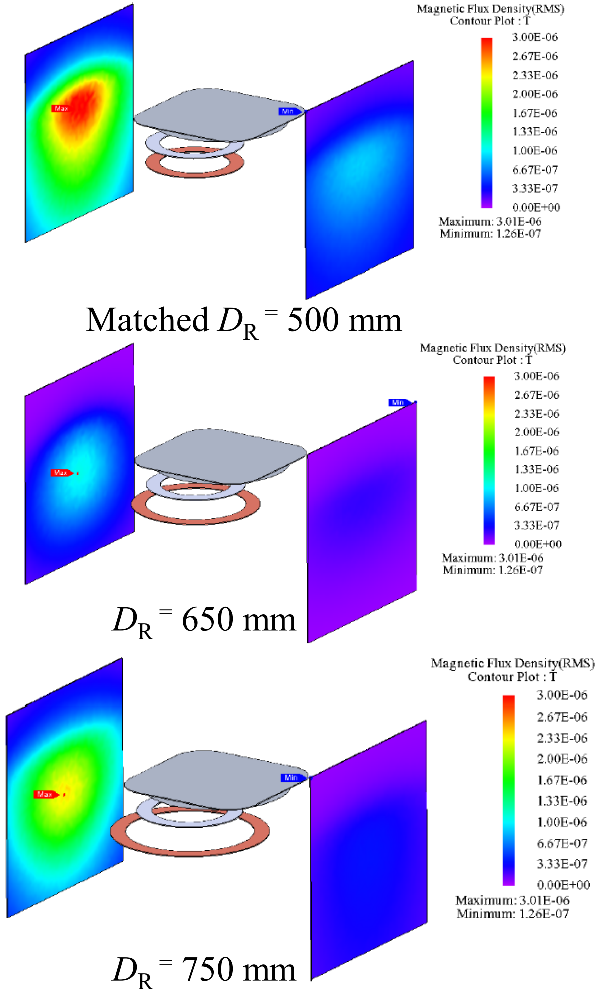

Anti-wound (reflection) coil 1/3 the turns ratio

Reflection coil ~30% larger has excellent leakage

Coupling factors typically 2/3rds require 2.3x VA

Reference [26], [33]

A Demonstration System at EVS24

2kW IPT Charger

Vehicle controller

Charger: 2kW single phase supply

220mm airgap

Polarised Couplers

Polarised Designs: Solenoid

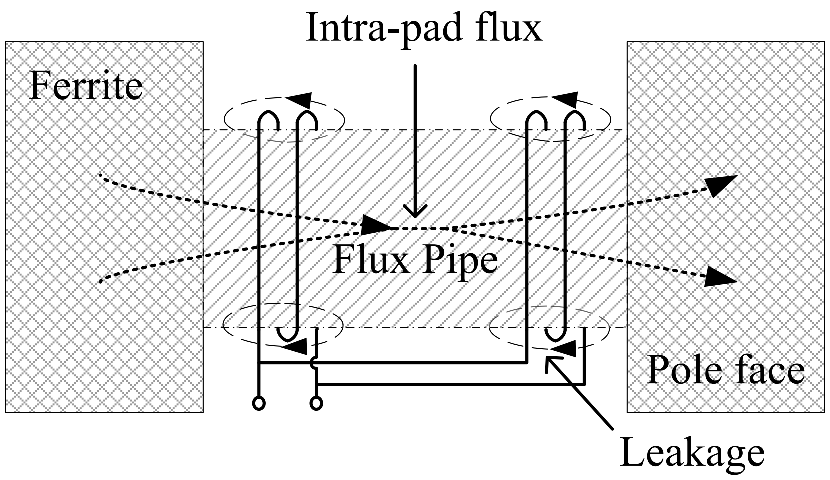

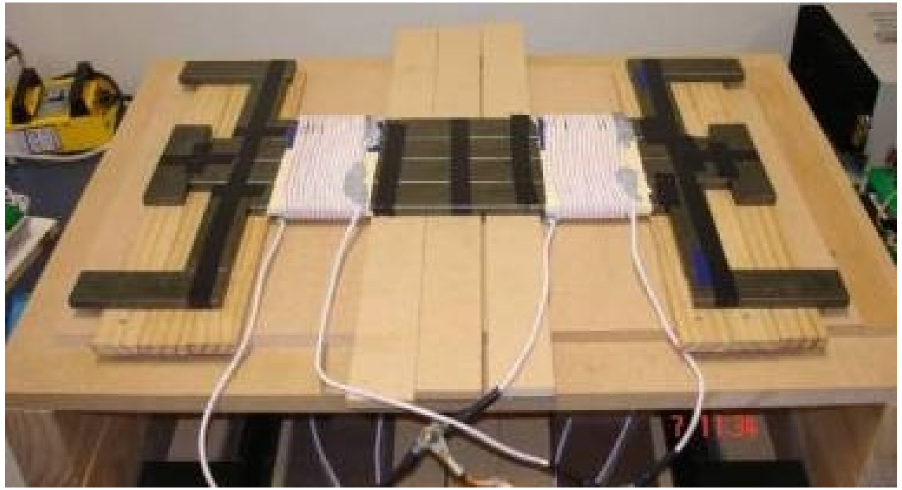

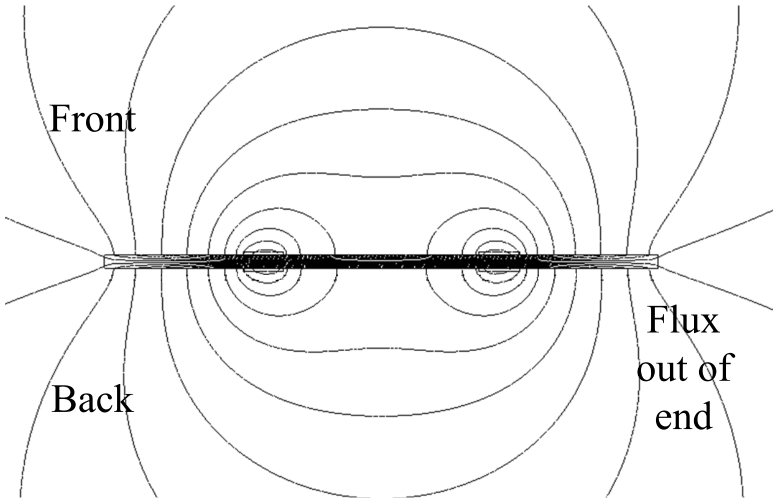

Flux pipe:

- encourages pole separation
- flux path has greater height

Issues:

- Fields on both sides & ends
- Hard to control leakage

Reference [8],[22]

Circular vs. Solenoid Coupler

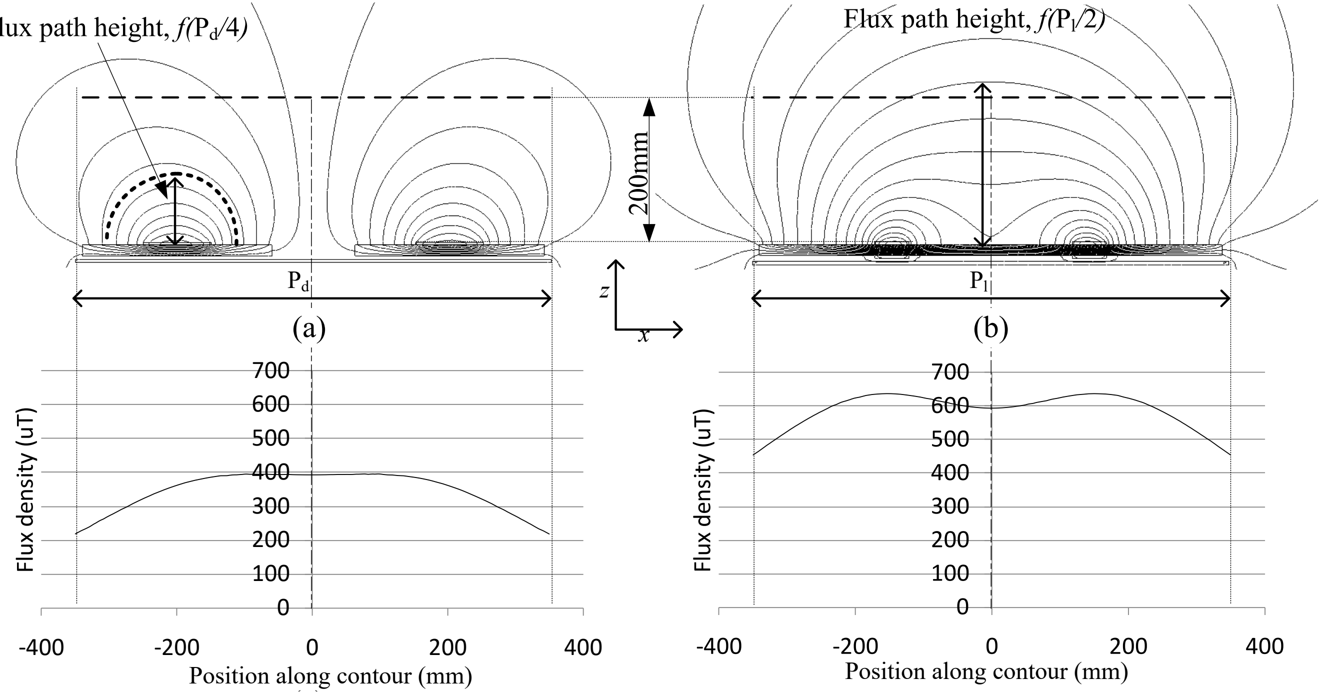

Circular Q_L (~ 300 at 20kHz)

Solenoid aluminium shield creates large losses

I_1 = 23A/coil at 20kHz

- Q_L without shielding is 260
- Q_L with shielding is 86

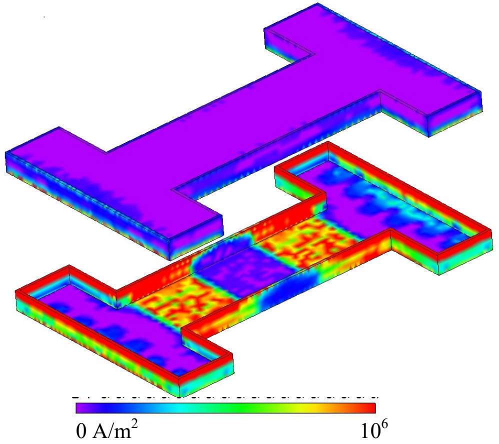

Reference [8],[22]

Improving the Magnetic Design

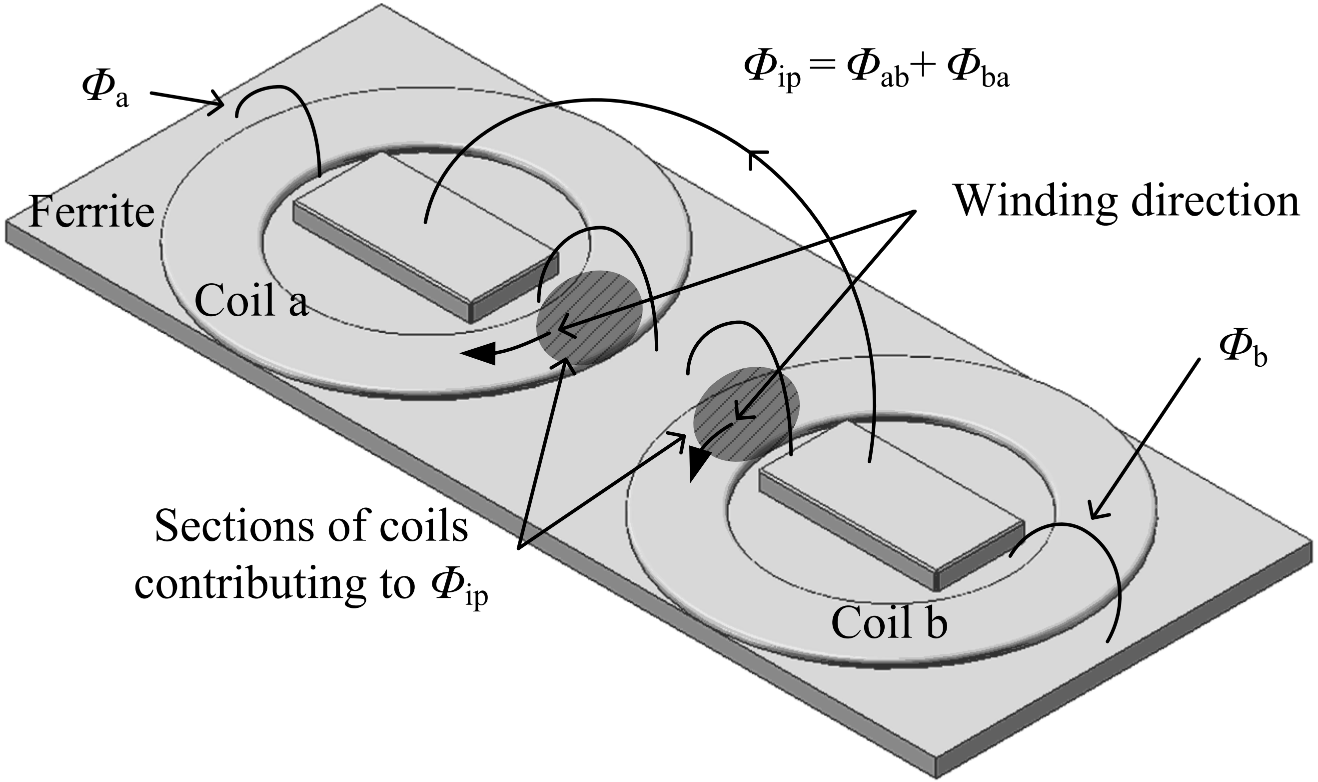

Equipotential surface

Polarised DD

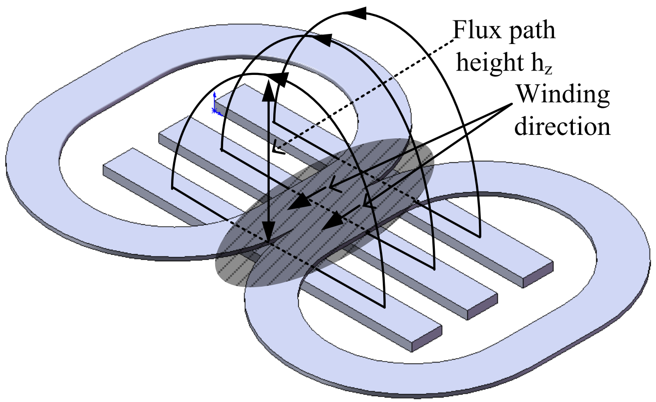

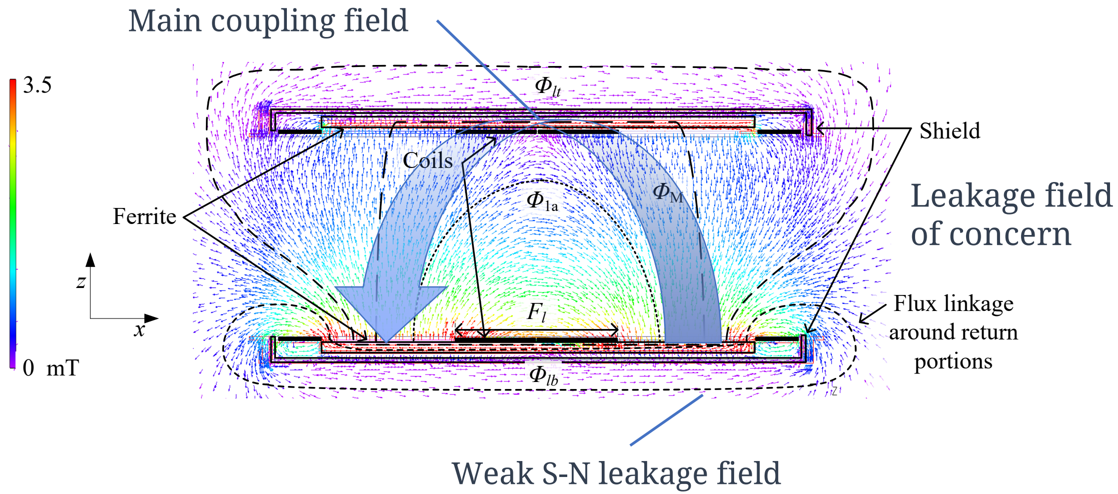

Ferrite strips:

- Reduce material and inductance

Coil winding:

- Creates a flux pipe (minimised winding length)
- Single sided flux paths with height ~ *pole seperation*/2

Q_L ~400 at 20kHz

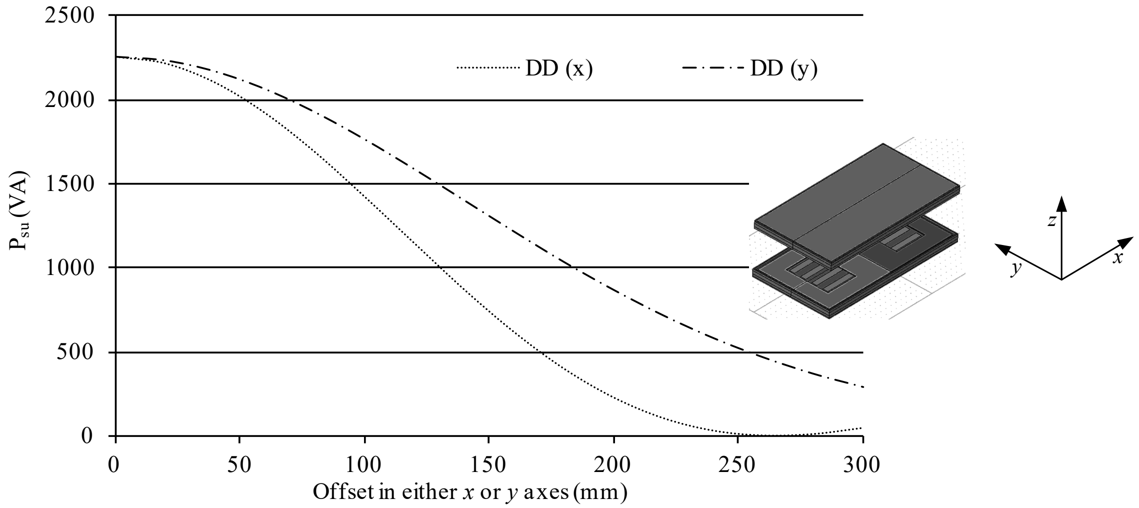

Performance with lateral offset

Reference [8],[22]

Ferrite-less DD Primaries

(a) Ferrite & Aluminium DD (b) Ferrite-less DD (c) Reduced ferrite DD

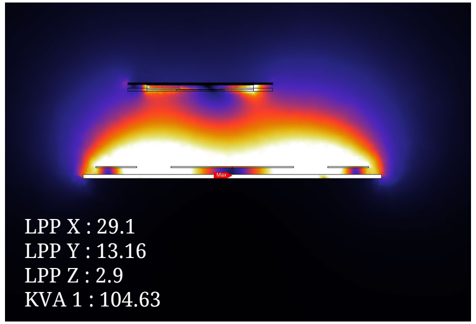

Main coil (640 x 460)
28 ferrite blocks

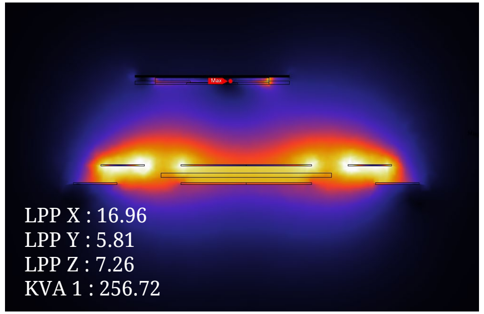

No ferrite
Reflection coil (760 x 520)

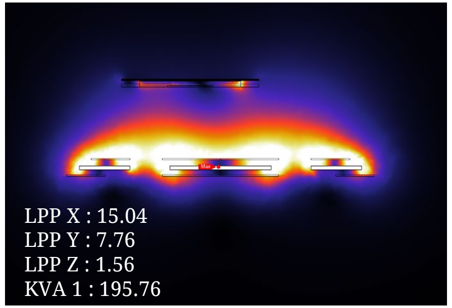

4 blocks ferrite 125x100
Reflection coil (760 x 520)

Anti-wound (reflection) coil 1/3 the turns ratio & ~30% larger
Ferrite-less coupling factors typically 2/3rds require 2.5 x VA
Partial ferrite coupling factors ~75% require ~1.9 x VA
Leakage can be lower!

Reference [53], [54]

Simple Coil Comparisons

For similar: Pad Areas & Inductances
Driving VA & Frequency
Secondary VA

Transfer height d/4

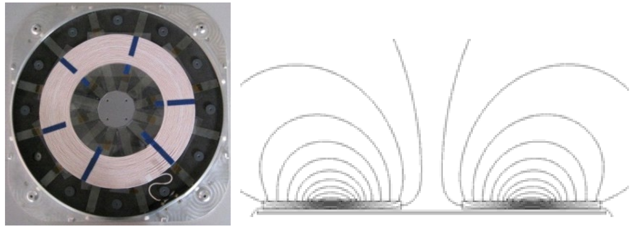

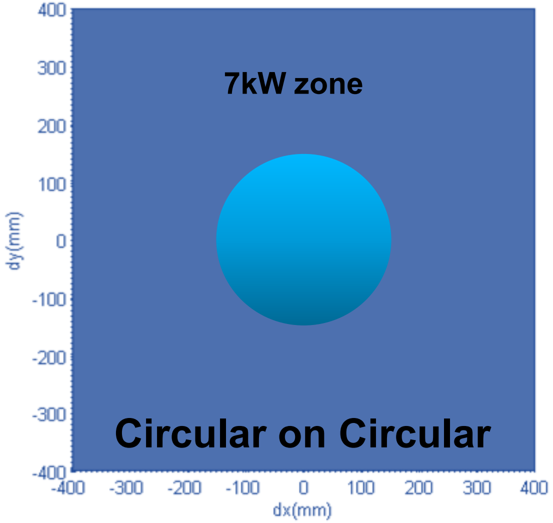

Leakage naturally constrained with external pole

7kW output at 125mm

Charging Area
Circular < 2 x Polarised

Transfer height ~d/2

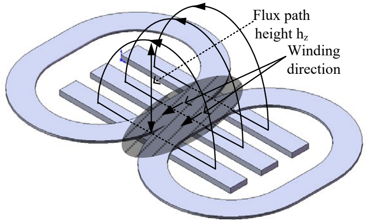

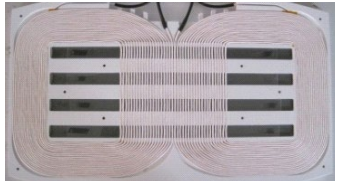

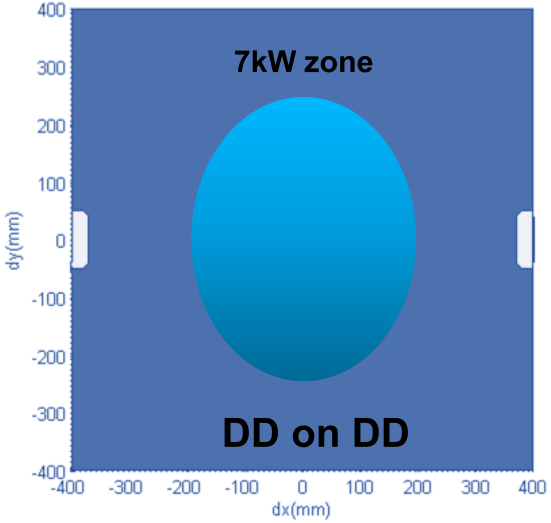

Tolerance v.s. higher leakage due to auxiliary poles

Reference [8],[22]

Interoperability (7 kW)

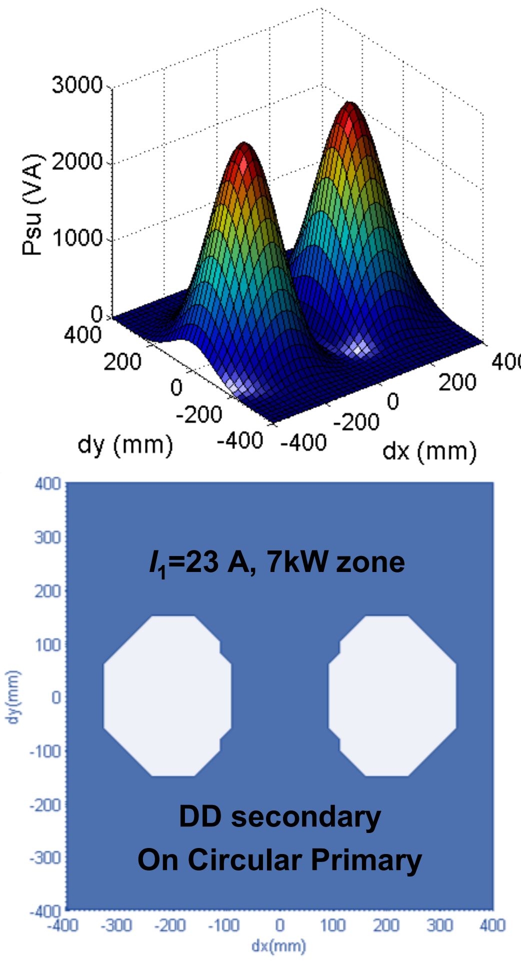

$$P_{su} = k^2 V A_1$$

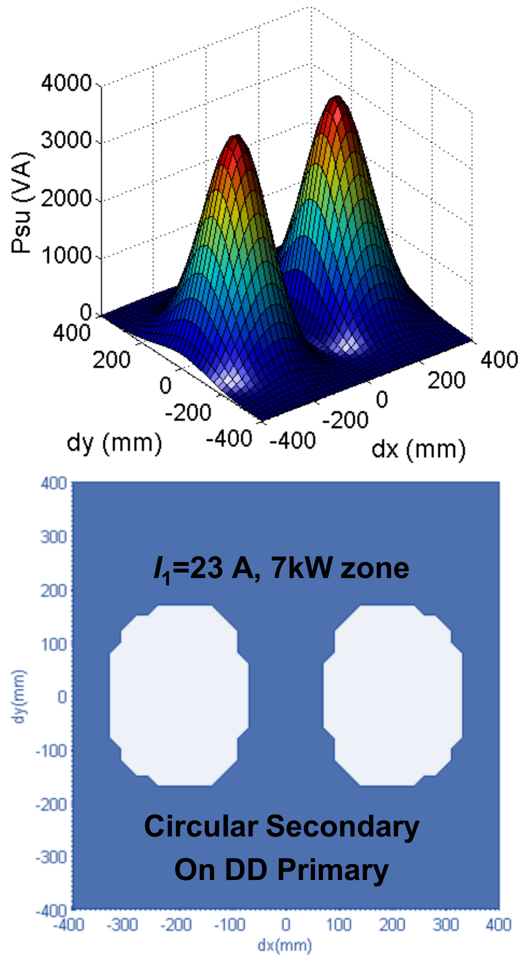

Reference [8],[22]

Evolution of Systems

Developed with HaloIPT 2010
Rolls Royce Phantom 102Ex

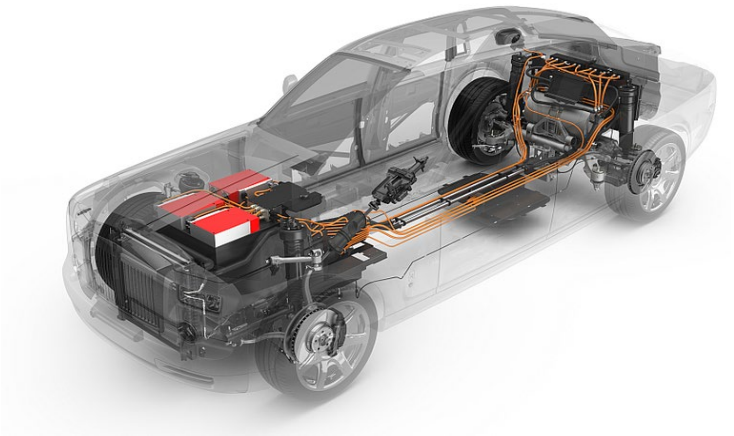

7kW charge system > 90% Efficiency

Courtesy of Qualcomm

Product ready with Qualcomm

11kW > 90% Efficiency

Future Systems with WiTricity
Power demand shifting upwards

SAE J2954 Compliance

Light Duty

Future LD and HD status

HD Considerations

SAE J2954 targets full Interoperability

- A test station is used for validation
  - Universal Ground Assembly (UGA)
  - Test station Vehicle Assemblies (VA) (WPT1-3, Z1-3)

- Classifications:
  - Public GAs: Class I
  - Private GAs: Class II

- Product Testing:
  - Class I GAs at all power and Z ranges with all test VAs
  - Class II GAs up to rating & over specified Z range with relevant VAs
  - Vehicle systems over their designed airgap on the UGA

- All systems tested:
  - ΔX: ± 75mm, ΔY: ± 100mm, Roll/Pitch: 2°, Yaw: 3°.
  - Over typical battery range (DC 280-420V) on test VAs
  - Must comply with EMF ICNIRP/Pacemaker leakage when powered
  - Must meet EMC Limits (82.8 dBuA/m in 79-90kHz band)
  - Must use communication sets (J29847-6), except proprietary VAs
  - Must not heat specified foreign above 80°c in 60s

Reference [59]

SAE J2954 Interoperability

THE UNIVERSITY OF AUCKLAND
Te Whare Wānanga o Tāmaki Makaurau
NEW ZEALAND

System Efficiency Targets:

AC Mains to Battery – matched systems deployed > 90%

Product VAs
- tested at full power must be ≥80% over all X,Y,Z range
- ≥85% when centred in the middle of the nominated Z range.

Class I (Public)
- Minimums at rated power of test VA

WPT Class of Test VA	At Centered Position	In Alignment Tolerance Area
WPT1	80%	75%
WPT2	82%	77%
WPT3	85%	80%

Class II (Private/Fleet …)
- Minimums at rated power of test VA

WPT Class Difference of Test VA	At Centered Position and Over Alignment Tolerance Area
Same Power Class	80%
One Power Class Difference	77%
Two Power Class Difference	75%

Reference [59]

Future Light & Heavy Duty Vehicle Status

- LD Future Power levels from 20 - 60kW planned for taxi etc.
  - WPT4 22kW, WPT5 60kW
  - Vehicle side magnetics are made small and designed for raised primary
  - Flush mounted designs for public deployment

- HD under development
  - Focus on output power 20-500kW ideally with 90% efficiency
  - Flush and buried mounted magnetics
  - Often matched designs with vehicle systems twice size of LD
  - Parking Zones (±100mm, ±100mm)
  - Leakage limits same
  - Safety in managed parking can use cameras and qualified personnel

WPT 4 & 5 Systems ...

Cambridge & Warwick (50kW)

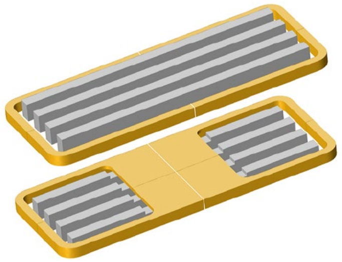

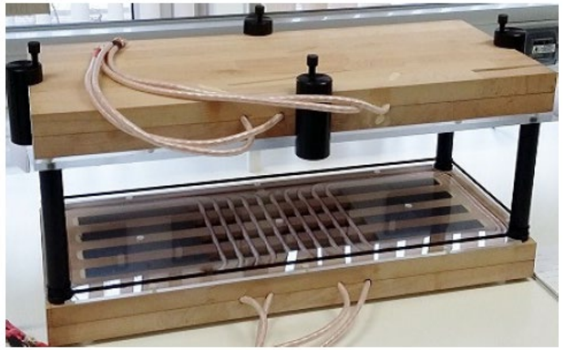

Fig. 4. Photo of constructed full-size WPT pads

ORNL

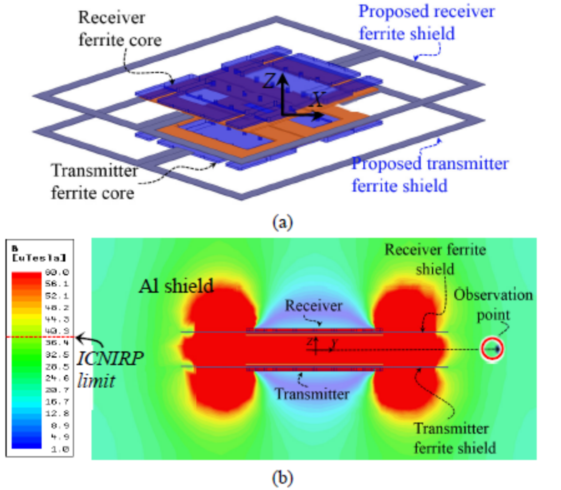

Fig. 8. (a) Proposed magnetic shield using the ferrite bars and (b) resulting peak flux density distribution on the YZ plane showing that the EMF emissions have been reduced below the ICNIRP limit.

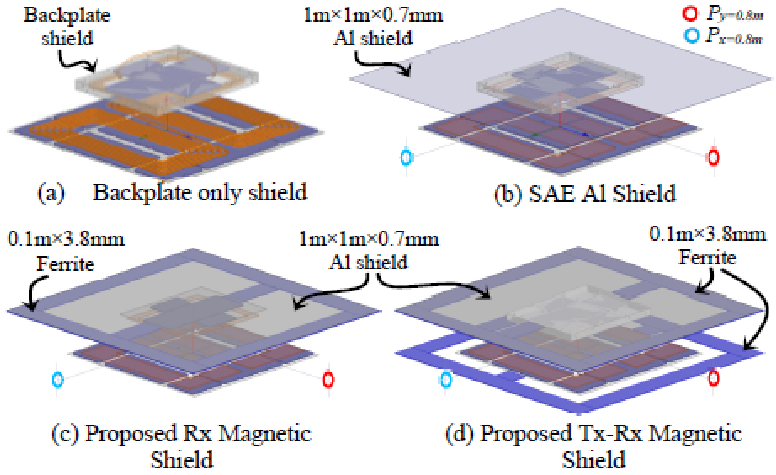

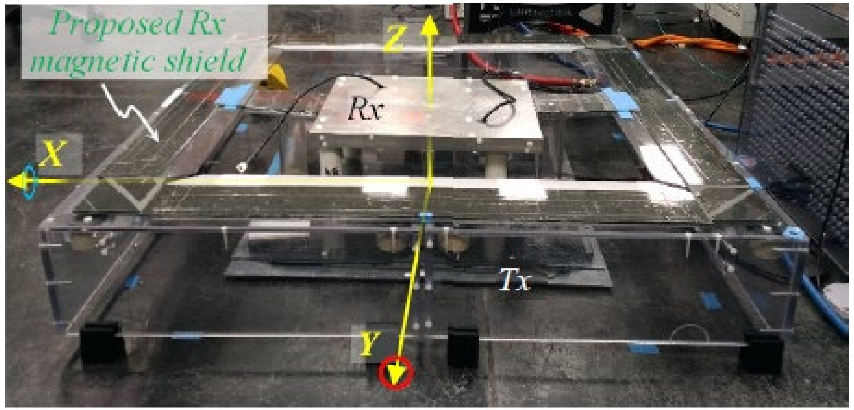

Reference [50,51]

Ferrite and Wiring Considerations

Flux crowding (partial saturation) influenced by:

- Ferrite Grouping & chosen Spacing
- Wiring and exits

50 kW Prototype

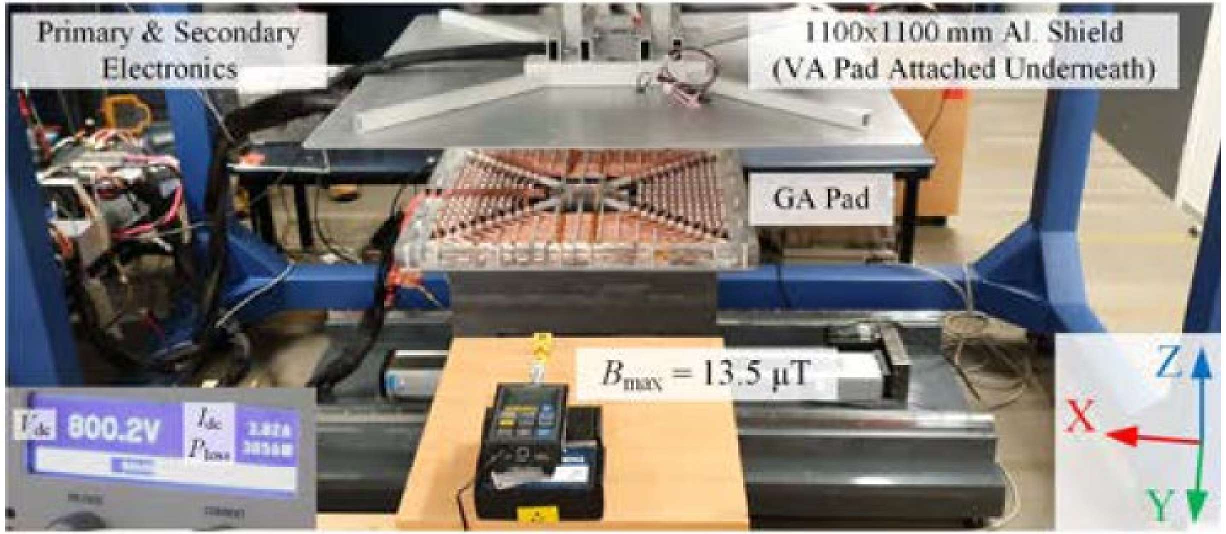

Reference [64]

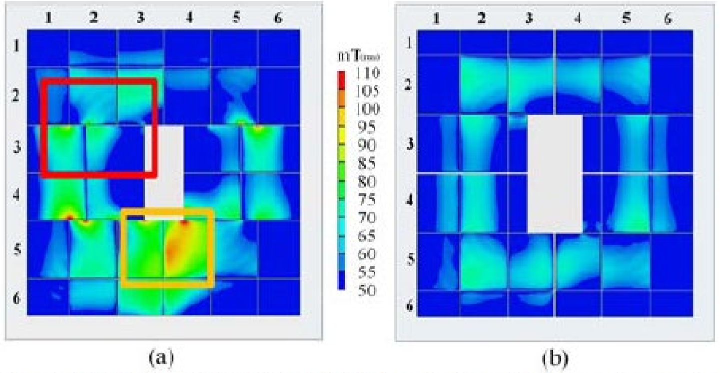

Fig. 5. (a) Mk1 and (b) Mk2 50 kW GA prototype FEA |B| contour plots.

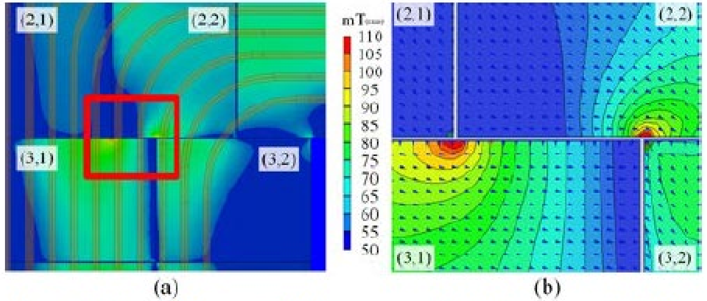

Fig. 9. (a) Top left region of Mk1 prototype FEA |B| contour plot. (b) Closeup of red outlined region with overlaid B vector plot.

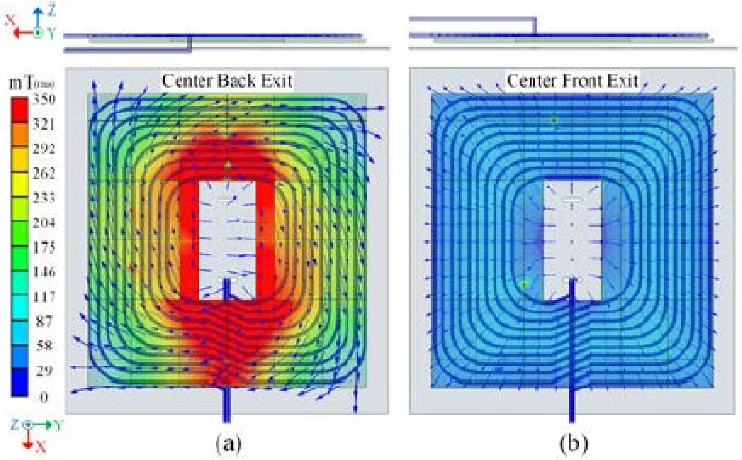

Fig. 12. (a) Top and side view of 50 kW Mk2 GA when coil exits through the back. (b) Coil exits through the front. B vector plots shown

FOD Considerations

- Surface flux using Ultrasonic or impedance measurement
  - Detection objects directly on GA pad surface during charging
  - Metallic Foreign Objects (MFO)
    - Paper clips, Nails, Coins, Cigarette Packets
- Living Foreign Objects (LFO) - ultrasonics or capacitive
    - Pets, Small Children
- Field levels for humans <15uT, small objects to avoid heating (mT)

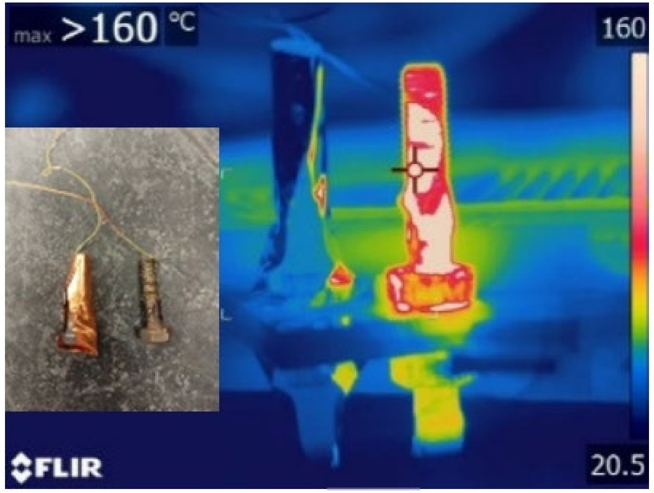

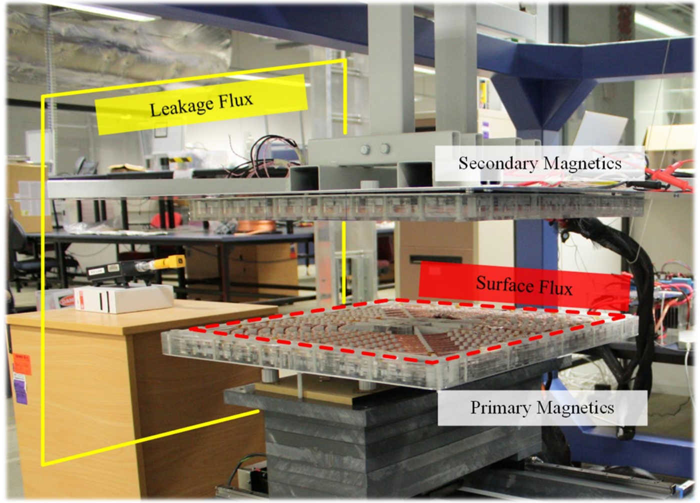

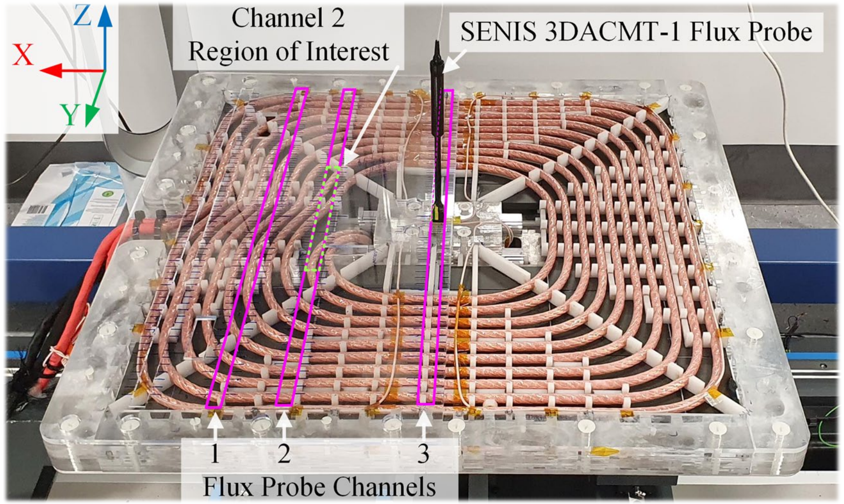

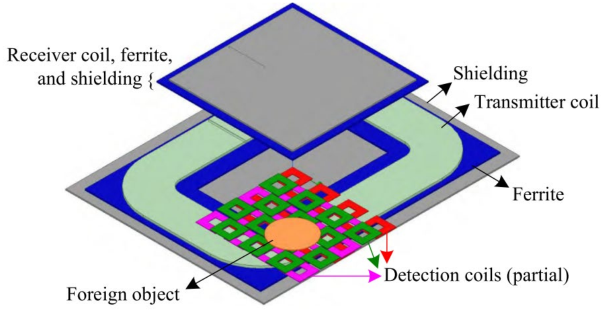

Fig. 9. A detection coil set in a WPT system.

Reference [61,62,63]

What are decoupled coils?

References [22]-[25]

Mutual decoupling

- Overlapped coil sees B in two opposing directions
- Overlap size & field strength determines the degree of mutual coupling

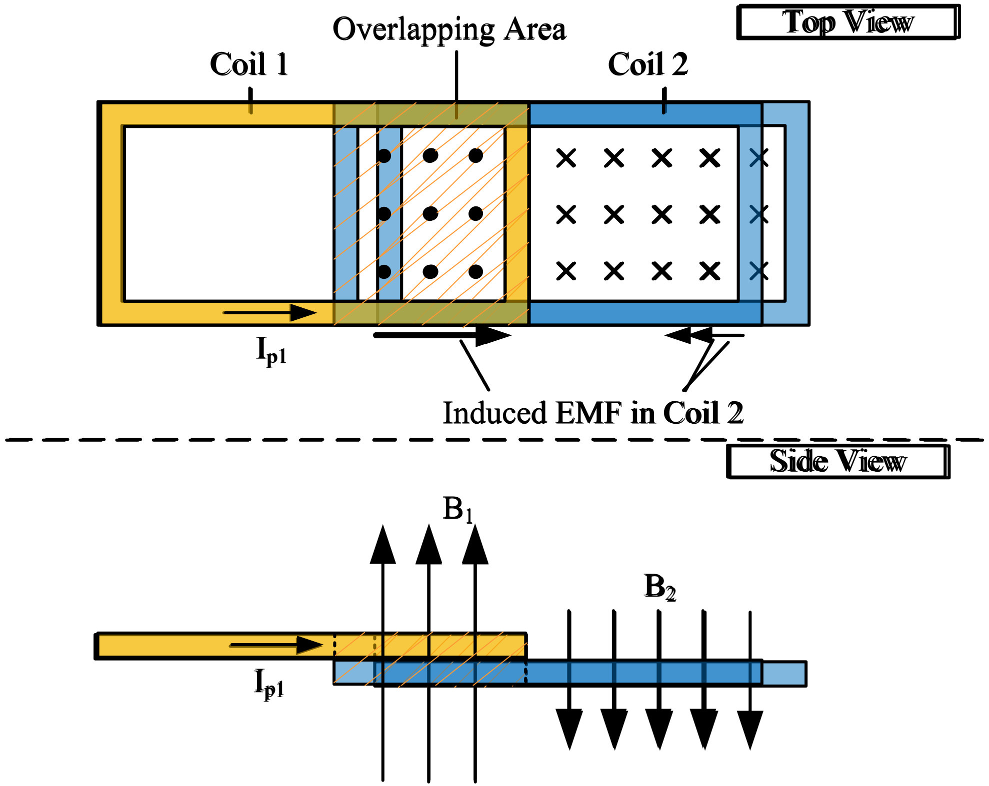

Mutual Decoupling

Minimizing mutual coupling between the primary coils

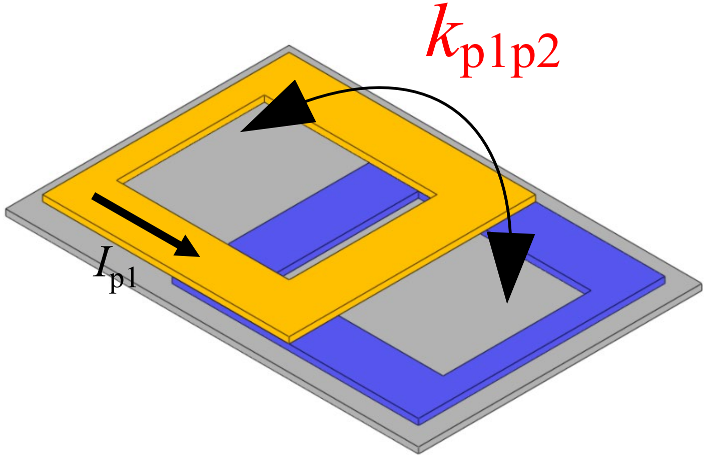

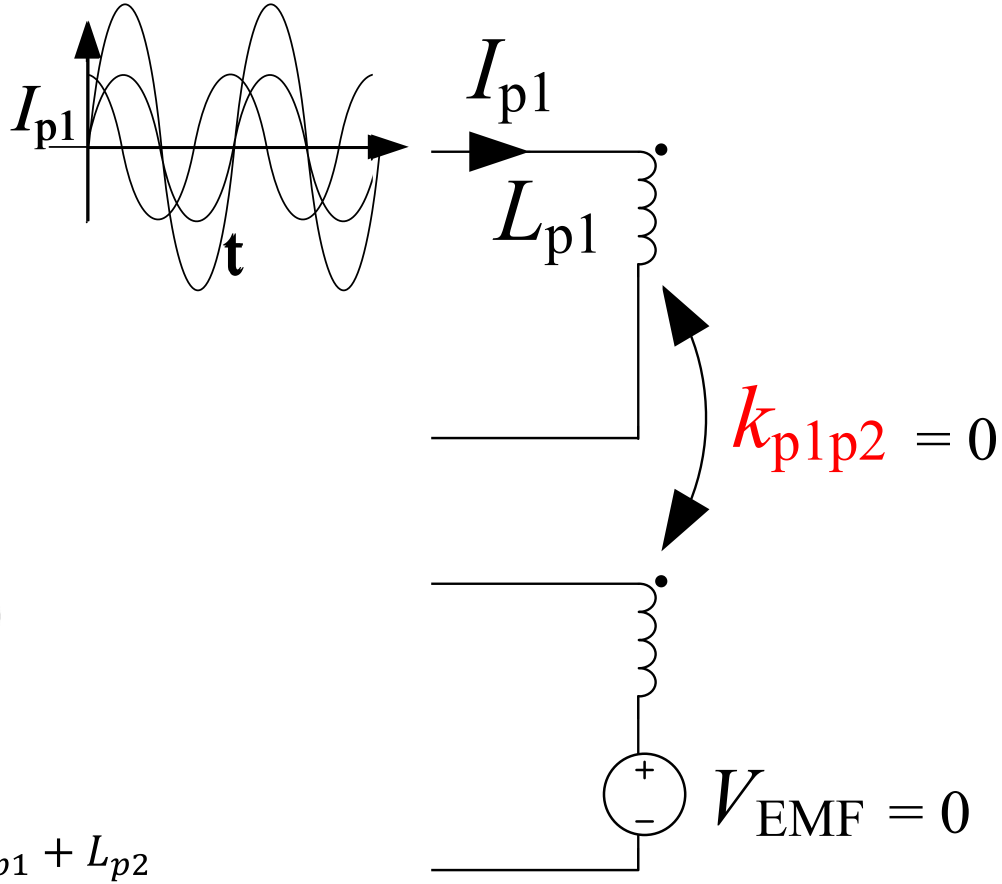

$$L_{ptotal} = L_{p1} + L_{p2} \pm 2M_{p1p2} = L_{p1} + L_{p2}$$

Multi-Coil Primaries

Single sided combining non-polarized & polarized

- Increase local coupling
- Improve interoperability
- Enable higher power with lower leakage
- Better ferrite usage
- Increased system complexity

DDQ or Bipolar Primary Driving Circuit

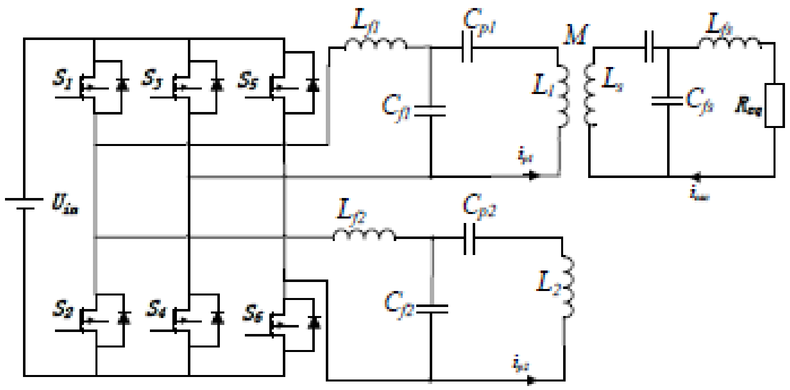

Fig. 5 multiple legs inverter with LCC topology

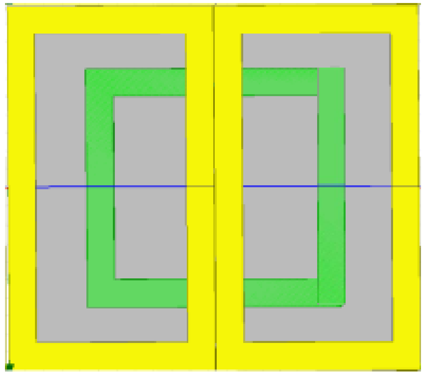

Fig. 2 DDQ coupler

Chonqing University, China

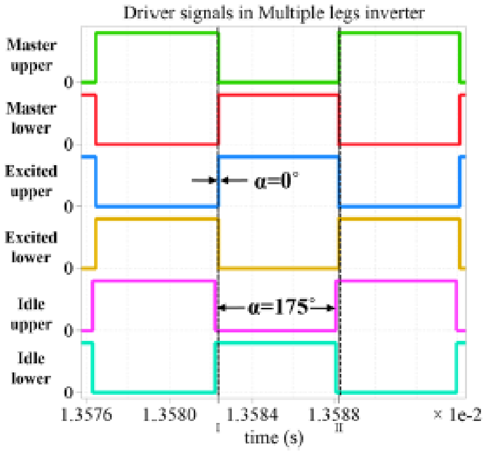

Fig. 6 Driver signals for multiple legs inverter

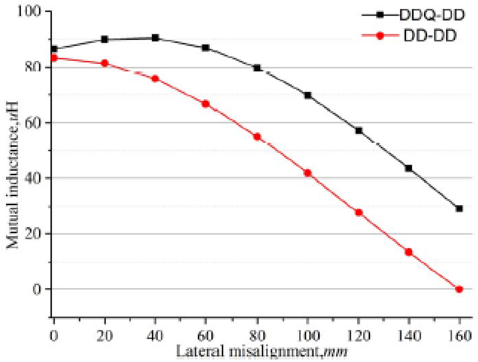

(a) Comparison with the mutual inductance variation between DDQ to DD coils and DD to DD coils
(Sample A:primary coil DDQ, secondary coil DD,
Sample B: primary coil DD, secondary coil DD)

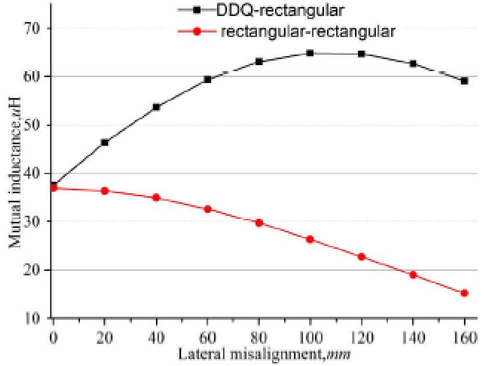

(b) Comparison with the mutual inductance variation between DDQ to rectangular coils and rectangular to rectangular coils
(Sample C: Primary coil DDQ, secondary coil rectangular,
Sample D: primary coil rectangular, secondary coil rectangular)
Fig. 3 Mutual inductance variation with different couplers and lateral misalignment

Reference [32]

Leakage flux control of BPPs

Severe misalignment (250mm)

Both BP coils vs. powering only the best coupled coil

Using 1 BP coil shows lower primary VA with better power out and lower leakage

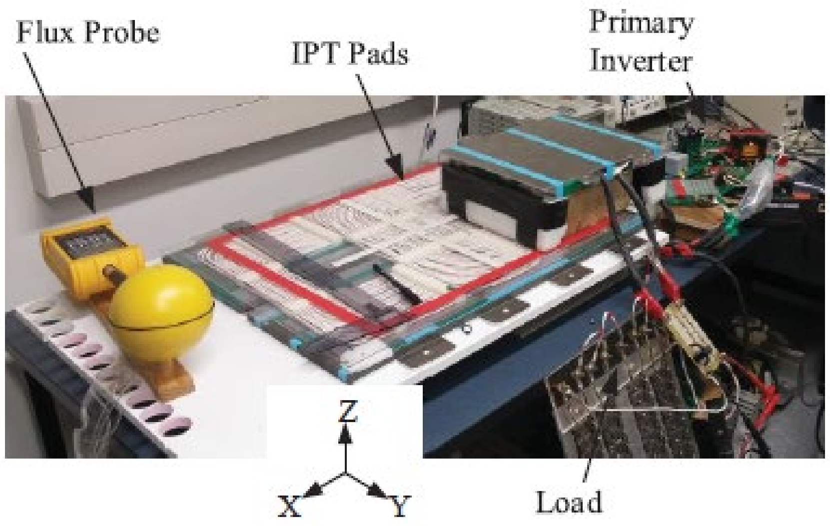

Fig. 7. A laboratory IPT system with a BPP primary and DDP secondary misaligned.

TABLE II
SIMULATED LEAKAGE FLUX ALONG X AXIS AT 800 mm FOR A FIXED $I_1 = 27.69$ A AS Q_2 VARIES AT THE MOST MISALIGNED POSITION OF (-250,100) MM.

		$S_1 = 20.5$ kVA		$S_{1a} = 10.2$ kVA	
Q_2	I_{coil} (A)	$X_{LN,12}$ (μT)	$P_{o,12}$ (W)	$X_{LN,1a2}$ (μT)	$P_{o,1a2}$ (W)
0	2.44	28.17	0	14.96	0
1	3.45	28.17	166	15.49	239
2	5.45	28.19	332	15.88	479
3	7.72	28.23	498	16.31	719
4	10.07	28.28	664	16.76	959
5	12.45	28.35	829	17.22	1198
6	14.85	28.42	995	17.70	1438
7	17.26	28.51	1061	18.17	1678
8	19.68	28.61	1327	18.64	1917
9	22.11	28.73	1493	19.11	2157
10	24.53	28.86	1658	19.58	2396

Secondary Control Needed (within limits)

Both secondary & primary control = lower loss and lower leakage

TABLE III
MEASURED VALUES TO OBTAIN 1 kW UNDER DOUBLE COIL OPERATION (S = SERIES, P = PARALLEL TUNING).

Load R (Ω)	I_1 (A)	I_{coil} (A)	V_{out} (V)	I_{out} (A)	P_{out} (W)	P_{in} (W)	η (%)	$X_{LN,12,m}$ (μT)	Q_2	PPL_X ($\frac{W}{\mu T}$)	$Y_{LN,12,m}$ (μT)	PPL_Y ($\frac{W}{\mu T}$)
4Ω S	27.69	15.78	63.82	15.78	1007.1	1066.3	94.44	29.63	6.3	33.75	4.16	240.4
8Ω S	38.69	11.01	90.7	11.01	998.6	1090	91.62	41.27	3.3	24.23	5.68	176.1
8Ω P	38.01	36.18	89.4	11.18	999.5	1094.3	91.33	37.7	3.3	26.53	4.09	244.5
12Ω P	32.15	43.27	109.4	9.16	1002.1	1073.2	93.75	32.48	4.9	30.79	4.52	221.2
16Ω P	29	49.65	125.9	7.94	999.6	1068.4	93.56	29.89	6.5	33.46	5.41	184.8

All values in this table are measured

TABLE V
LEAKAGE FLUX FOR A MISALIGNED BPP-DDP SYSTEM WITH SINGLE COIL OPERATION FOR 1 kW OUTPUT, (S = SERIES, P = PARALLEL TUNING).

	I_1 (A)	I_{coil} (A)	$X_{LN,1a2}$ (μT)	PPL_X ($\frac{W}{\mu T}$)	$Y_{LN,1a2}$ (μT)	PPL_Y ($\frac{W}{\mu T}$)	P_{out} (W)
Simulation Results							
4Ω S	21.29	15.78	15.89	62.93	3.23	309.6	1000
16Ω P	21.78	52.48	15.79	63.33	3.29	304.0	1000
Practical Validation							
4Ω S	22.44	15.41	14.94	66.93	2.49	401.6	994
16Ω P	24.92	50.42	16.97	58.9	2.535	394.5	992

Multicoil Surface GA

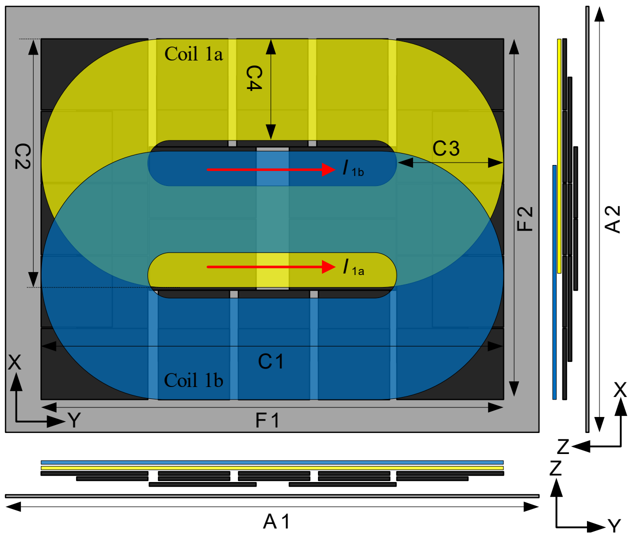

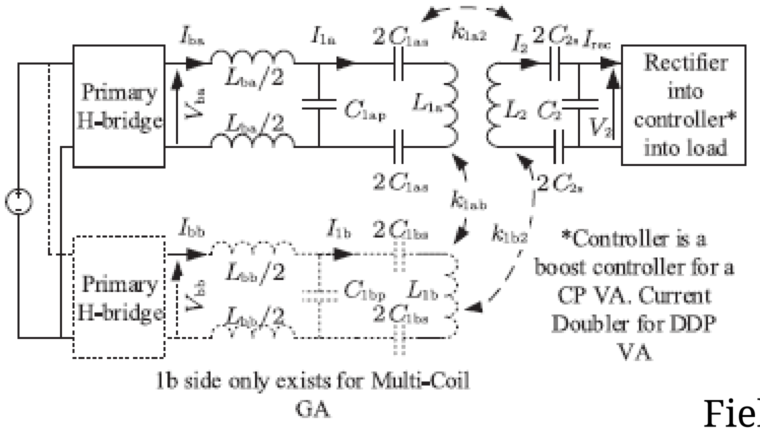

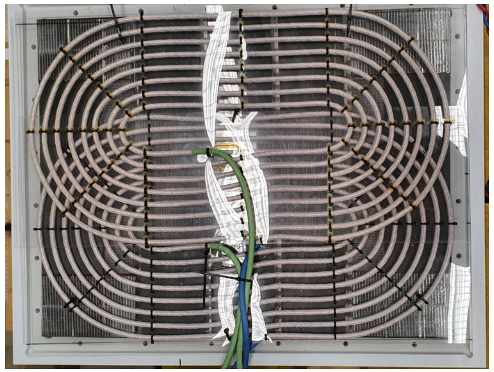

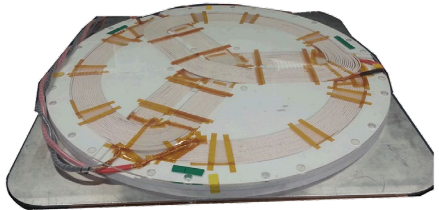

Tri-polar UoA.

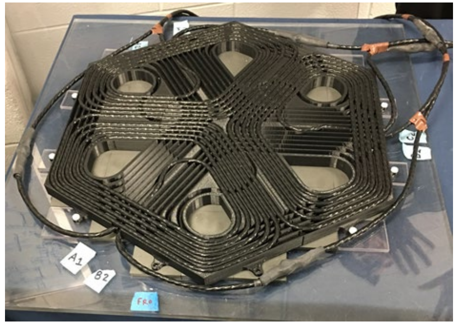

3 phase 120° rotated DDs ORNL.

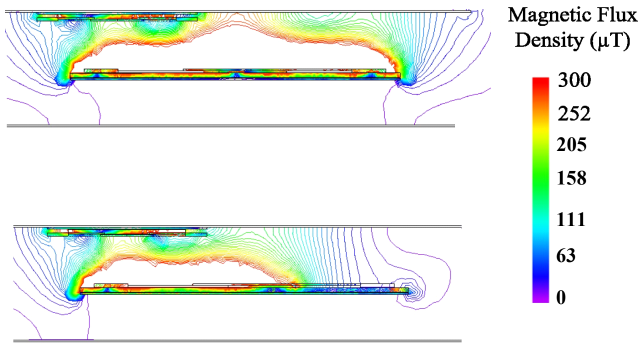

Field shaping increases efficiency & lowers leakage

Multicoil/multiphase exploits interoperability and improves ferrite use & leakage

References [22]-[25],[27], [32], [49-56]

Example UGA @ WPT2/Z2 VAs

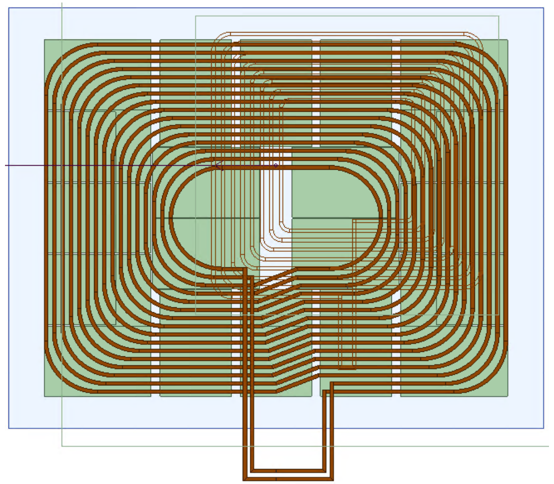

Tested at rated power
Max offsets

UGA-CP

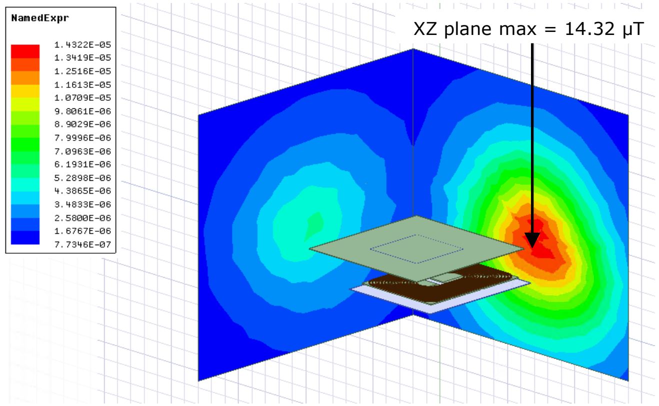

UGA-DDP

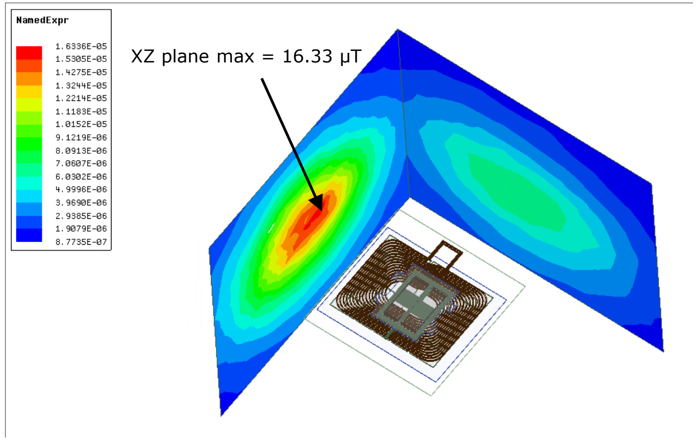

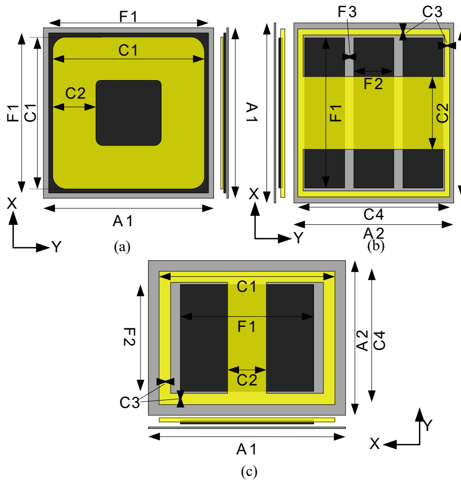

References [22]-[25],[27], [32], [49-56]

Multi-Coil Primary: WPT2/Z2 VAs

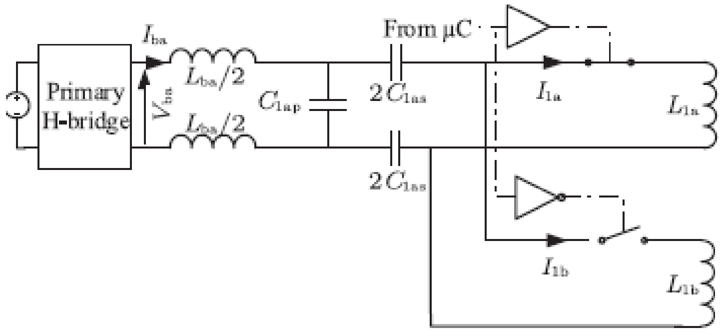

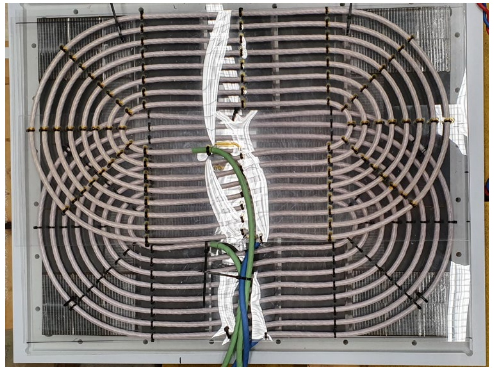

MCP-CP

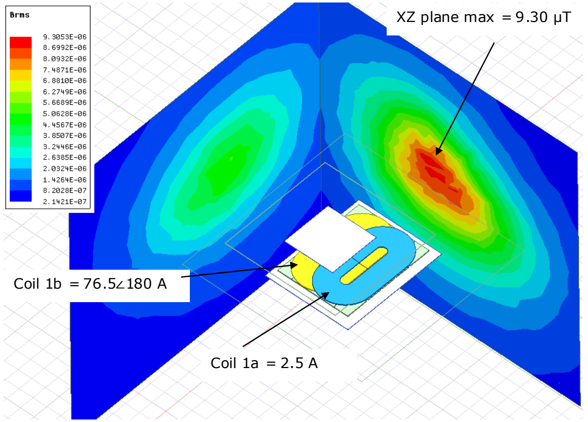

MCP-DDP

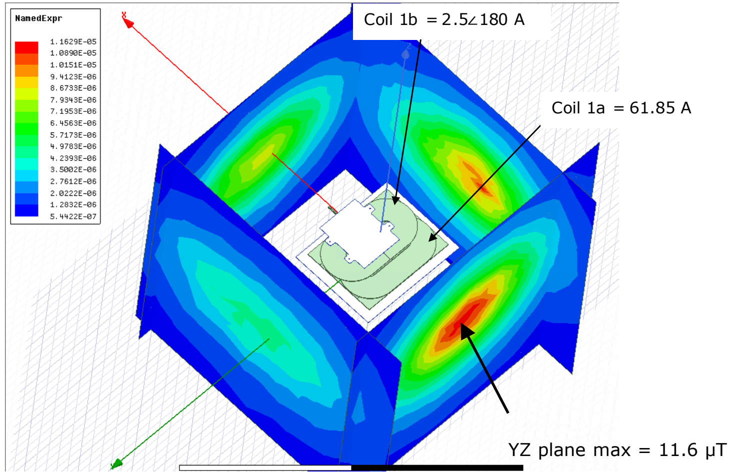

References [22]-[25],[27], [32], [49-56]

Tri-polar Pads

- Mutually decoupled coils
- Rotationally tolerant to all including polarised and circular
- Has capability to boost VA in added coil for high power
- Compatible will all other technologies
- Can be used to reduce flux leakage at offset by as much as 50% for identical power transfer

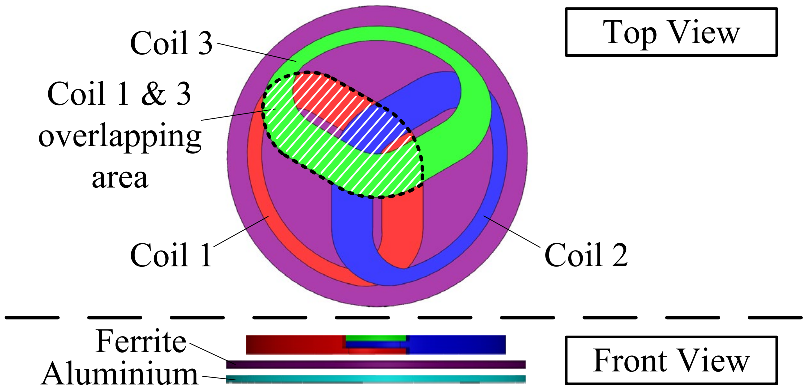

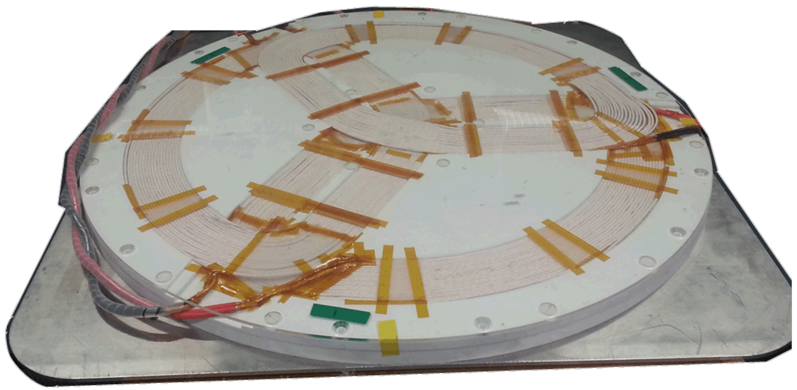

References [22]-[25],[27], [32], [49-56]

1/2/3 Phase Tripolar pad

Mutually decoupled primary pad

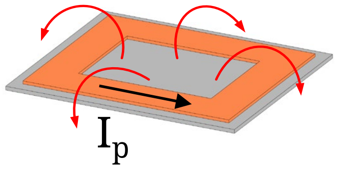

Non-polarised

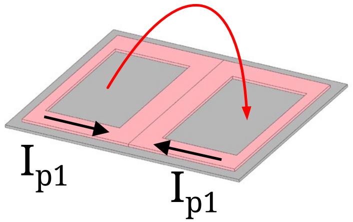

Polarised

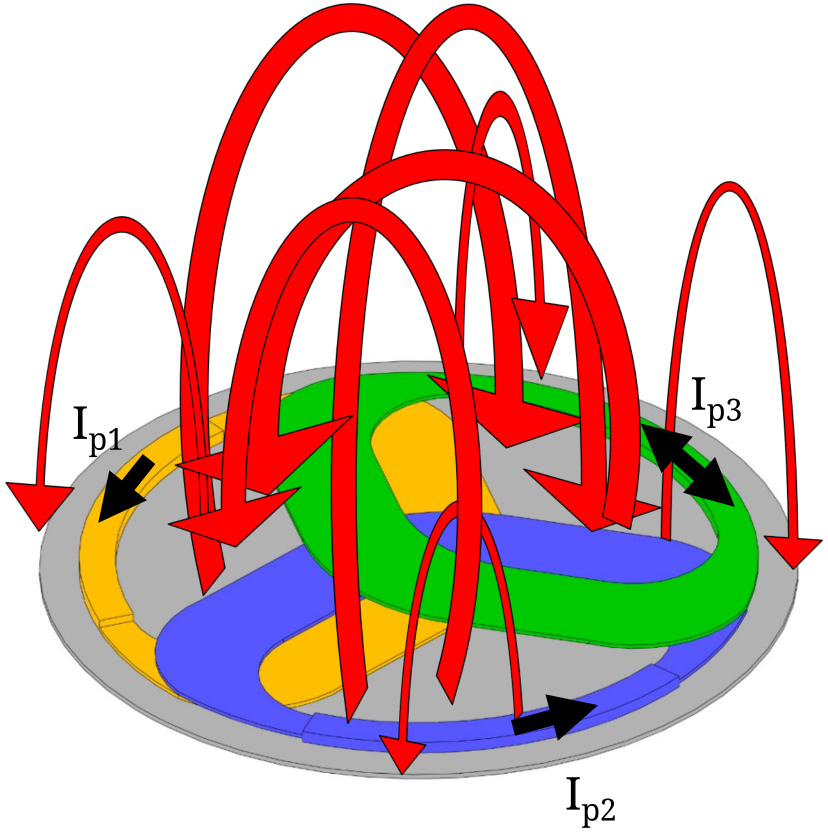

Tripolar Pad

References [22]-[25],[27], [32], [49-56]

Tripolar Pad Primary

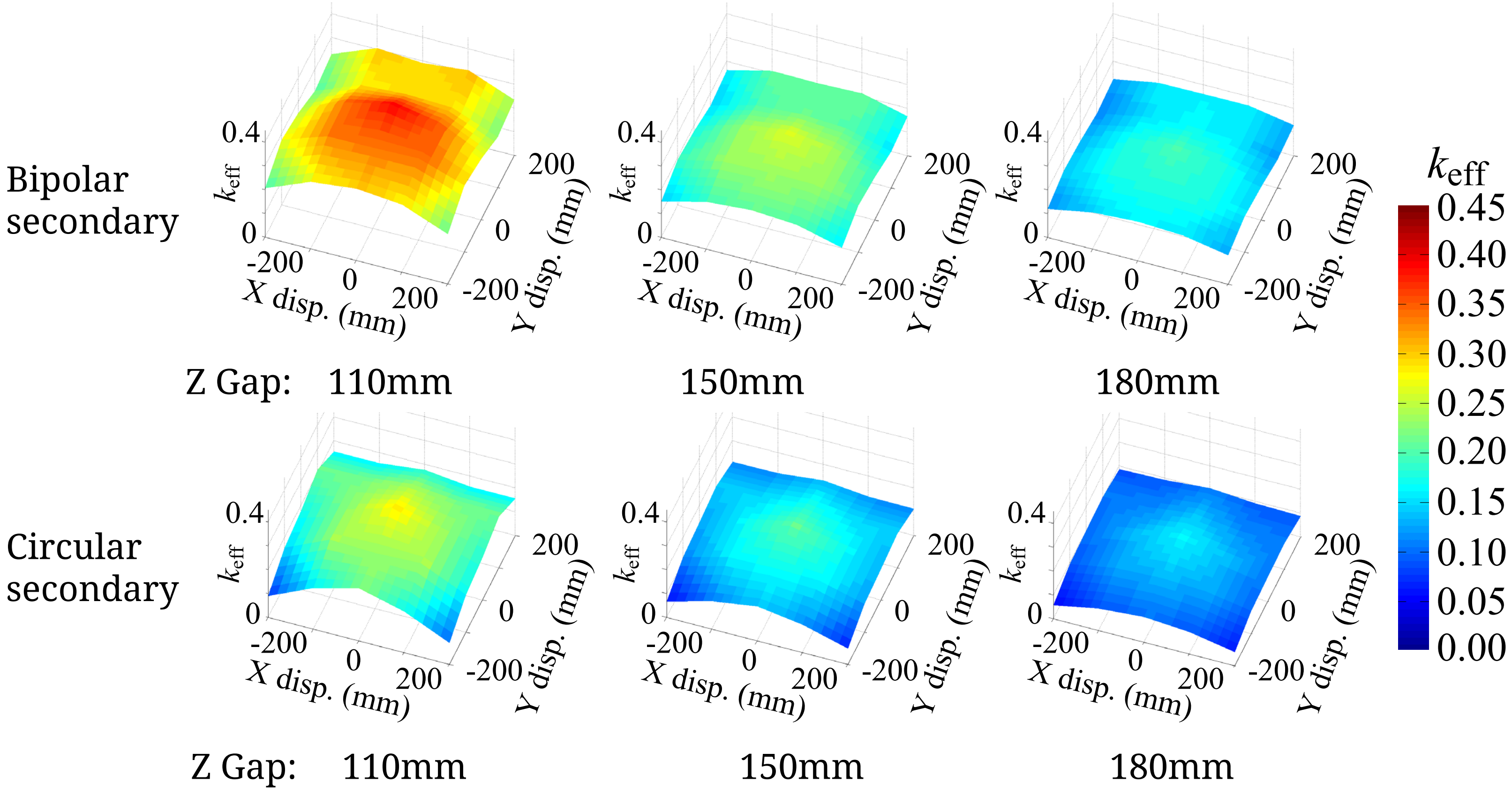

TPP primary to BPP and CP secondary with optimised primary currents at different air gaps and secondary sizes

Primary: TPP - 670mm diameter pads (coil 600mm), Sec: CP – 450mm x 450mm, BPP – 356mm x 576mm

References [22]-[25],[27], [32], [49-56]

20 kW Topologies Evaluated

CP or TPP primaries to CP or TPP secondary

- Identical Cu, Fe, and Al
- 680mm diameter pads (600mm coil diameter)
- 150mm air gap
- Designed for 20kW at 85kHz

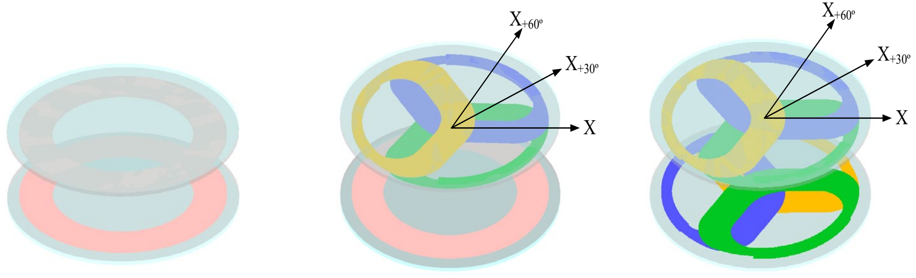

CP-CP CP-TPP TPP-TPP

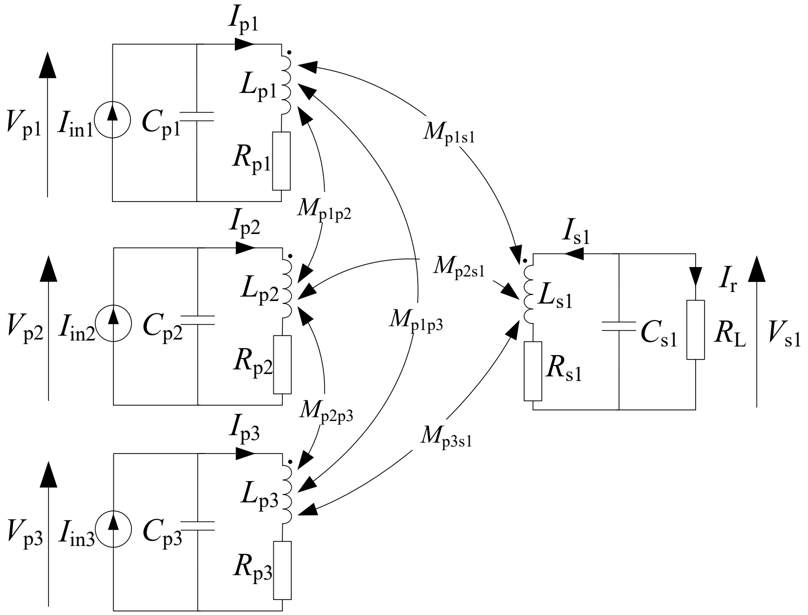

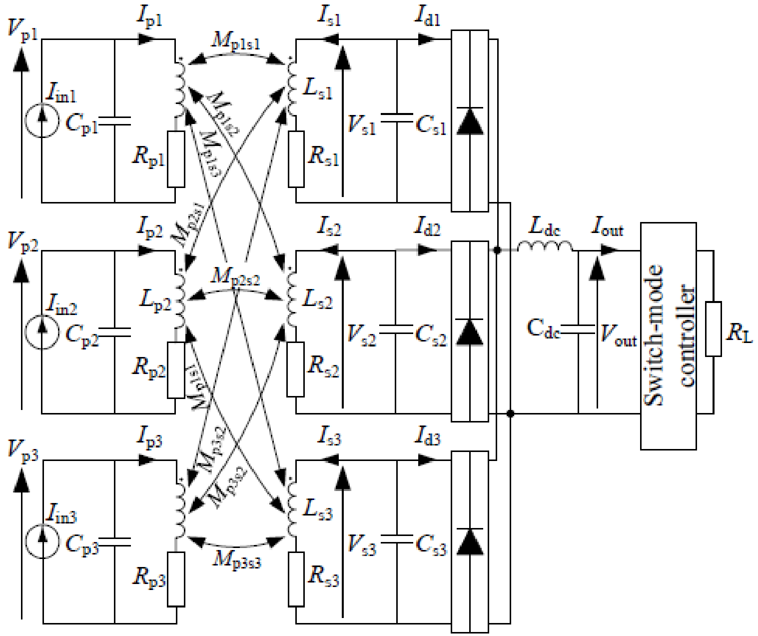

References [22]-[25],[27], [32], [49-56]

Each coil of the TPP is driven from an LCL tuned inverter

Effective Coupling Factor (k_{eff})

Multicoil Pads with Decoupled (independent) Windings

- $k_{\mathrm{eff}} = \sqrt{\frac{\sum S_{\mathrm{u}}}{\sum VA_{\mathrm{p}}}} = \sqrt{\frac{S_{\mathrm{u1}} + S_{\mathrm{u2}} + S_{\mathrm{u3}}}{VA_{\mathrm{p1}} + VA_{\mathrm{p2}} + VA_{\mathrm{p3}}}}$
- $P_{\mathrm{out}} = k_{\mathrm{eff}} \sqrt{\sum VA_1 \sum VA_2}$

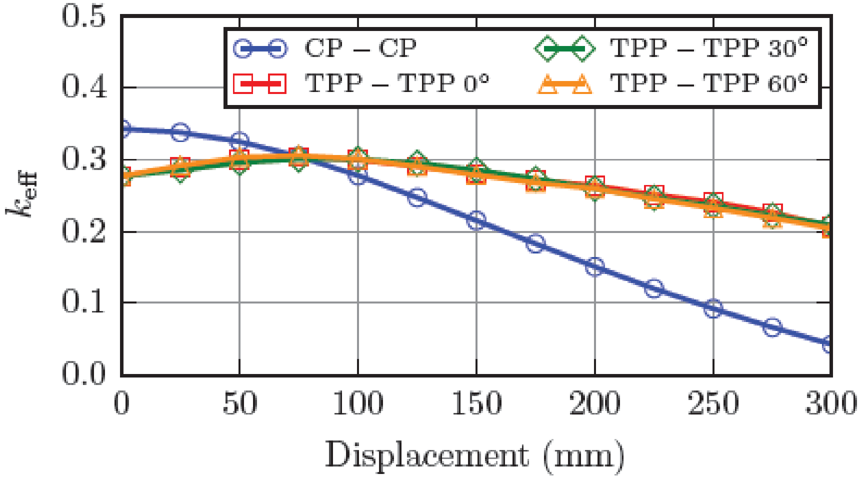

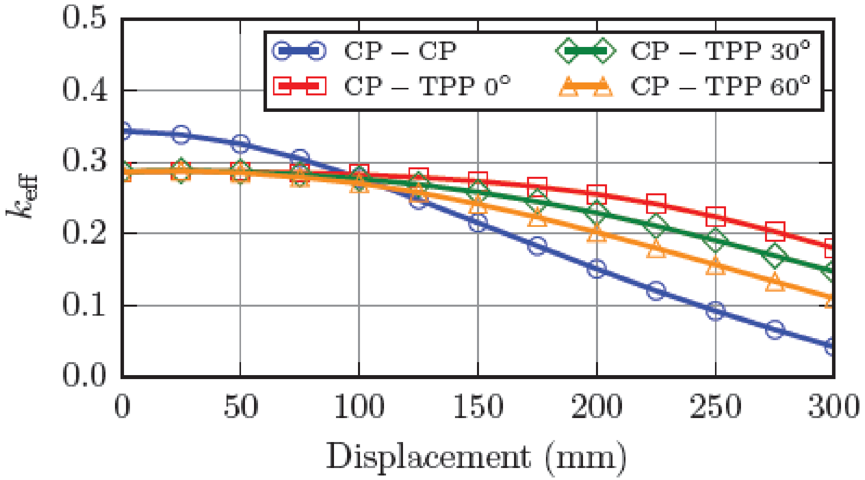

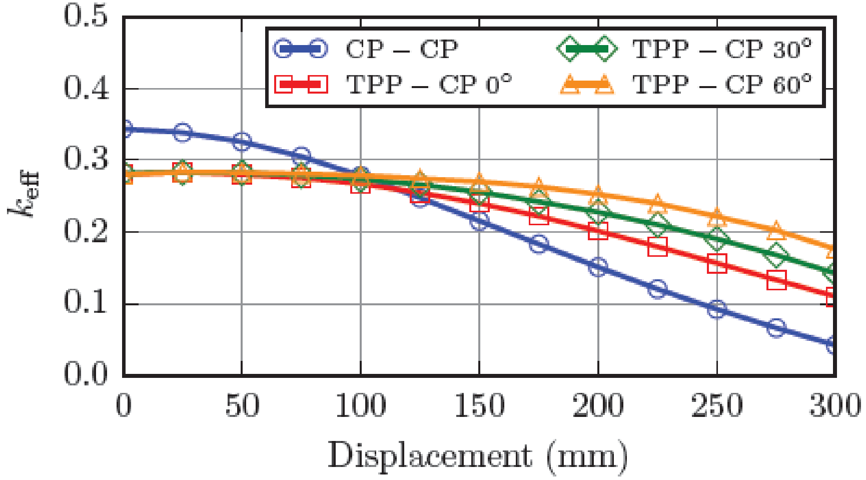

References [22]-[25],[27], [32], [49-56]

Impact on Leakage

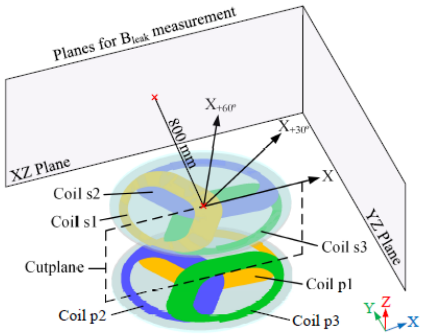

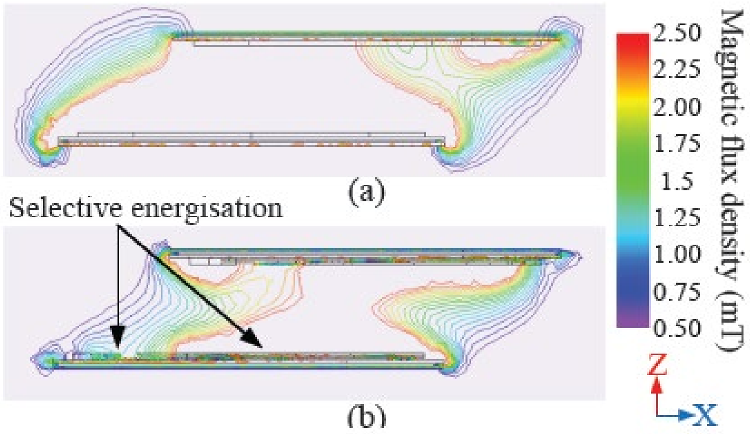

(a) CP-CP and (b) TPP-TPP

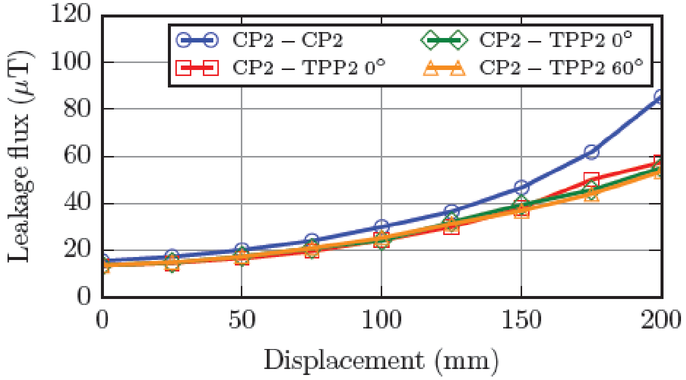

Fig. 14: B_{leak} for CP-CP and CP-TPP for 20 kW at 150 mm air gap.

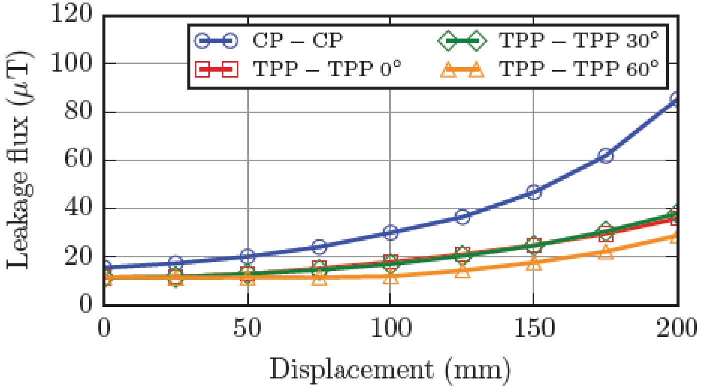

Fig. 13: B_{leak} for CP-CP and TPP-TPP for 20 kW at 150 mm air gap.

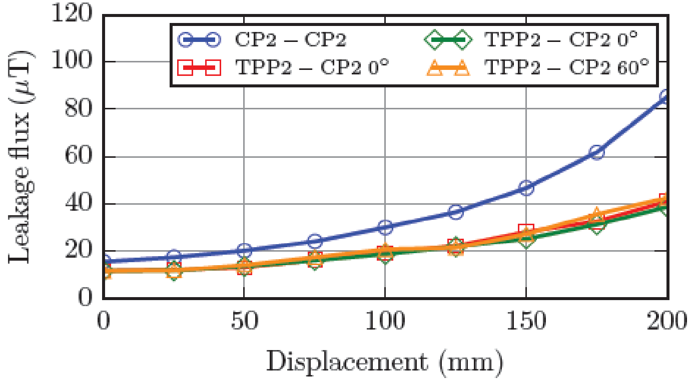

Fig. 15: B_{leak} for CP-CP and TPP-CP for 20 kW at 150 mm air gap.

References [22]-[25],[27], [32], [49-56]

Ratings of Electronics for 20 kW

TABLE II: Distribution of real and apparent power in CP-CP and TPP-TPP systems*

	CP-CP 360 V_{out}		CP-CP 800 V_{out}		TPP-TPP 0° 360 V_{out}							
(mm)	(kVA)	(kW)	(kVA)	(kW)	(kVA)			(kVA)	(kW)			(kW)
Disp.	S_p	P_p	S_p	P_p	S_{p1}	S_{p2}	S_{p3}	$S_{p\ total}$	P_{p1}	P_{p2}	P_{p3}	$P_{p\ total}$
100	99.74	20.83	42.95	21.26	26.31	5.96	28.25	60.52	8.56	3.09	9.59	21.24
Disp.	S_s	P_s	S_s	P_s	S_{s1}	S_{s2}	S_{s3}	$S_{s\ total}$	P_{s1}	P_{s2}	P_{s3}	$P_{s\ total}$
100	53.76	20.19	129.15	20.19	35.69	33.98	32.64	102.31	8.27	5.91	5.94	20.12

Summary:
Leakage reduction of 43%

Component ratings each phase of TPP, against CP:
TPP/phase: H-bridge & rectifiers ½ rating of CP, resonant components 1/3 of CP

References [22]-[25],[27], [32], [49-56]

Multicoil Vehicle COUPLERS

- Provide wider misalignment tolerance
- Better transition for stationary to dynamic
- Reduced sensitivity to varying coupling
- Improved system efficiency

Multi-coil DDQ and Bipolar Secondaries

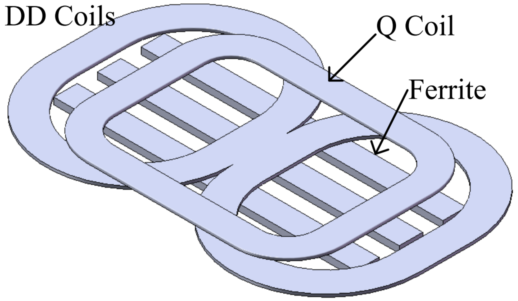

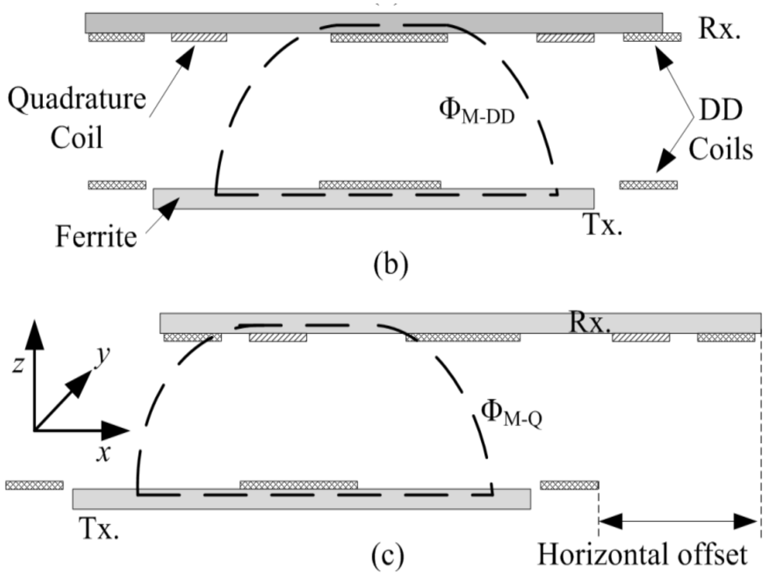

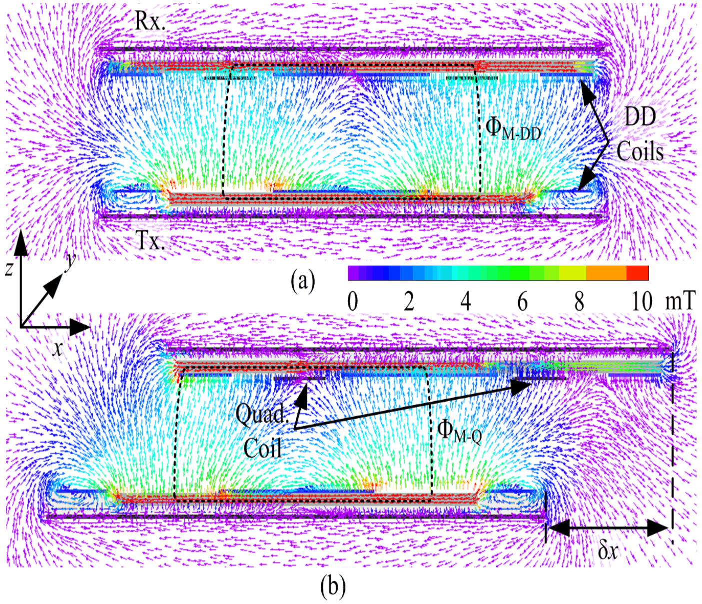

DDQ combines DD & Circular
Improves secondary lateral tolerance
- DD captures horizontal flux at centre
- Circular captures vertical flux at centre

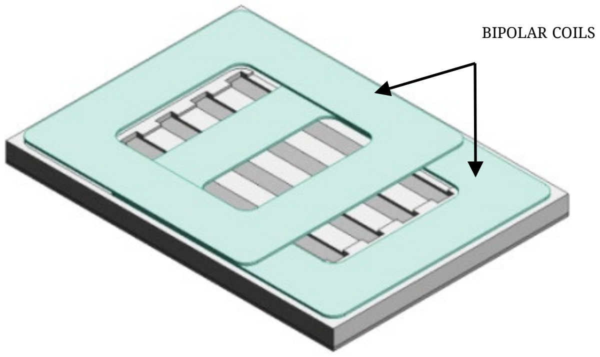

Bipolar:
Requires 25-30% less copper than DDQ
Power capture < 10% difference from DDQ

References [22]-[25]

Multi-coil Secondary Comparisons

Both include two independent coils each with high Q_L

- Enable similar power transfer
- Either coil can be shut down when not needed to maximise ζ

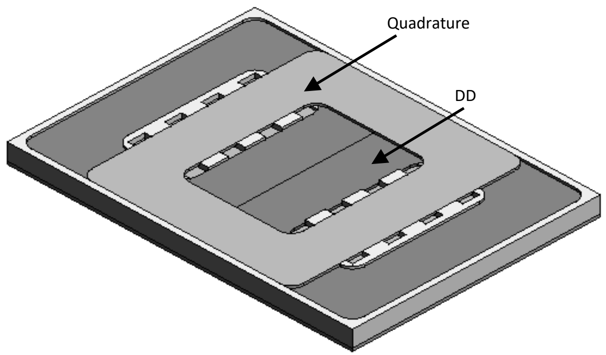

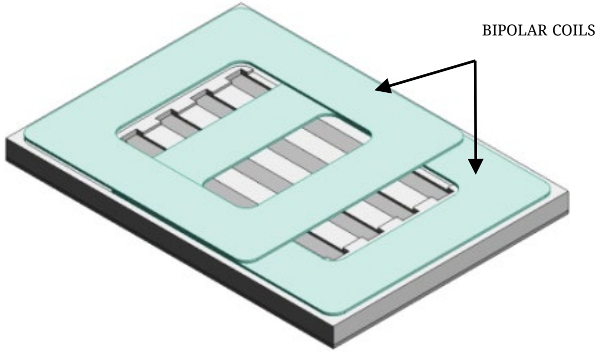

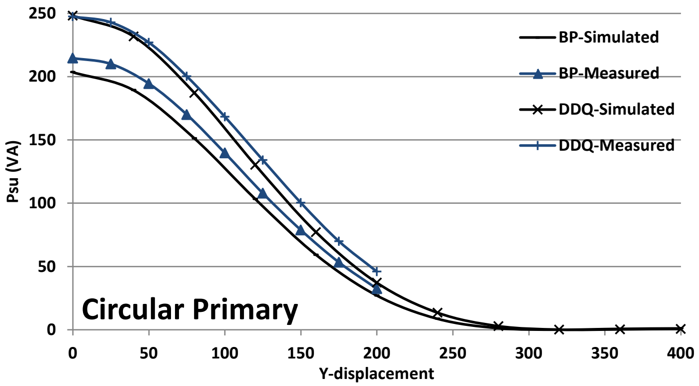

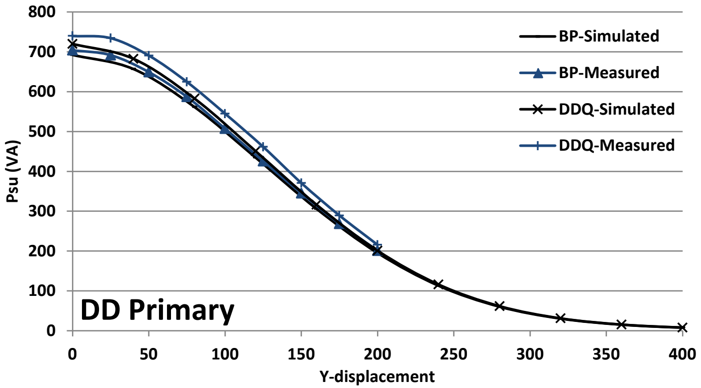

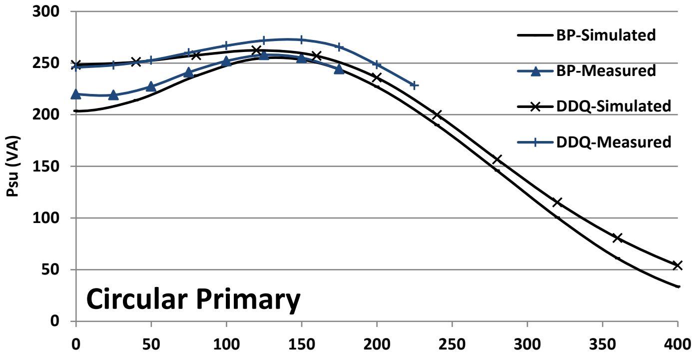

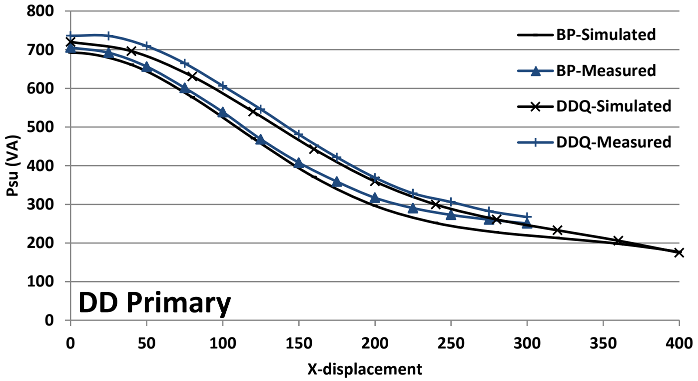

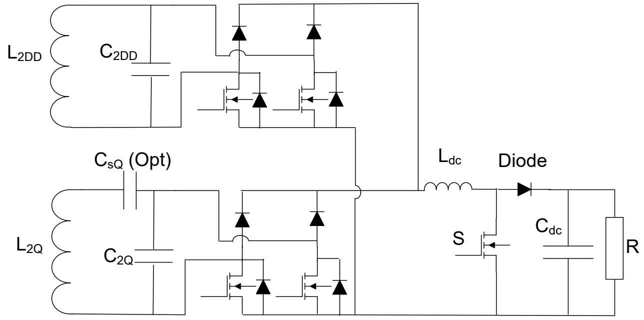

Ex: Combining current sourced secondaries when the primary current is controlled

References [22]-[25]

Multi-coil Secondaries on Various Primaries

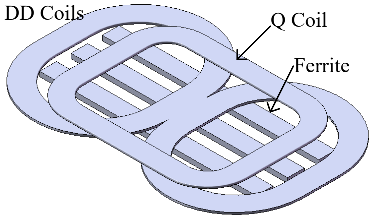

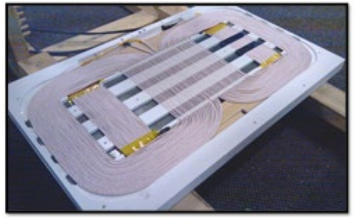

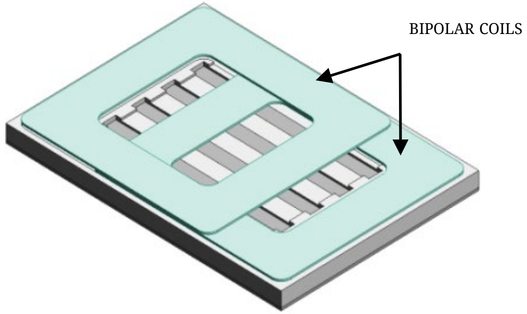

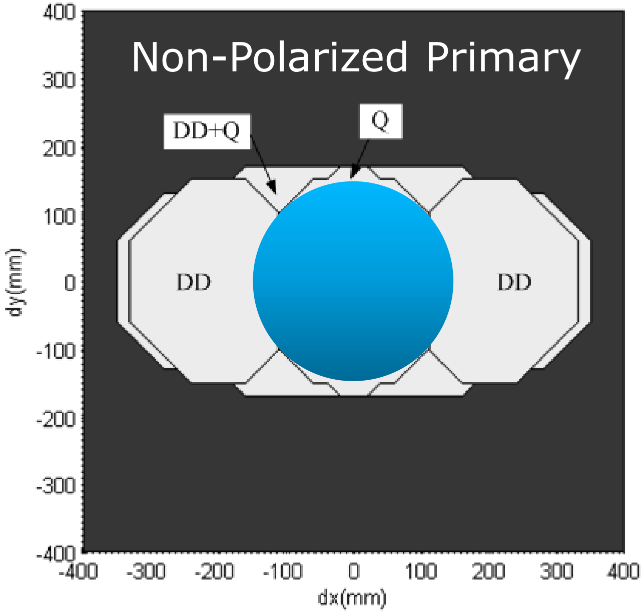

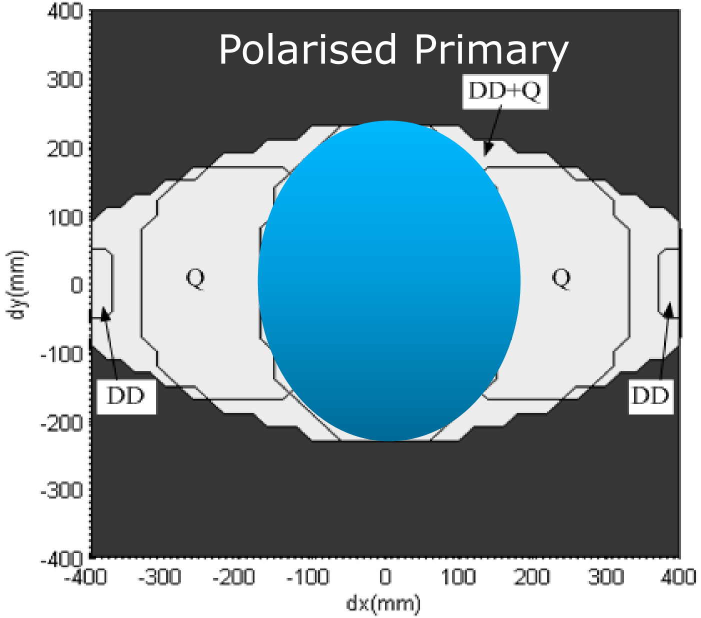

Power transfer zone is 3 x larger
Higher lateral parking tolerance possible
Minimises power pulsations in dynamic applications

Bipolar Interoperability

Coupling factors for mismatched primary and secondary pads

- Bipolar, circular and solenoid options of identical area

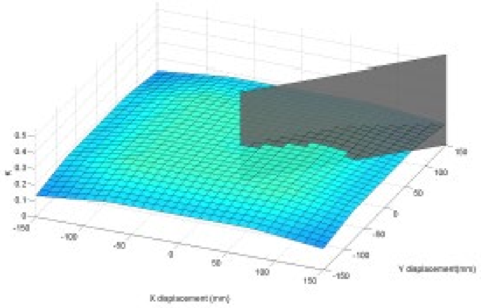

(a) CP P1-CP S2

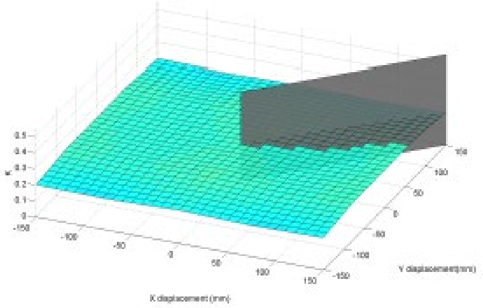

(b) CP P1-BPP S2

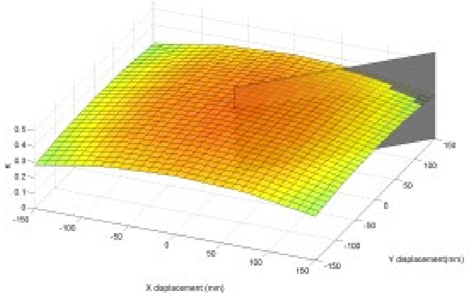

(e) SP P1-SP S2

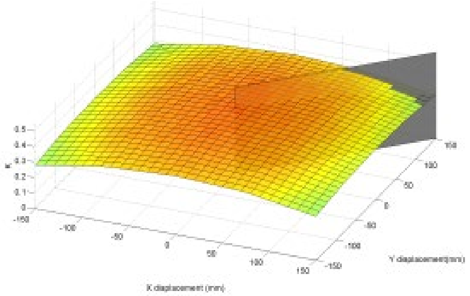

(f) SP P1-BPP S2

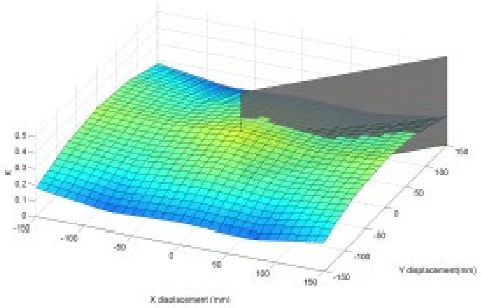

(c) BPP P1-CP S2

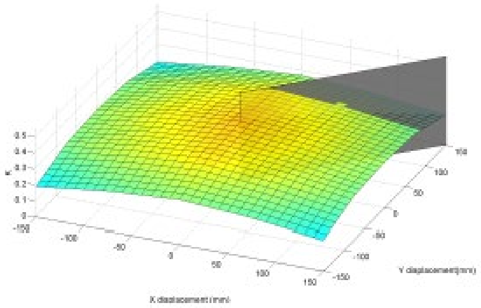

(d) BPP P1-BPP S2

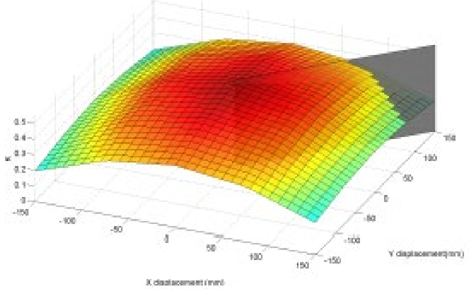

(g) BPP P1-SP S2

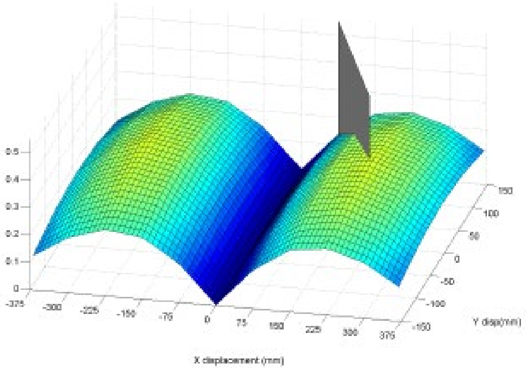

(h) CP P1-SP S2

Intermediate Couplers

Resonant Repeaters

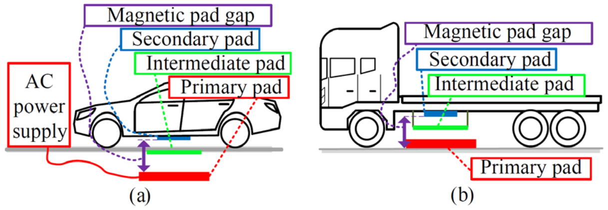

Fig. 1: Overview of a three-coil IPT system where the intermediate is (a) placed flush on the road or (b) attached to the vehicle

Resonant repeaters applications

- Extending power transfer over a large gap using high quality ferrite-less coils
- Domino effect splitting can be effective for splitting and movement – e.g. robotics
- Co-planar magnetics series/parallel shows it only improves series tuned primaries by lowering the current from the inverter

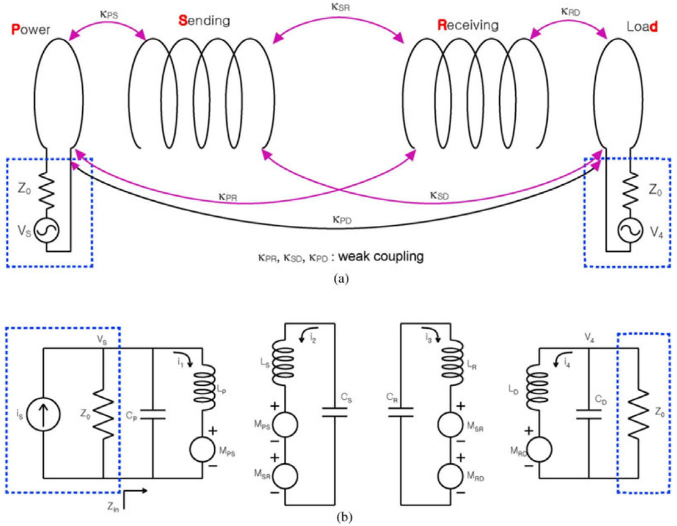

Fig. 8. (a) Wireless power system with two coil-resonators, a power driving coil and a load coil, and (b) the equivalent circuits [36] (Copyright IEEE).

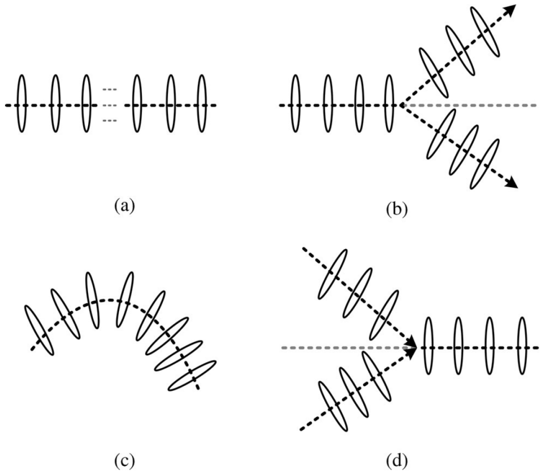

Fig. 9. Examples of domino-resonator arrangements [60]. (a) Straight chain. (b) One chain splitting into two. (c) Curved chain. (d) Two chains emerging into one (Copyright IEEE).

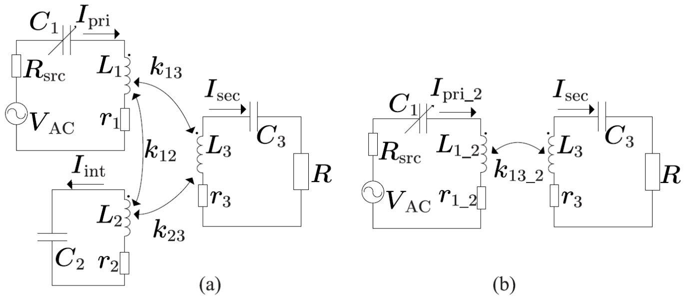

Fig. 15. Series–series-tuned systems with losses in the (a) three coil configuration and (b) its two coil equivalent system.

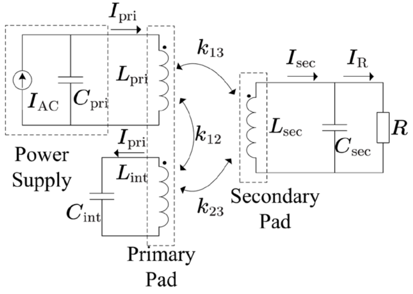

Fig. 2. Three coil, parallel–parallel IPT system with coplanar intermediate coupler in the primary pad.

References [65]-[70]

Intermediates in use for Traffic lighting:

Road studs with flat pick-ups – using resonant intermediate power boost in late 90's

Installation
- Saw cut (10mm x 60mm)
- Backfill epoxy/bitumim
- Glue stud into recess
- Active node/spacer placed beneath

resonant intermediate

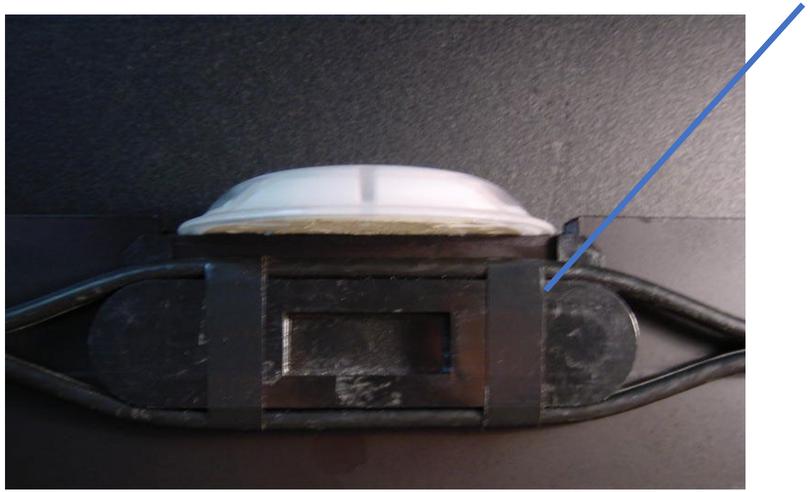

Coupler Improvements in Coupling?

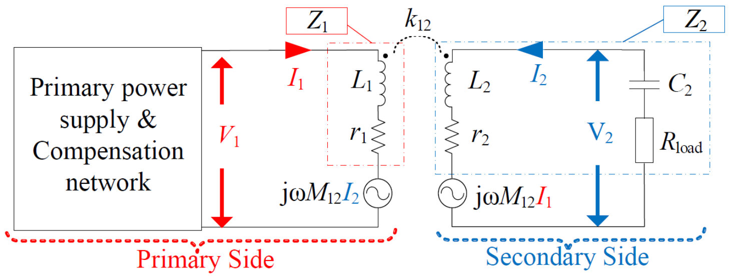

Fig. 2: Mutual inductance model of two-coil IPT system with series tuning on the secondary

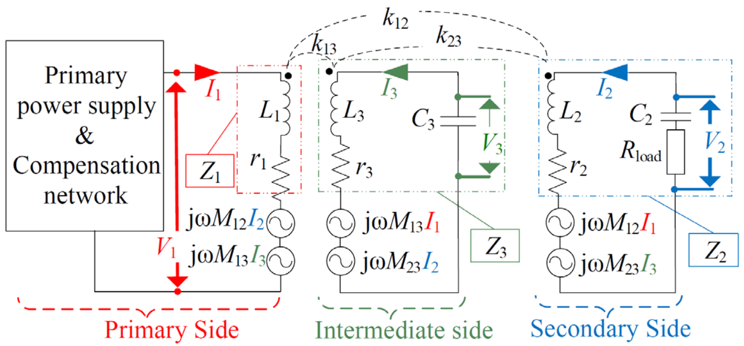

Fig. 3: Model of a three-coil IPT system with an intermediate resonant pad and series tuned secondary

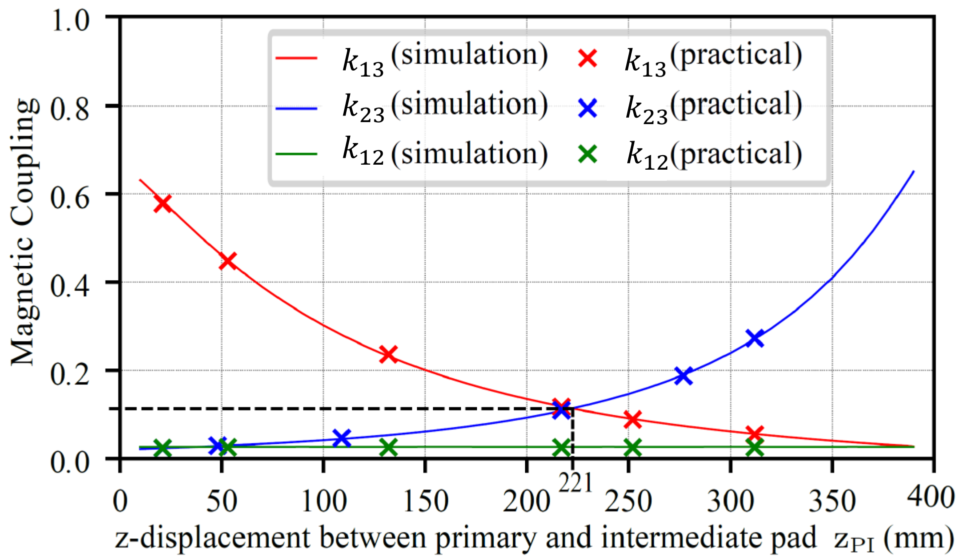

k's with changing position of intermediate

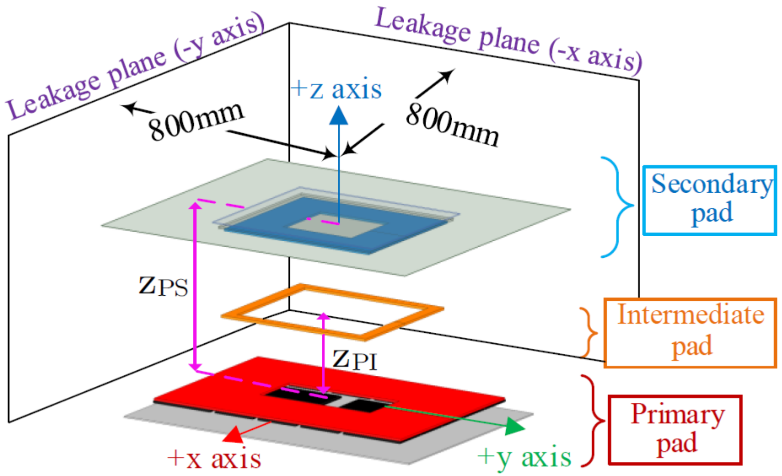

Fig. 5: Layout of the three-coil IPT system

$$\frac{I_2}{I_1} = -\frac{M_{13}}{M_{23}} = -\frac{k_{13}}{k_{23}}\sqrt{\frac{L_1}{L_2}}$$

$$\frac{I_3}{I_1} = -\frac{M_{12}}{M_{23}} - j\frac{M_{13}R_{load}}{\omega M_{23}^2}$$

$$P_{load} = \left(\frac{M_{13}}{M_{23}}\right)^2 I_1^2 R_{load}$$

Reference [70]

Coupler Assessments of two coil versus 3 coil

1: UGA:WPT3 Z3

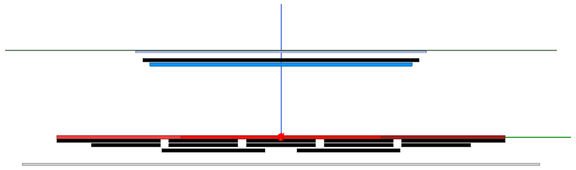

2: Matched Secondary

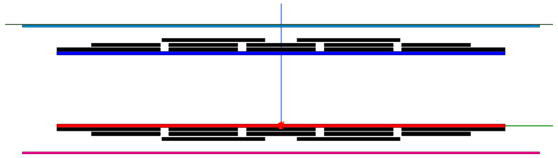

3: Improved volume VA

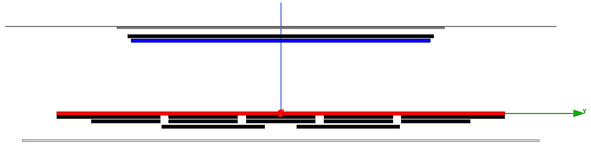

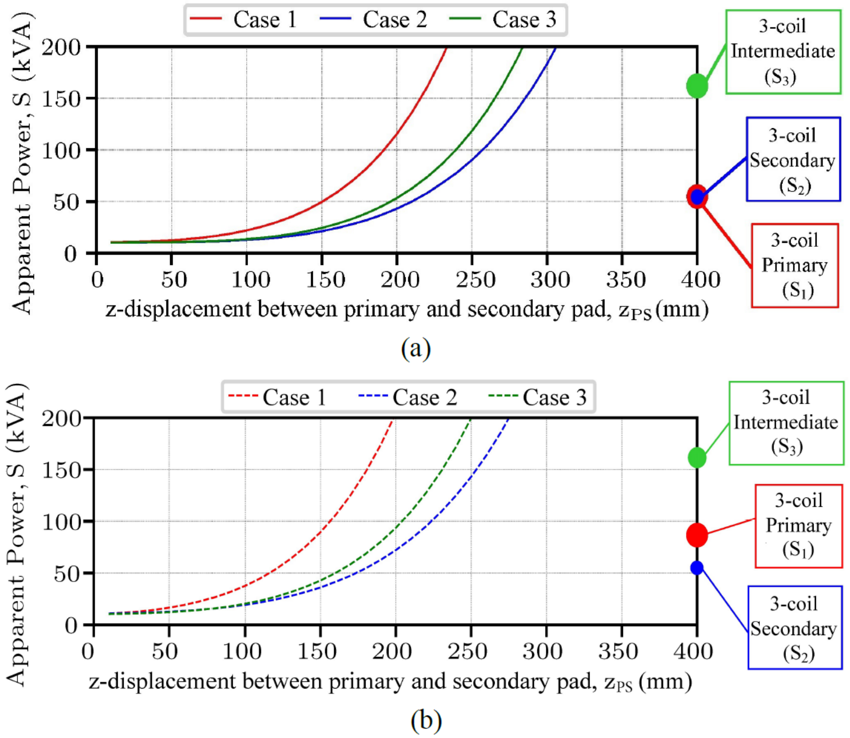

Fig. 9: Comparison of the apparent power when pads (a) centred (b) offset

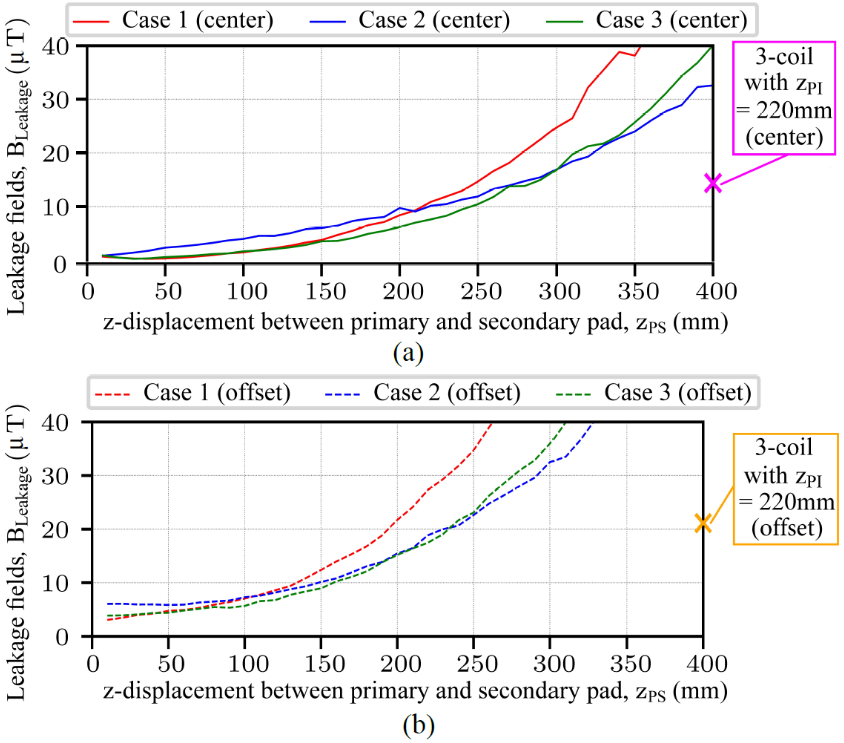

Fig. 10: Comparison of the leakage fields in the worst axis when (a) centred and (b) offset

Reference [70]

Future Road Systems

Stationary & Dynamic
Around town: little & often

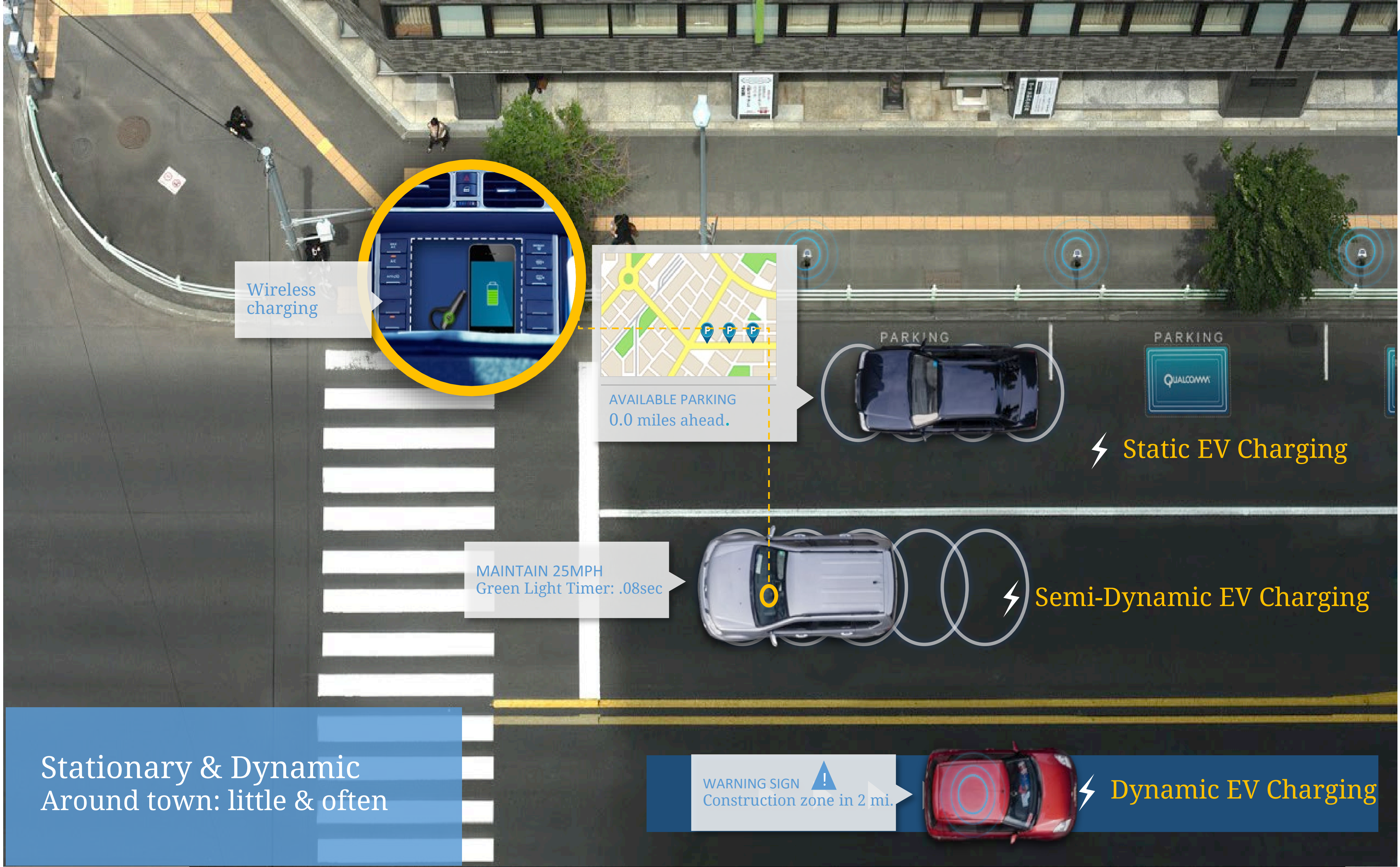

Roadway Vision

Static, Semi-dynamic, Smart Cities (rail, bus…), Long haul

Taxi-lanes/High Capacity Highways

- Sequentially Energised Pads
- Independently controlled, can track at > 100km/h
- Automated vehicle recognition, billing …

Vision Challenges:

- Compatibility
- Robustness
- Longevity

Dynamic Options

- Track options

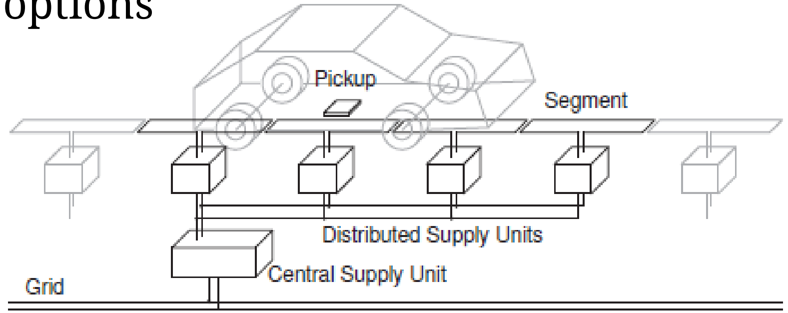

Fig. 1: Segment layout of a dynamic charging system

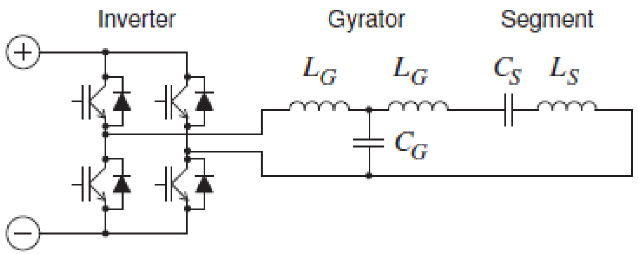

Fig. 3: Circuit of a primary WPT supply unit

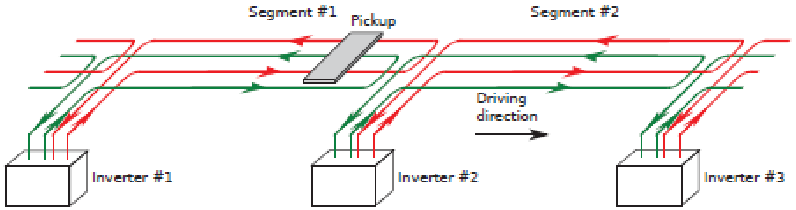

Fig. 6: Dual-phase WPT track parallel to the track

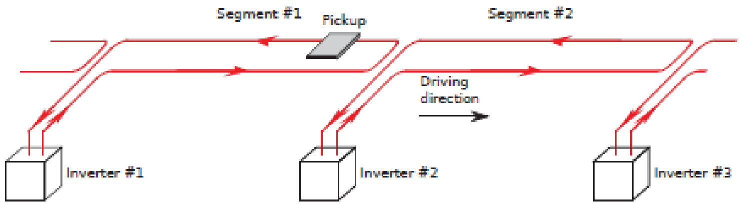

Fig. 4: Single-phase WPT track parallel to track

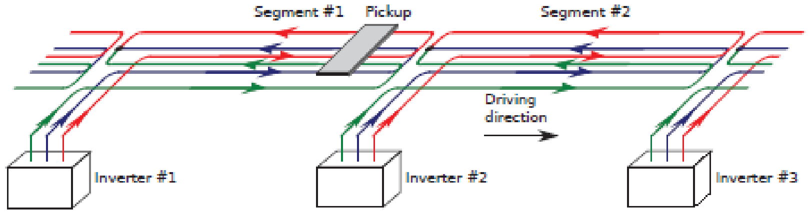

Fig. 7: Three-phase WPT track parallel to track

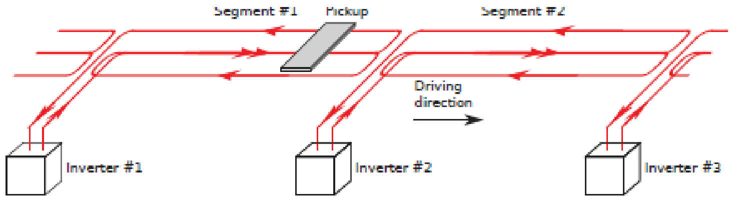

Fig. 5: Single-phase WPT track parallel to track with bipolar sturcture

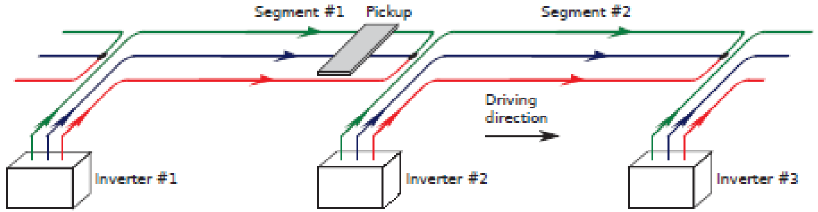

Fig. 8: Three-phase WPT track parallel to track with a star point at the end of segment

Reference [34]

Dynamic Options

- 3 phase always better
- Linear lower cost but meander has higher tolerance and power

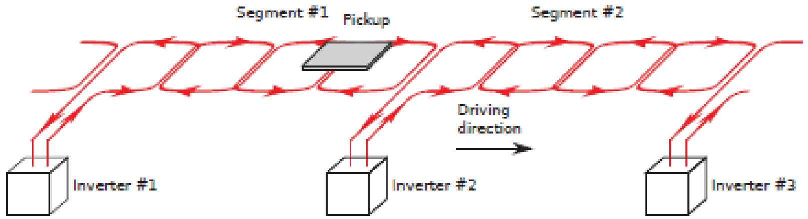

Fig. 11: Single-phase WPT meander track

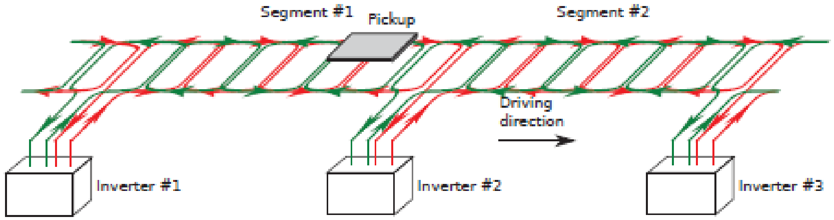

Fig. 13: Dual-phase WPT meander track

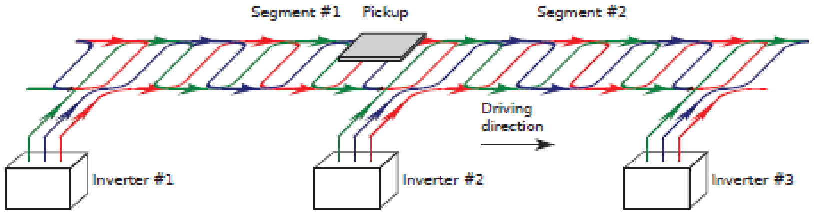

Fig. 14: Three-phase WPT meander track

Reference [34]

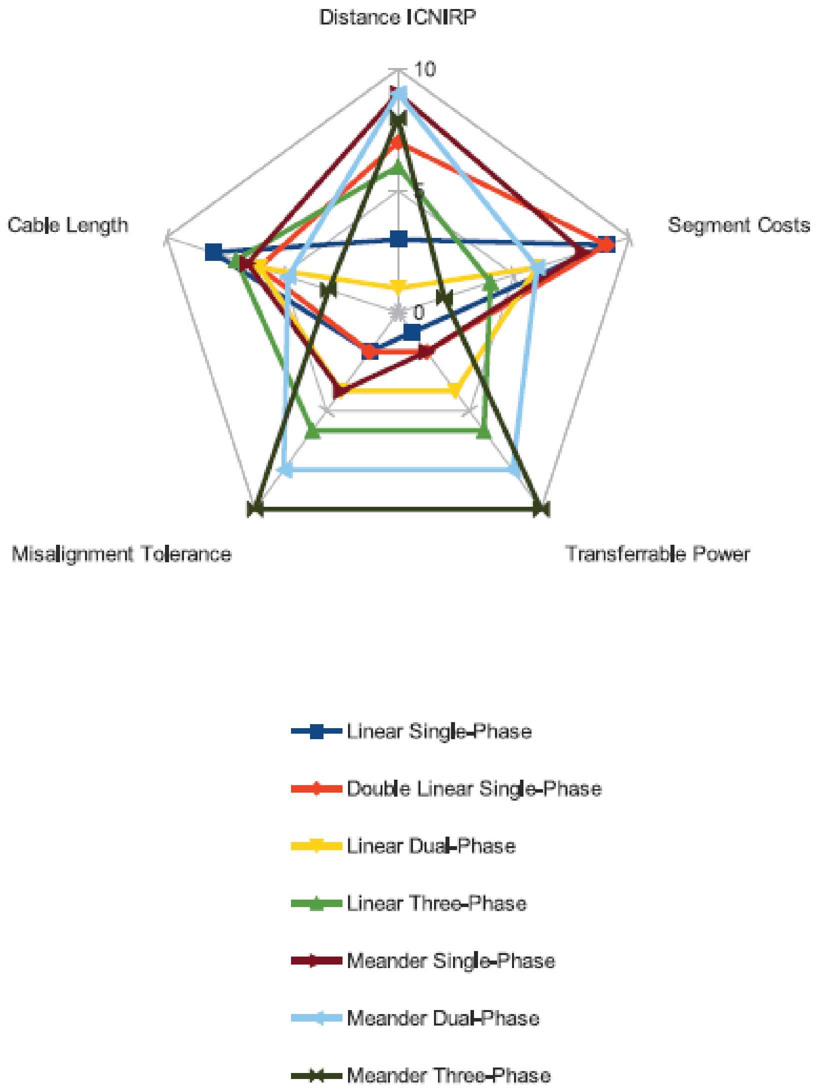

Lumped or Track?

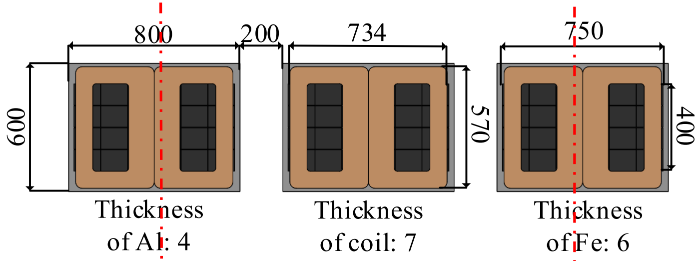

Single phase lumped DD Pads

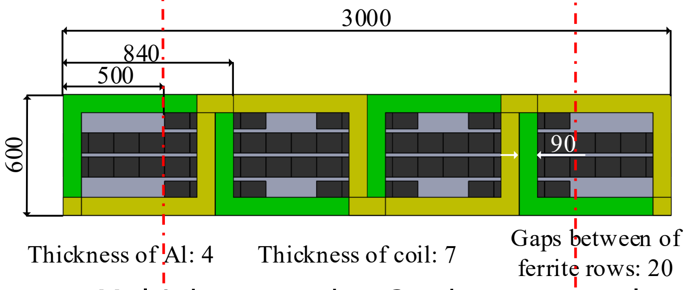

Multiphase track – 2 phase example

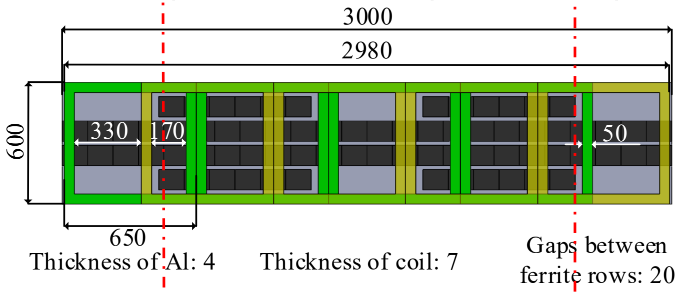

Modified 2 phase track

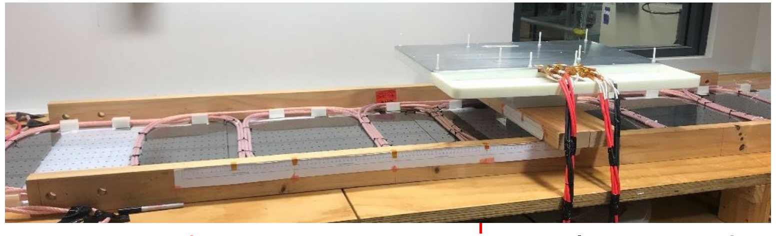

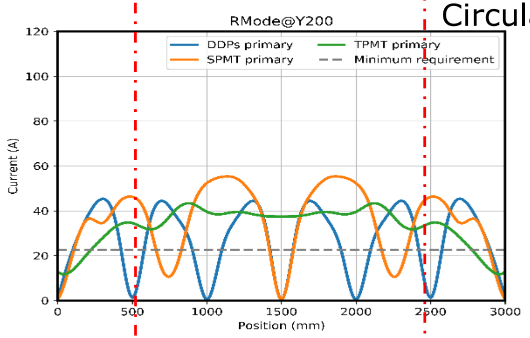

Circular Secondary

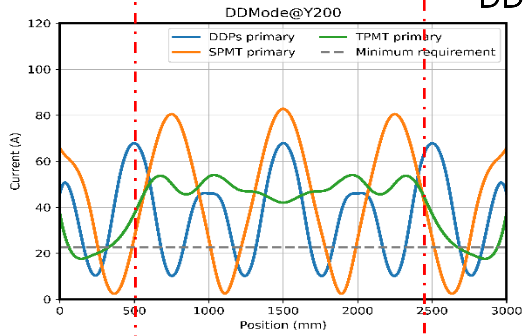

DD Secondary

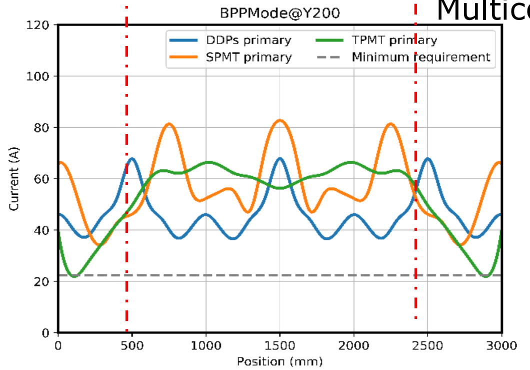

Multicoil Secondary

Reference [57] Plus applications in References [27]-[32],[34]-[48],[57]-[58]

Track Roadway Systems

Example systems

KAIST Various Generations

Polarised only track and secondary has power nulls

http://olev.kaist.ac.kr/en/index.php

20-100kW
17 cm gap
Inductive strips sized for Bus

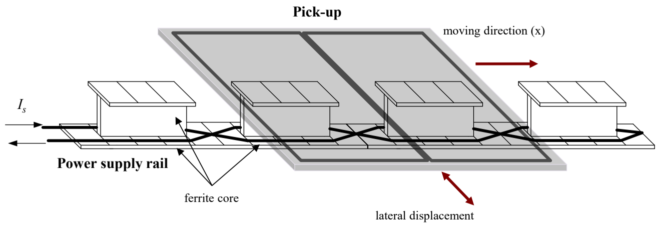

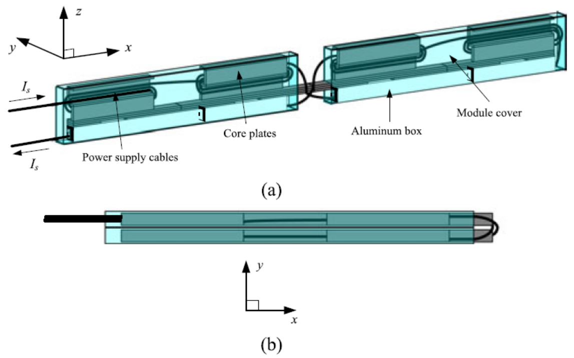

Fig. 5. Configuration of the ultra-slim S-type power supply modules including two magnetic poles [41]. (a) Bird's eye view for two unfolded modules. (b) Top view of a folded module.

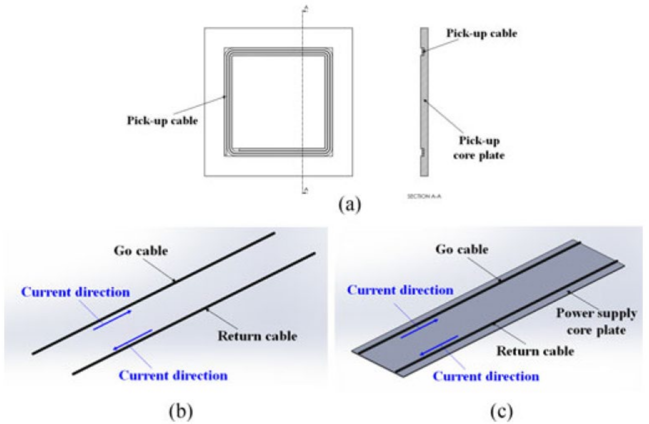

Fig. 9. Conceptual scheme of the proposed coreless power supply rail for both RPEVs and SCEVs [84]. (a) A rectangular pick-up coil for SCEVs in accordance with the SAE J2954. (b) Proposed coreless power supply rail. (c) Conventional power rail used for the 3G and 3G+ OLEVs.

Reference [2],[9],[35].[36]

Bombardier Dynamic IPT

*www.primove.**bombardier**.com*

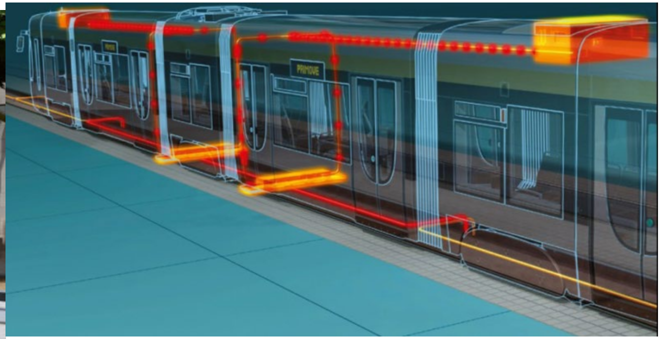

Light Rail: Continuous 270kW power, buried cables replaces catenaries

Bus: Dynamic trials lowered pads at controlled height, Stationary lowered for 100-200kW

Reference [2]

IABG INTIS

- 200kW Backbone
- 30kHz double U core
- 30kW @ 10cm

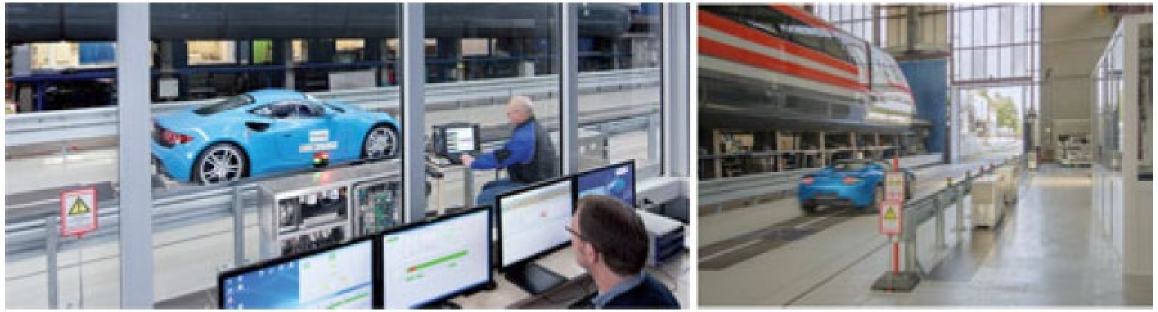

Fig. 22. INTIS test center having a 25-m-long track for the IPTS of SCEVs and RPEVs [90].

Fig. 23. Test frame for a pick-up (left) and double U-type power supply rail (right) used in the test center [90].

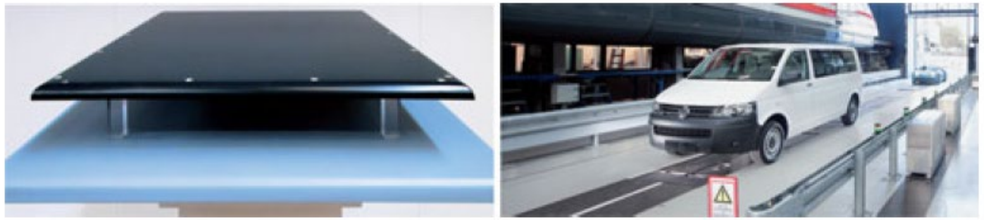

Fig. 24. Power supply rails and pick-up coils for SCEVs (left) and RPEVs (right) developed by INTIS [91].

Reference [37]

Nissan

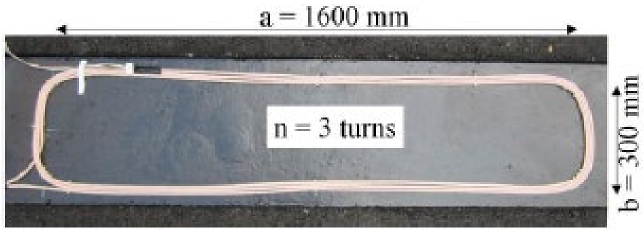

Figure13: Photograph of the transmitter coil embedded in the test road

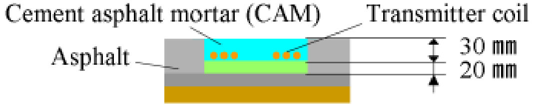

Figure15: Schematic cross-sectional view of the test road

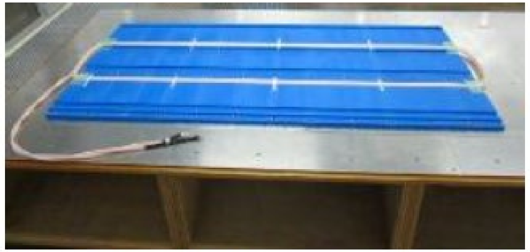

Figure2: Photograph of the measured transmitter coil

Figure14: Photograph showing the paving of the test road

Figure18: Photograph of the receiver coil installed at the rear of the test EV

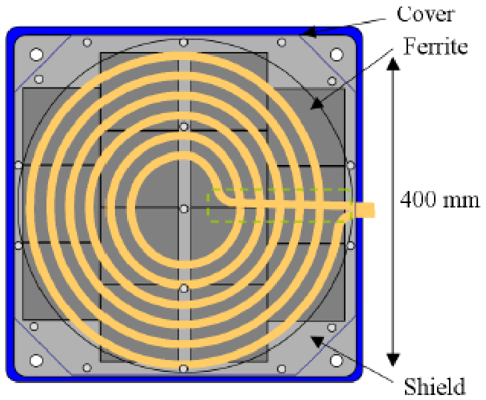

Figure4: Schematic of the receiver coil used in this study

Reference [38]

Lumped Roadway Systems

Example systems

University of Tokyo

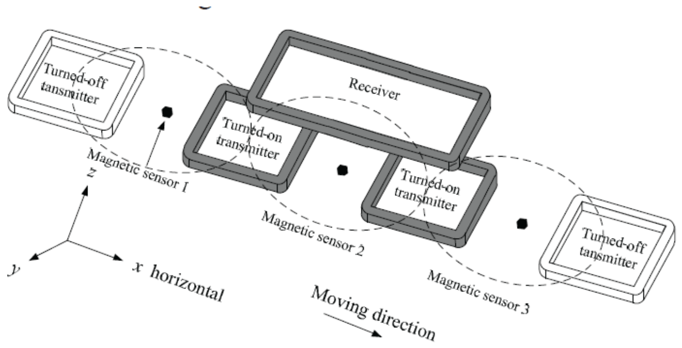

Fig. 4. Diagram of EV positioning using magnetic sensor

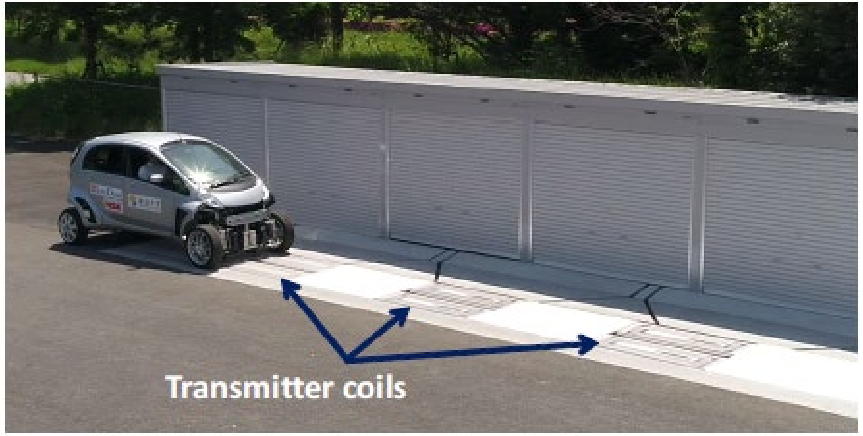

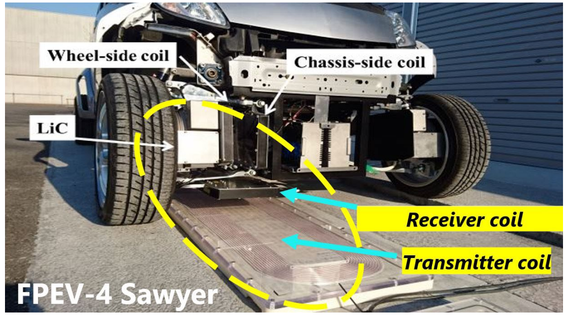

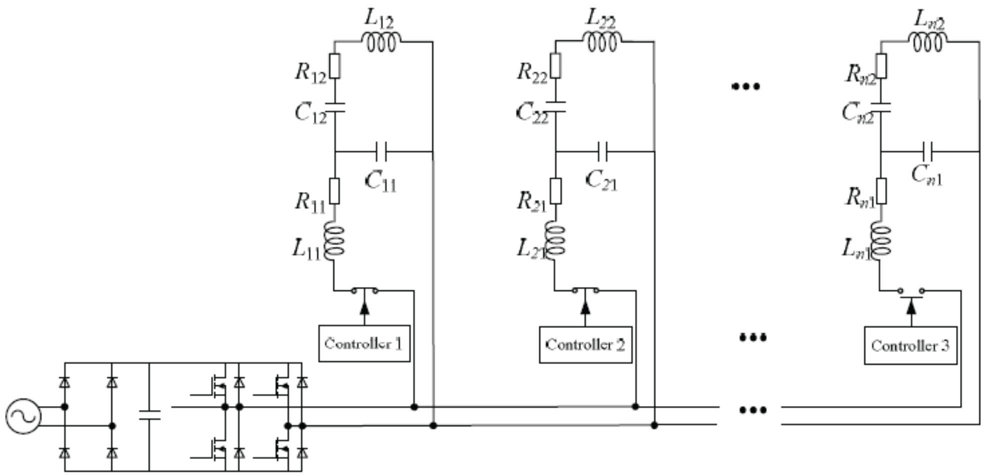

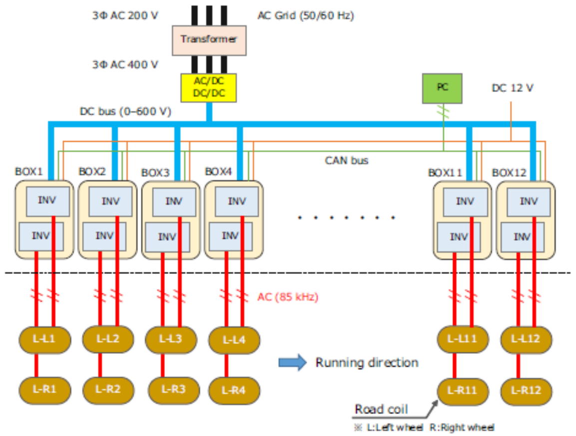

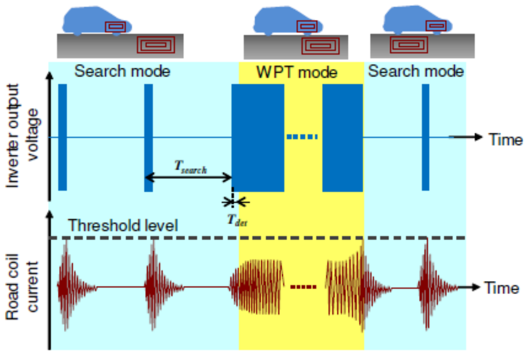

Fig. 8. Concept of sensorless vehicle detection system.

References [39,40]

ORNL

Figure 8. ORNL's EVWPT experimental facility.

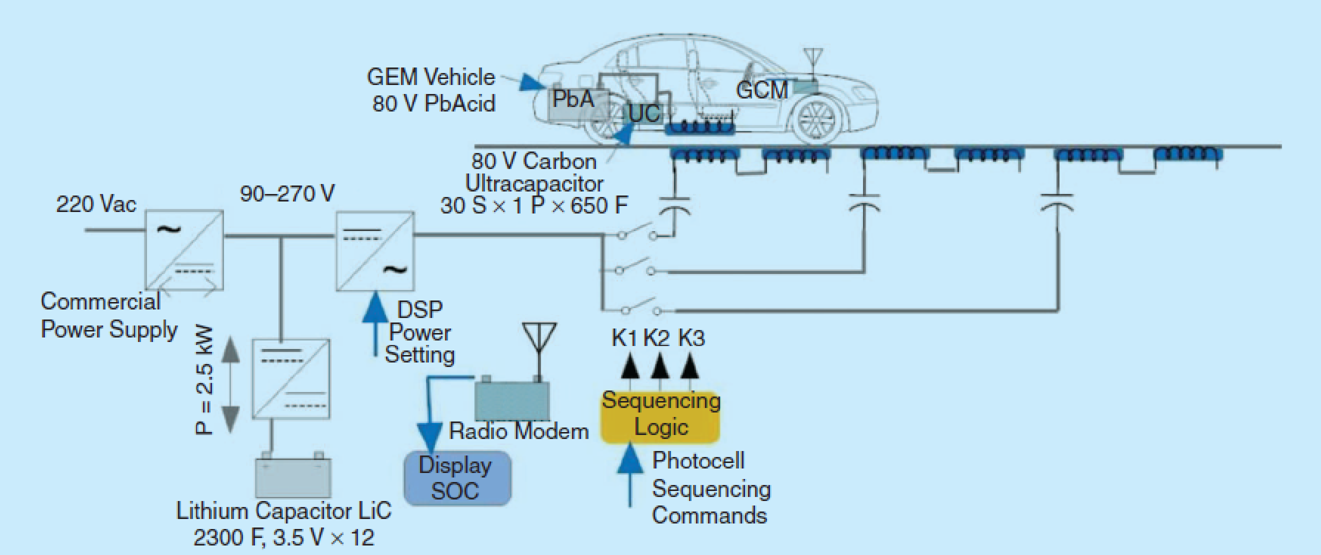

Figure 11. Functional diagram of the ORNL in-motion experimental facility.

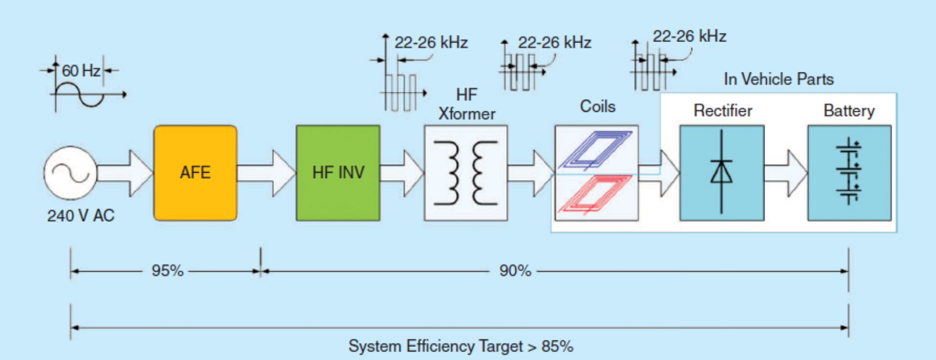

Figure 3. Functional diagram of laboratory WPT.

Power Pulses followed by Nulls
Overcome using two offset coils and ultra capacitors but reduces potential capture.

Reference [43]

TUG Bulgaria (FP7 fast in Charge)

- 30kW system
- Primary has 4cm think cover
- Dynamic at 15-20km/hr

a) b)

Fig. 1. Charging infrastructure – a) static; b) dynamic.

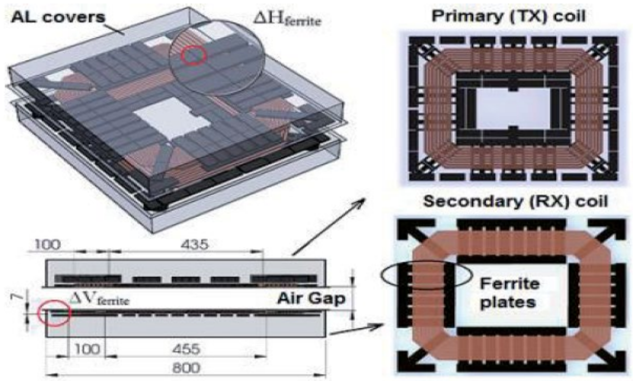

a) b)

Fig. 5. Real tests – a) static and b) dynamic

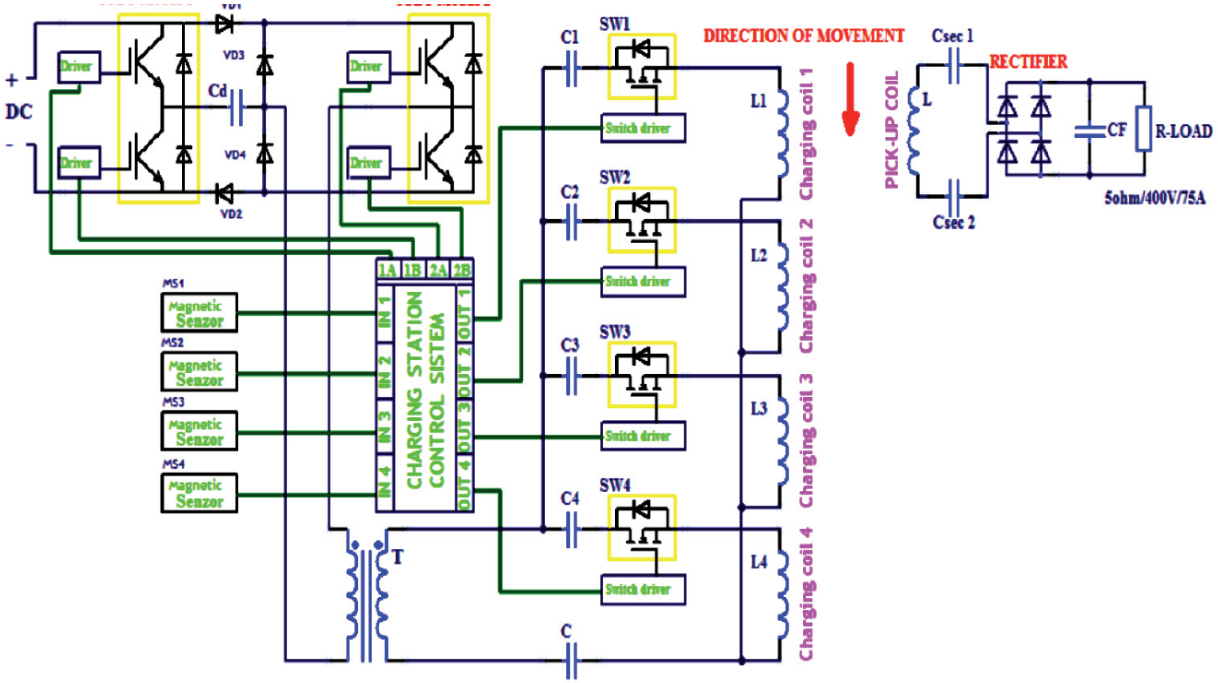

Fig. 4. Dynamic charging infrastructure

Reference [44]

CAS (China)

- (LCC) = LCL 2.34kW power transfer
- Studying switch on and cross transfer of power

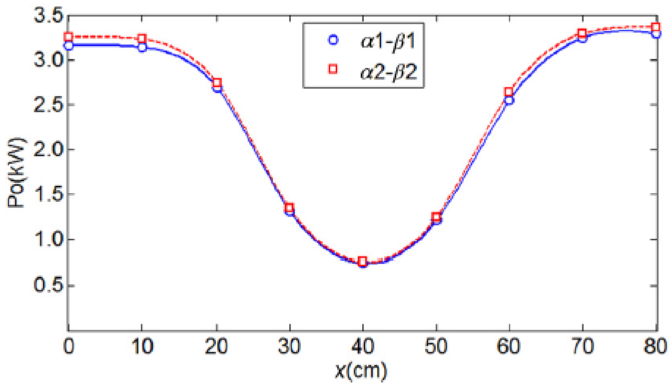

Fig. 14. Measured P_o at different position within a dynamic WPT unit.

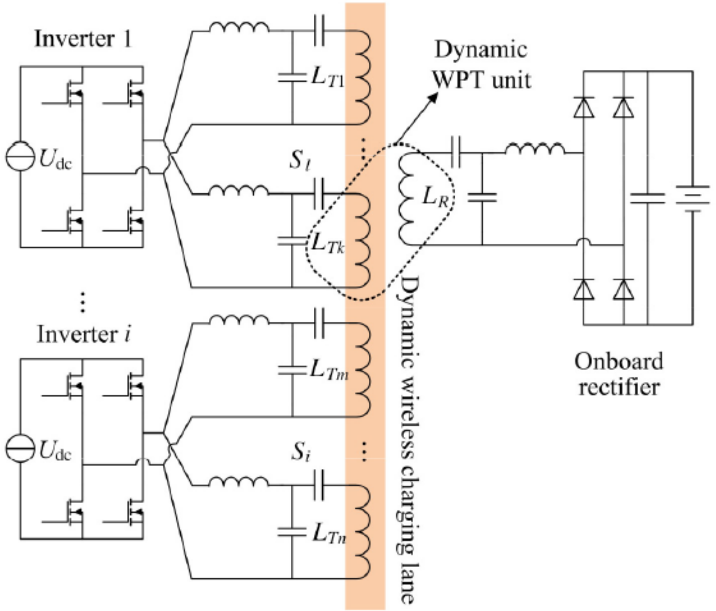

Fig. 2. Configuration of a general wireless power transfer system for dynamic wireless EV charging.

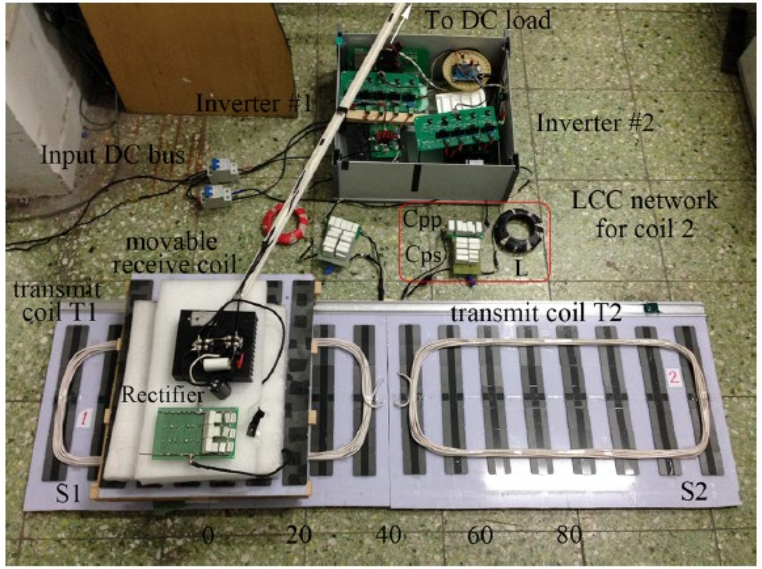

Fig. 12. Photograph of our dynamic EV charging-oriented WPT prototype.

Reference [45]

One inverter driving multiple DD Primaries to a DDQ Secondary

A closely coupled primary decoupler is used to shut off unused primaries

- S_a used to vary reflected load to regulate Ip

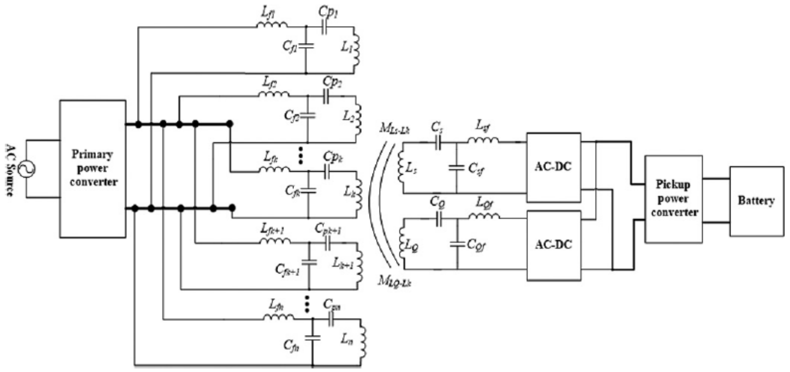

Fig. 4. Multi-LCC networks for the dynamic WPT system.

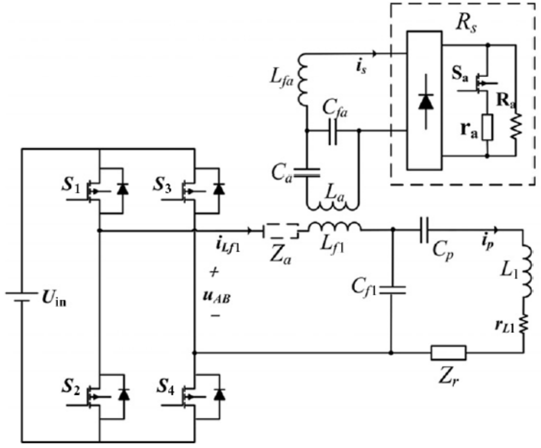

Fig. 8. Primary coil current regulation circuit.

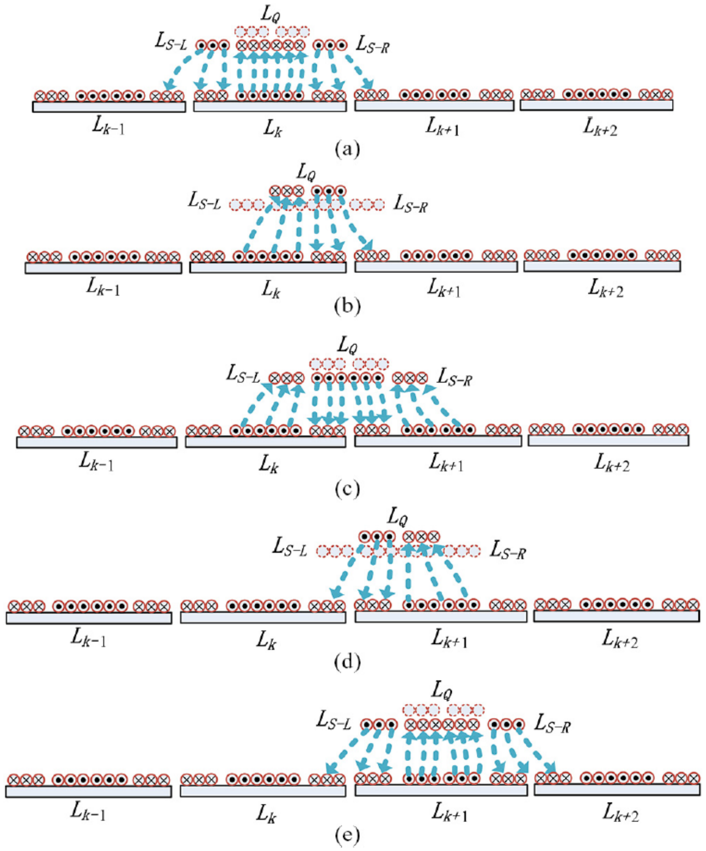

Fig. 6. Coils coupling diagram. (a) Reference point I. (b) Reference point II. (c) Reference point III. (d) Reference point IV. (e) Reference point V.

References [46,47]

Politecnico di Torino

- FABRIC CWD: 50 Tx's:
- Each: 1.5m x 50cm, spaced 50cm.
- 630Vdc stabilised backbone

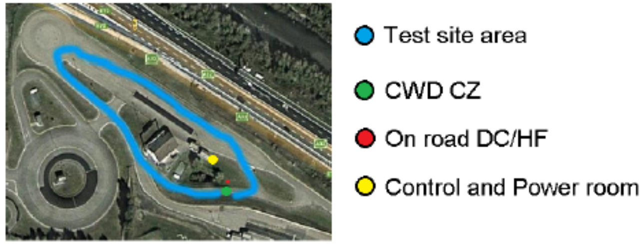

Fig. 10: Map of the Italian test site of eCo-FEV

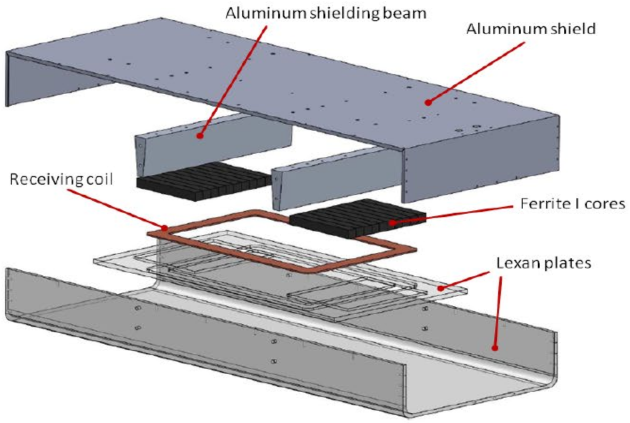

Fig. 11: 3D model of the receiving structure.

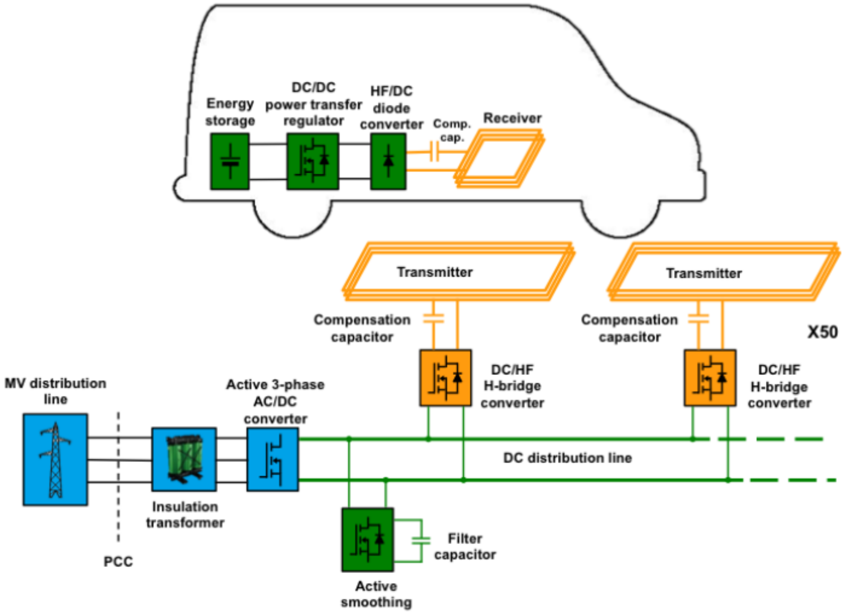

Fig. 9: Electrical infrastructure for the dynamic IPT proposed by the team of the Politecnico di Torino.

Fig. 12: Back of the vehicle during the CWD operation. Under the vehicle plane is visible the receiving structure mounted.

Reference [48]

UoA Roadway

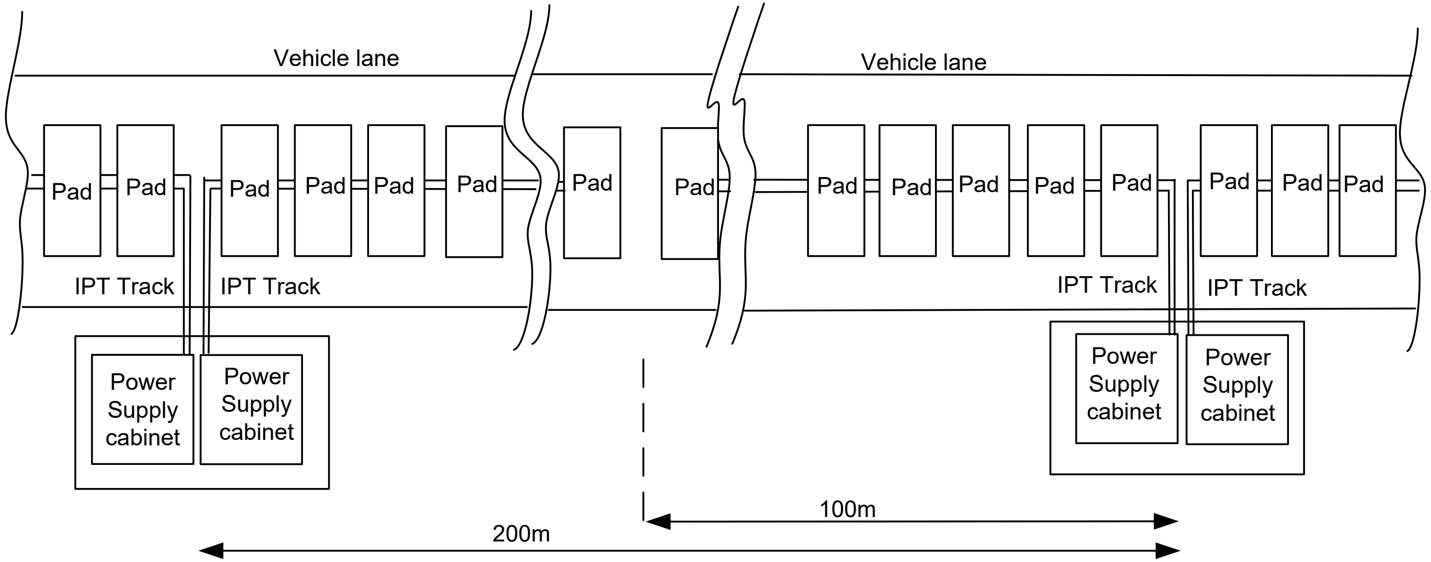

- Sequentially Energised Pads under the Vehicle
- Coupled power to each independently controlled pad
- No DC or mains under roadway

References [8],[27]-[31]

UoA Prototype: Slow moving Taxi-Rank System

- Evaluation of various systems
- 10kW/vehicle system
- Energised only under vehicle
- 20/50kW systems under development

Single phase DD Primaries

Multicoil Bipolar Secondary

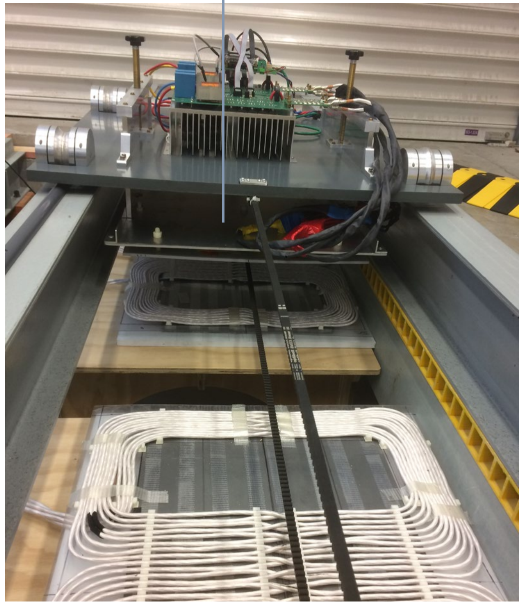

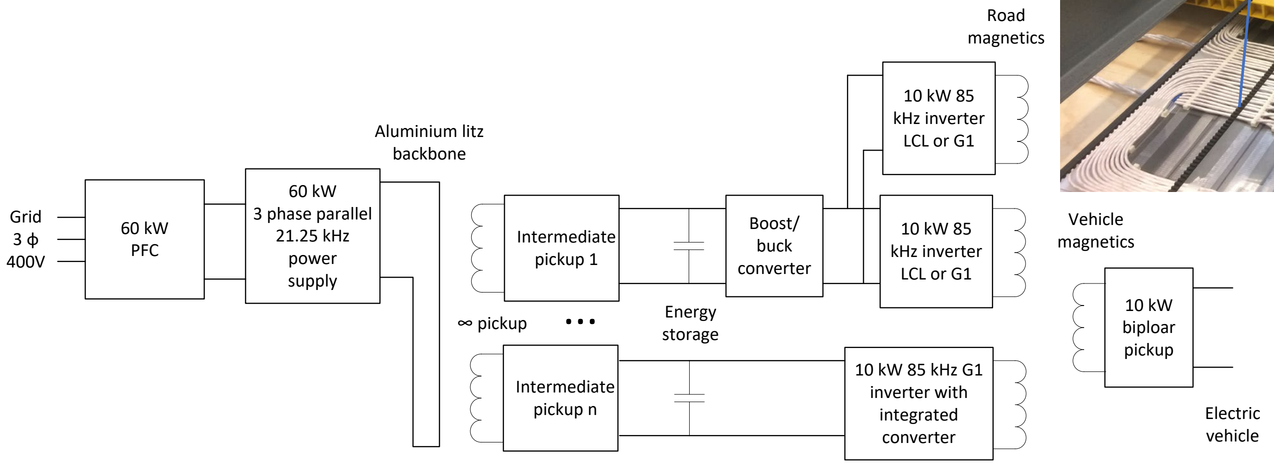

System Opeartion

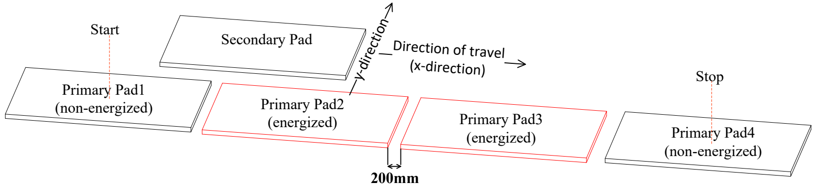

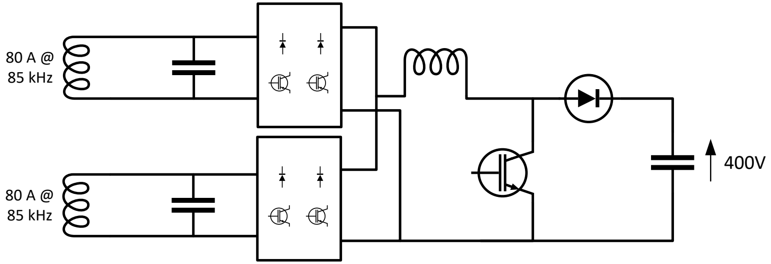

- DDP primary (600mm x 775mm)
- Gap between adjacent primary pads (200mm)
- BPP secondary (350mm x 700mm)

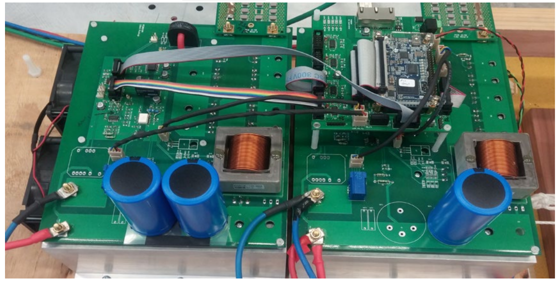

Received current too high:
Multicoil lowers by switching off a coil, raising efficiency

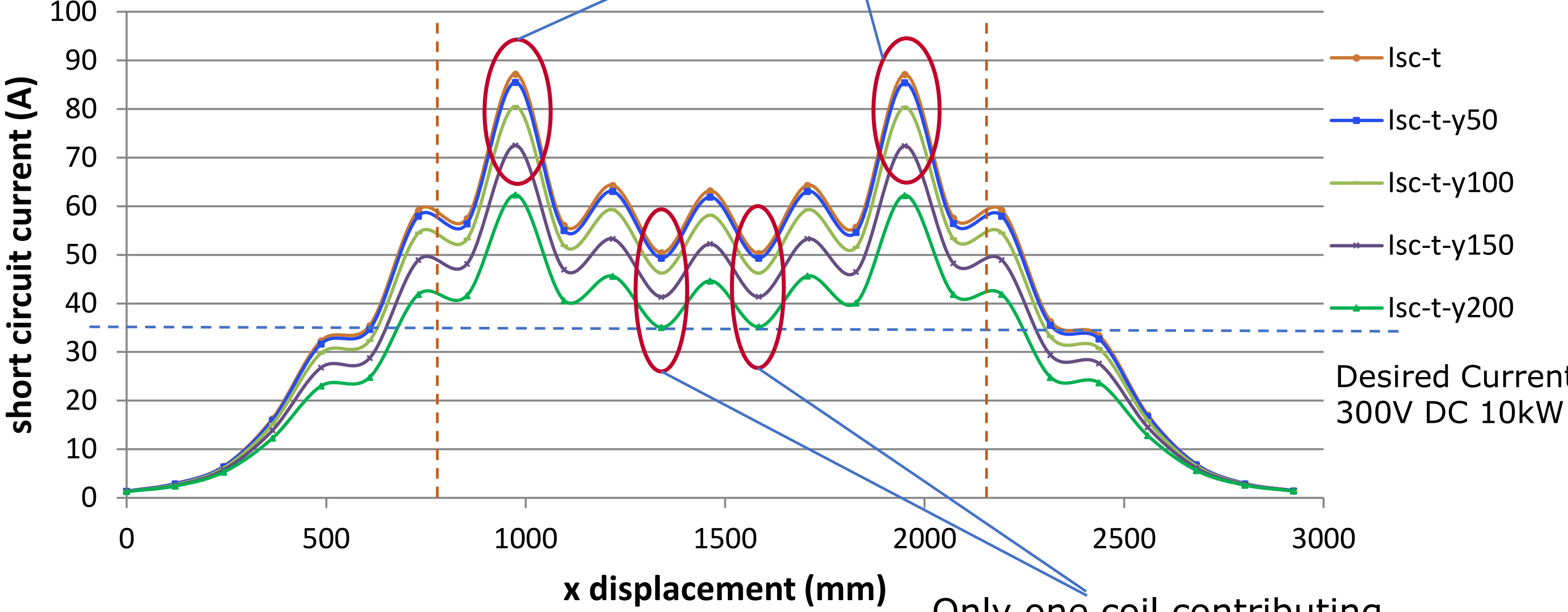

Desired Current
300V DC 10kW

Only one coil contributing
Multicoil turns off coil not contributing

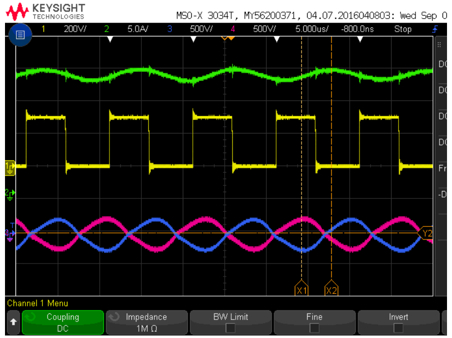

Both Coils Operating

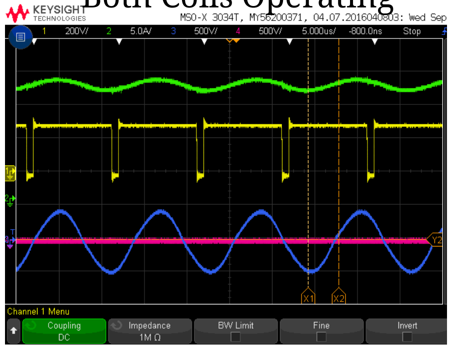

Coil B shorted

Inverter turn on at slow speeds

- Slow vehicle movement (~0.8m/s) speed synchronised
  - If not phase synchronised energy transferred between base pads
- If free resonance > set level in base pad then turn on.
- Turn off when I_{bridge} is low

Slow vehicle movement

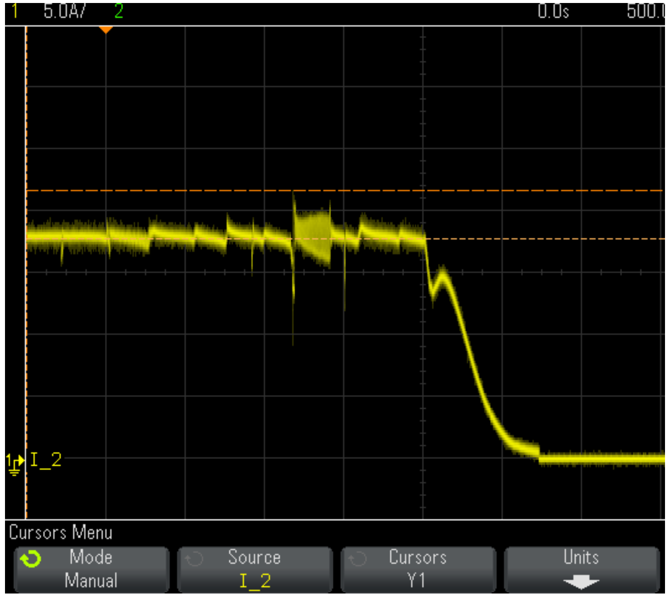

5.5 kW, Voltage = 300,
Output Current = 17.8 A

Qualcomm Halo (WiTricty) DEVC

- No DC or mains under road
- Sequentially Energised Multicoil in road
- 2 x DD 10kW pads (20kW) vehicle

100 m, 20 kW Dynamic Track

100m, 20kW Dynamic Track

Sequential Energisation along the track

In-Road Research Challenges

- Compatibility
  - traffic mixes (different heights)
  - Road construction, (most not concrete and larger movement)
  - Varying energy demands,
  - Flexible grid supply

- Robustness and reliability

- Impact of road construction

Conclusions

- Resonant WPT
  - Imagined 1890s
  - Rediscovered in 1970-80s
  - Commercially practical mid-late 90s in niche markets

- Stationary Charging
  - Single coil options accepted by OEMs for first application
  - Multi-coil topologies promising for high power, wide tolerance
  - Ferrite-less designs under investigation for robustness

- Moving applications
  - Industrial track systems are well established, but transportation options being evaluated
  - Greater freedom requires multi-coil designs on primary or secondary
  - Vehicular systems require robust design considering LD and HD

DD-DD Ansys Stationary Charging Example

Objectives of matched pads analysis:

- Set the ferrite Al and copper regions
- Set excitation to 25A 85kHz RMS
- Evaluate when pads aligned: L1, L2, M and k
- Use rectangle cut plans to evaluate
  - B in the core
  - B Leakage field at 800mm

Questions

Biographies

Dr Duleepa Thrimawithana

Duleepa J. Thrimawithana (M09-SM18) received his BE in Electrical Engineering (with First Class Honors) in 2005 and his Ph.D. in power electronics in 2009 from The University of Auckland, Auckland, New Zealand. From 2005 to 2008, he worked in collaboration with Tru- Test Ltd. in Auckland as a Research Engineer in the areas of power converters and high-voltage pulse generator design. He joined the Department of Electrical and Computer Engineering at The University of Auckland in 2009 where he currently works as a Senior Lecturer. He has co-authored over 130 international journal and conference publications and holds 18 patent families on wireless power transfer technologies. In recognition of his outstanding contributions to engineering as an early career researcher, Dr. Thrimawithana received the Jim and Hazel D. Lord Fellowship in 2014. His main research areas include wireless power transfer, power electronics and renewable energy.

Prof. Grant Covic

Grant Covic (S'88-M'89-SM'04) is a full professor with the Electrical, Computer, and Software Engineering Department at The University of Auckland (UoA). He began working on inductive power transfer in the mid 90's, and by early 2000's was jointly leading a team focused on AGV and EV charging solutions. He has published more than 200 international refereed papers in this field, worked with over 30 PhDs and filed over 40 patent families, all of which are licensed to various global companies in specialised application fields. Together with Prof. John Boys he co-foundered HaloIPT and was awarded the NZ Prime Minister's Science Prize, amongst others for successful scientific and commercialization of this research. He is a fellow of both Engineering New Zealand, and the Royal Society of New Zealand. Presently he heads inductive power research at the UoA, is directing a government funded research program on stationary and dynamic wireless charging of EVs within the road, while also co-leading the interoperability sub-team within the SAE J2954 wireless charging standard for EVs.

Key References

1. http://en.wikipedia.org/wiki/Nikola_Tesla
2. Covic G.A. and Boys J.T. "Inductive power transfer", Proceedings of the IEEE, **101** no. 6, 2013, pp. 1276-1289
3. Hui, S.R. "Planar Wireless Charging Technology for Portable Electronic Products and Qi" Proceedings of the IEEE, **101** no. 6, 2013, pp. 1290-1301
4. Garnica J., Chinga R.A. and Lin J. "Wireless Power Transmission: from far field to near field" Proceedings of the IEEE, **101** no. 6, 2013, pp. 1321-1331
5. Ho j. Kim S. and Poon A.S.Y. "Midfield wireless powering for implantable devices" Proceedings of the IEEE, **101** no. 6, 2013, pp. 1369-1378
6. Popovic Z. et al. "Low Power far-field wireless powering for wireless sensors", Proceedings of the IEEE, **101** no. 6, 2013, pp. 1397-1401
7. Hui, S.Y.R. ;   Wenxing Z.;   Lee, C.K. "A Critical Review of Recent Progress in Mid-Range Wireless Power Transfer" IEEE Trans. Power Electronics, **29** no 9, 2014, pp 4500 - 4511
8. Covic G.A. and Boys J.T. "Modern trends in inductive power transfer for transportation applications" IEEE Transactions Emerging and Selected Topics in Power Electronics , **1**, no 1, pp 28-41.
9. Choi S.Y., Gu B.W. Jeong S.Y., Rim C.T. "Advances in wireless power transfer systems for roadway powered electric vehicles" in press IEEE Transactions Emerging and Selected Topics in Power Electronics early access pp 1-14 August 2014, DOI: 10.1109/JESTPE.2014.2343674
10. Boys J.T., Covic G.A. and. Green A.W. "Stability and Control of inductively coupled power transfer systems", *IEE Proc. EPA*, **147**. pp 37-43
11. Keeling N.A., Covic G.A. and Boys J.T. "A unity power factor IPT pick-up for high power applications", *IEEE Trans. Industrial Electronics Society,* **57**, no 2, pp. 744-751, Feb., 2010

Key References

12. Huang C-Y., Boys, J.T., Covic, G.A. “LCL Pick-up Circulating Current Controller for IPT systems” *IEEE Trans. Power Electronics Society*, **28** no. 4 April 2013, pp. 2081-2093.
13. Wang, C.S, Covic G.A. and Stielau, O. H. “Investigating an LCL Load Resonant Inverter for Inductive Power Transfer Applications”, *IEEE Trans., Power Electronics Society,* **19,** no. 4, 995-1002, 2004
14. Boys J.T., Huang C-Y. and Covic G.A. “Single phase unity power-factor IPT system”, The 34th Annual IEEE Power Electronics Specialists Conference PESC 08 June 15-22nd Rhodes Island Greece 2008, pp. 3701-3706.
15. Hao H. Covic G.A. and Boys J.T. “A parallel topology for Inductive Power Transfer power supplies” *IEEE Trans. Power Electronics,* **29** no. 3 March 2014, pp. 1140-1151.
16. Boys, J.T., Elliott G.A.J. and Covic, G.A. “An Appropriate Magnetic Coupling Co-efficient for the design and Comparison of ICPT Pick-ups” *IEEE Trans. Power Electronics Society*, **22,** no. 1, pp. 333-335, Jan. 2007
17. Elliott G.A.J., Covic, G.A., Kacprzak, D. and, Boys, J.T. “A New Concept: Asymmetrical Pick-ups for Inductively Coupled Power Transfer Monorail Systems” *IEEE Trans. on Magnetics*, **42,** no. 10 pp. 3389-3391, 2006
18. Covic G.A., Boys J.T., Kissin M. and Lu H. “A three-phase inductive power transfer system for roadway power vehicles” *IEEE Trans., Industrial Electronics Society,* **54,** no. 6, pp. 3370-3378, Dec. 2007
19. Elliott G.A.J., Raabe S., Covic G.A. and Boys J.T. “Multi-phase pick-ups for large lateral tolerance contactless power transfer systems”, IEEE Trans. Industrial Electronics Society, **57**, no. 5, pp 1590-1598, May 2010
20. Raabe S., Covic G.A. “Practical design considerations for contactless power transfer systems quadrature pick-ups”, IEEE Trans. Industrial Electronics Society, **60** no. 1, Jan 2013, pp. 400-409
21. Budhia M. , Covic, G.A. and Boys J.T.; "Design and Optimisation of Magnetic Structures for Lumped Inductive Power Transfer Systems", *IEEE Trans. Power Electronics Society*,**26** no 11. pp. 3096-3108, Nov. 2011.

Key References

22. Budhia M., Boys J.T, Covic, G.A. and Huang C-Y. "Development of a single-sided flux magnetic coupler for electric vehicle IPT charging systems", *IEEE Trans. Industrial Electronics Society*, **60** no. 1, Jan 2013, pp. 318-328
23. Zaheer, A. ; Hao, H. ; Covic, G.; Kacprzak, D. "Investigation of Multiple Decoupled Coil Primary Pad Topologies in Lumped IPT Systems for Interoperable Electric Vehicle Charging *" IEEE Transactions on Power Electronics*, **30**, pp. 1937-1955, 2015.
24. Kim S., Covic G.A. and Boys J.T. "Tripolar Pad for Inductive Power Transfer Systems for EV Charging" *IEEE Trans. Power Electronics Society* , pp 1-13, available early access 2016 DOI: 10.1109/TPEL.2016.2606893
25. Nagendra G.R., Covic G.A. and Boys J.T. "Determining the physical size of inductive couplers for IPT EV systems" *IEEE Trans. Journal of* JESTPE, **2** no. 3, Sept. 2014, pp. 571-583
26. Tejeda, A. , Carretero, C., Boys, J. T., & Covic, G. A. (2016). Core-less Circular Pad with Controlled Flux Cancellation for EV Wireless Charging. *IEEE Transactions on Power Electronics*, pp1-12. available early access DOI:10.1109/TPEL.2016.2642192
27. Lin F.Y., Covic G.A. , Boys J.T. "Evaluation of Magnetic pad sizes and topologies for electric vehicle charging", *IEEE Trans. Power Electronics Society*, **30** no. 11, Nov. 2015, pp. 6391-6407.
28. Budhia M., Covic, G.A. and Boys J.T. "Magnetic Design of a Three-Phase Inductive Power Transfer System for Roadway Powered Electric Vehicles" *IEEE Vehicle power and propulsion conference,* VPPC'10, Sept 1-3 Lille, France 2010
29. Zaheer, A., Neath, M., Beh, H. Z. Z., & Covic, G. A. "A Dynamic EV Charging System for Slow Moving Traffic Applications." *IEEE Trans. on Transport. Electrification*, pp1-18., 2016, DOI:10.1109/TTE.2016.2628796
30. Nagendra G.R., Chen L., Covic G.A. and Boys J.T. "Detection of EVs on IPT Highways" *IEEE Trans. Journal of JESTPE*, **2** no. 3, Sept 2014, pp. 584-597.
31. Kamineni, A., Neath, M. J., Zaheer, A., Covic, G. A., & Boys, J. T. "Interoperable EV detection for dynamic wireless charging with existing hardware and free resonance". *IEEE Trans. on Transport. Electrification*, pp.1-12. 2016, DOI:10.1109/TTE.2016.2631607

Key References

32. L. Xiang, Y. Sun, Z. Ye, Z. Wang and S. Zhou "Combined primary coupler design and control ofe EV dynamic wireless charging system" IEEE Wow workshop 2016 pp. 174-179.
33. Y. H. Sohn, B. H. Choi, E. S. Lee, and C. T. Rim, "Comparisons of magnetic field shaping methods for ubiquitous wireless power transfer," in Proc. IEEE PELS Workshop Emerg. Technol., Wireless Power, 2015, pp. 1–6.

Selected track based roadway examples

34. F. Turki, V. Staudt, A. Steimel "Dynamic Wireless EV Charging fed from Railway Grid: Magnetic Topology Comparison" IEEE ESARS pp 1-8, 2015
35. C. C. Mi, G. Buja, S. Y. Choi, and C. T. Rim, IEEE"Modern Advances in Wireless Power Transfer Systems for Roadway Powered Electric Vehicles" IEEE Trans IES 63 no 10, 2016, pp 6553 -6544
36. V. X. Thai, S. Y. Choi, B. H. Choi, J. H. Kim, and C. T. Rim "Coreless Power Supply Rails Compatible with Both Stationary and Dynamic Charging of Electric Vehicles" IEEE IFEEC 2014 pp. 1-5
37. INTIS "Wireless charging Evs unplugged" IHS Automotive 6 no 5 pp. 8-11, 2015
38. K. Throngnumchai, A. Hanamura, Y. Naruse, K. Takeda "Design and Evaluation of a Wireless Power Transfer System with Road Embedded Transmitter Coils for Dynamic Charging of Electric Vehicles" EVS27 2013 pp. 1-10

Key References

Selected lumped based roadway examples

39. K. Song, C. Zhu, K.-E. Koh, D. Kobayashi, T. Imura & Y. Hori, “Wireless Power Transfer for Running EV Powering Using Multi-Parallel Segmented Rails” IEEE WoW PELs workshop 2015 pp. 1-6
40. K. Song, C. Zhu, K.-E. Koh, D. Kobayashi, T. Imura & Y. Hori “Modeling and Design of Dynamic Wireless Power Transfer System for EV Applications” IEEE IECON 2015 pp. 1-6
41. S. Lukic and Z. Pantic “Cutting the cord” IEEE Elect Mag 2013 pp. 57-64
42. S. Lukic and Z. Pantic “Reflexive Field Containment in Dynamic Inductive Power Transfer Systems” IEEE Trans PELS29 no 9, 2014 pp. 4592-4602.
43. J. M. Miller, P.T. Jones, J.-M. Li, and O. C. Onar, “ORNL Experience and Challenges Facing Dynamic Wireless Power Charging of EV’s” IEEE circuits and systems magazine, Q2, 2015. pp. 40-53,
44. N. Madzharov, and V. Petkov “Innovative solution of static and dynamic contactless charging station for electrical vehicles” PCIM Europe 2016 pp. 1-8
45. Y. Guo, L. Wang, Q. Zhu, C.Liao, and F. Li “Switch-On Modeling and Analysis of Dynamic Wireless Charging System Used for Electric Vehicles” IEEE Trans IES 63, no 10 2016 pp. 6568-6579
46. S. Zhou and C.C. Mi “Multi-Paralleled LCC Reactive Power Compensation Networks and Their Tuning Method for Electric Vehicle Dynamic Wireless Charging” IEEE Trans IES 63, no 10, 2016 pp. 6546-6556
47. F. Lu, H. Zhang, H. Hofmann, C.C. Mi A “Dynamic Charging System With Reduced Output Power Pulsation for Electric Vehicles” IEEE Trans IES 63, no 10, 2016, pp. 6580-6590
48. V. Cirimele, M. Diana, F. Freschi,“Inductive power transfer for automotive applications: state-of-the-art and future trends” IEEE Trans IAS, 2018 pp. 1-11

Key References

Selected Additional References

49. B. J. Varghese, A. Kamineni and R. A. Zane “Investigation of a DD2Q Pad Structure for High Power Inductive Power Transfer” IEEE wpw 2019 pp 1-6
50. A. Ridge, K. K. Ahamad, R. McMahon, J. Miles “Development of a 10 kW Wireless Power Transfer System” IEEE wpw 2019 pp. 1-6
51. V. P. Galigekere et. al. ,“Design and Implementation of an Optimized 100 kW Stationary Wireless Charging System for EV Battery Recharging” IEEE ECCE 2018 pp. 3587-3592
52. M. Mohanmmad et. al. “Design of an EMF Suppressing Magnetic Shield for a 100-kW DD-Coil Wireless Charging System for Electric Vehicles” IEEE APEC 2019 pp 1521-1527
53. M. G. S. Pearce; G. A. Covic ; J. T. Boys, “Robust Ferrite-less Double D Topology for Roadway IPT Applications”, IEEE Transactions on Power Electronics, 2018
54. M. G. S. Pearce; G. A. Covic ; J. T. Boys “ Reduced Ferrite Double D pad for Roadway IPT Applications” , IEEE Transactions on Power Electronics, vol. 36, no. 5, pp. 5055-5068, May 2021
55. J. Pries, V. P. N. Galigekere, O. C. Onar, G-J Su. “50-kW Three-Phase Wireless Power Transfer System Using Bipolar Windings and Series Resonant Networks for Rotating Magnetic Fields” IEEE Trans. Power Electronics 35, no. 5, pp. 4500-4517, May 2020
56. F. Lin, G. A. Covic, and M. Kesler “Design of a SAE Compliant Multicoil Ground Assembly” IEEE Journal of Emerging and Selected Topics in Industrial Electronics, vol. 1, no. 1, pp. 14-25, July 2020
57. W. Chen, F. Lin, G. A. Covic and J. T. Boys, "Evaluation of a Meandering Track Primary Topology for EV Roadway Charging," in IEEE Journal of Emerging and Selected Topics in Industrial Electronics, vol. 1, no. 1, pp. 26-35, July 2020
58. V. Zahiri Barsari, D. J. Thrimawithana and G. A. Covic, "An Inductive Coupler Array for In-Motion Wireless Charging of Electric Vehicles," in IEEE Transactions on Power Electronics, doi: 10.1109/TPEL.2021.3058666.
59. SAE J2954 “Wireless Power Transfer for Light-Duty Plug-in/Electric Vehicles and Alignment Methodology”, 20-10-2020 https://www.sae.org/standards/content/j2954_202010/
60. K. Hata, T. Imura, H. Fujimoto, Y. Hori, D. Gunji “Charging Infrastructure Design for In-motion WPT Based on Sensor-less Vehicle Detection System” IEEE wpw 2019 pp 1-6

Key References

Selected Additional References

61. M. Mohammad, O. C. Onar, J. L. Pries, V. P. Galigekere, G. -J. Su and J. Wilkins, "Thermal Analysis of a 50 kW Three-Phase Wireless Charging System," 2021 IEEE Transportation Electrification Conference & Expo (ITEC), 2021
62. J. Lu, G. Zhu and C. C. Mi, "Foreign Object Detection in Wireless Power Transfer Systems," in IEEE Transactions on Industry Applications, vol. 58, no. 1, pp. 1340-1354, Jan.-Feb. 2022
63. P. A. J. Lawton, F. J. Lin and G. A. Covic, "Reducing and Validating Surface Flux Emissions for High-Power Wireless Charging Systems," 2022 IEEE Wireless Power Week (WPW)
64. P. A. J. Lawton, F. J. Lin and G. A. Covic, “Magnetic Design Considerations for High-Power Wireless Charging Systems” IEEE Trans. PELs pp 1-10, 2022.
65. J. T. Boys, “Inductive power transfer across an extended gap,” Patent WO/1998/050993 Nov. 12, 1998.
66. Y. H. Kim, S. Y. Kang, S. Cheon, M. L. Lee, J. M. Lee, and T. Zyung, “Optimization of wireless power transmission through resonant coupling,” in Proc. SPEEDAM, 2010, pp. 1069–1073.
67. W. X. Zhong, C. K. Lee, and S. Y. R. Hui, “General analysis on the use of tesla’s resonators in domino forms for wireless power transfer,” IEEE Trans. Ind. Electron., vol. 60, no. 1, pp. 261–270, Jan. 2013.
68. W. X. Zhong, C. Zhang, X. Liu, and S. Y. R. Hui, “A methodology for making a 3-coil wireless power transfer system more energy efficient than a 2-coil counterpart for extended transmission distance,” IEEE Trans. Power Electron., vol. 30, no. 2, pp. 933–942, Mar. 2014
69. A. Kamineni, G. A. Covic, and J. T. Boys “Analysis of Coplanar Intermediate Coil Structures in Inductive Power Transfer Systems” IEEE Trans. PELs Vol 30 no 11, Nov. 2015, pp 6141-6151
70. A. Bilal, S. Kim,, F. Lin, and G. Covic “Analysis of IPT Intermediate Coupler System for Vehicle Charging Over Large Air Gaps” IEEE Journal of Emerging and Selected Topics in Pwr. Elec. pp 1-10
71. Budhia M., Covic, G.A. and Boys J.T. “Magnetic Design of a Three-Phase Inductive Power Transfer System for Roadway Powered Electric Vehicles” IEEE Vehicle power and propulsion conference, VPPC’10, Sept 1-3 Lille, France 2010
72. Kissin, M. L. G., Boys J. T. and Covic, G. A. "Interphase Mutual Inductance in Poly-Phase Inductive Power Transfer Systems IEEE Trans., Industrial Electronics Society, 56, no. 7, pp. 2393-2400, July, 2009